Physiological, biochemical and molecular analyses of the drought stress responses of two contrasting wheat varieties

Sellwane Jeanette Moloi

2007105915

Thesis submitted in fulfilment of the requirements for the degree Doctor of Philosophy (PhD) in Botany in the Department of Plant Sciences, Faculty of Natural and Agricultural Sciences, University of the Free State - Qwaqwa Campus

UNIVERSITY OF THE
FREE STATE
UNIVERSITEIT VAN DIE
VRYSTAAT
YUNIVESITHI YA
FREISTATA

Supervisor: Prof. Rudo Ngara

Co-supervisor: Prof. Stephen Chivasa

November 2024

DECLARATION

I, Sellwane Jeanette Moloi, declare that the PhD thesis that I herewith submit for the PhD qualification in Botany at the University of the Free State, is my independent work and that I have not previously submitted it for a qualification at another institution of higher education.

I, Sellwane Jeanette Moloi, hereby declare that I am aware that the copyright is vested in the University of the Free State.

I, Sellwane Jeanette Moloi, hereby declare that all royalties as regards intellectual property that was developed during the course of and/ or in connection with the study at the University of the Free State will accrue to the University.

SIGNED BY THE STUDENT	30 November 2024
---------------------------	--------------------------
Sellwane Jeanette Moloi	Date

DEDICATION

I dedicate this work to the light of my life, my daughter, Lindokuhle Mosa Moloi. This is for you, baby girl, and I hope you learn from my journey that you must work hard to achieve whatever you want.

ACKNOWLEDGEMENTS

First, I would like to thank God's gift of life and for giving me the strength to continue with this PhD degree when I felt that I was incapable or not good enough. I would also like to express my sincere gratitude to my supervisor, Prof. Rudo Ngara, for allowing me the opportunity to pursue this PhD degree under her supervision. Thank you, Prof, for the encouragement and for always believing that I am capable even when I felt this degree was an impossible task. I am forever grateful. To my co-supervisor, Prof. Stephen Chivasa and his research group at Durham University, United Kingdom, thank you for the iTRAQ and osmolyte analyses. I am grateful. I also want to thank Dr. Arun Gokul for his assistance with the biochemical assays and always being there to check if I was okay, thank you. I also thank Dr. Makoena Joyce Moloi for welcoming me in her lab and assisting me with the biochemical assays. Thank you "Lekgolokwe". I am also grateful for the financial support I received from the National Research Foundation throughout my degree, without the funding, this academic journey would have been more difficult. To the Plant Biotechnology Research Group, thank you guys, you became more than just lab partners, and I am thankful for the support. I also want to thank the Department of Plant Sciences colleagues for their support. To my friends and family, especially my mother and siblings, thank you all for always being there when I complained about this degree. You guys always made time for me, and I am grateful.

TABLE OF CONTENTS

LIST OF FIGURES

LIST OF TABLES

LIST OF ABBREVIATIONS

1D-SDS PAGE	One-dimensional sodium dodecyl sulfate-polyacrylamide gel electrophoresis
APS	Ammonium persulfate
APX	Ascorbate peroxidase
BSA	Bovine serum albumin
CBB	Coomassie Brilliant Blue
CHAPS	3-[(3-Cholamidopropyl) dimethylammonio]-1 propanesulfonate
cDNA	Complementary deoxy-ribonucleic acid
EDTA	Ethylenediaminetetraacetic acid
GPX	Guaiacol peroxidase
HILIC-MS	Hydrophilic interaction liquid chromatography-mass spectrometry
iTRAQ	Isobaric Tags for Relative and Absolute Quantitation
kDa	Kilodalton
KEGG	Kyoto Encyclopedia of Genes and Genomes
LC/MS	Liquid chromatography mass spectrometry
MOPS	3-(N-Morpholino)-propanesulfonic acid
qRT-PCR	Quantitative real-time polymerase chain reaction
MW	Molecular weight
ROS	Reactive oxygen species
RWC	Relative water content
RNA	Ribonucleic acid
SDS	Sodium dodecyl sulfate
SOD	Superoxide dismutase

STRING	Search Tool for Retrieval of Interacting Genes/Proteins
TAE	Tris-acetate-(ethylenedinitrilo)-tetraacetic acid
TBA	Thiobarbituric acid
TCA	Trichloroacetic acid
TEMED	N,N,N’,N’-Tetramethylethylenediamine
v/v	Volume to volume
w/v	Weight to volume

RESEARCH OUTPUTS FROM THIS STUDY

Conference presentations

1. **Moloi, S.J**., and Ngara, R. Screening wheat varieties for drought tolerance using physiological and growth parameters. Poster presentation delivered by Sellwane Jeanette Moloi at the South African Association of Botanists (SAAB), 46th Annual Conference, University of the Free State, QwaQwa campus, 7-10 January 2020. The poster won best poster in the Plant Physiology category.

2. **Moloi, S.J**., Moloi, M.J., Gokul, A., Chivasa, S., and Ngara, R. Physiological, biochemical and leaf proteomic analyses of wheat varieties to water limitation stress. Oral presentation delivered by Sellwane Jeanette Moloi at the University of Johannesburg Postgraduate Symposium, 24-25 October 2023. The presentation won the third-place prize in the PhD category.

Publications

1. Part of the Literature review chapter was published as a review paper:
   Moloi, S.J., and Ngara, R. (2023). The roles of plant proteases and protease inhibitors in drought response: a review. *Frontiers in Plant Science*, 14, 1165845. https://doi.org/10.3389/fpls.2023.1165845. Q1. Impact factor 4.1.

2. Results from Chapters 3, 4 and 5 were published as a research article:
   Moloi, S.J., Alqarni, A.O., Brown, A.P., Goche, T., Shargie, N.G., Moloi, M.J., Gokul, A., Chivasa, S., and Ngara, R. (2024). Comparative physiological, biochemical, and leaf proteome responses of contrasting wheat varieties to drought stress. *Plants, 13*, 2797. https://doi.org/10.3390/plants13192797. Q1. Impact factor 4.0.

ABSTRACT

Wheat (*Triticum aestivum*) is the second most widely grown cereal crop worldwide. It is primarily used for human consumption, animal feed, and industrial biofuels. However, the production of wheat is negatively affected by drought, and current climate models are predicting more frequent and severe drought episodes in the future. As such, agricultural productivity will be negatively affected. Therefore, understanding plant responses among plant varieties with different drought phenotypes could help identify traits related to drought tolerance and aid in developing more drought-tolerant crops. This study compared the physiological, biochemical, and molecular responses of the drought-tolerant (BW35695) and drought-susceptible (BW4074) wheat varieties to drought stress. The wheat plants were grown in potting soil for two weeks in a growth chamber before withholding water for 28 days. Drought stress significantly decreased soil moisture content in the water-deprived pots of both varieties relative to the well-watered controls. However, there was no significant difference in soil moisture content between the varieties, suggesting comparable levels of water deficit stress. Physiological and biochemical parameters such as leaf chlorophyll, carotenoid and relative water content (RWC), lipid peroxidation, reactive oxygen species (ROS), osmolyte content, and enzymatic antioxidant activities revealed striking differences between the varieties. The drought-tolerant wheat variety, BW35695, demonstrated remarkable resilience to the imposed drought stress by exhibiting higher leaf RWC, chlorophyll, carotenoid, and osmolyte content compared to the drought-susceptible variety, BW4074. Additionally, BW35695 mitigated drought-induced oxidative stress by enhancing the activities of superoxide dismutase (SOD) and guaiacol peroxidase (GPX) in both leaves and roots and reduced ROS accumulation and membrane lipid damage. The leaf proteome of the wheat varieties was analysed to identify drought-responsive leaf proteins using the isobaric tags for absolute and relative quantitation (iTRAQ) method coupled with mass spectrometry. A total of 1062 and 882

leaf proteins were positively identified in BW4074 and BW35695 wheat varieties, respectively, of which 69 and 110 were drought responsive. Most of the drought-responsive leaf proteins in BW35695 were involved in energy (28%) and protein synthesis/folding/degradation (25%). For BW4074, primary metabolism (23%), energy (23%) and protein synthesis/folding/degradation (20%) were the most represented protein functional groups. The rest of the drought-responsive leaf proteins had putative functions in defence/ROS detoxification (20% and 10%), transcription (4% and 7%), secondary metabolism (6% and 3%), and cell structure (2% and 1%) in BW4074 and BW35695, respectively. A Kyoto Encyclopedia of Genes and Genomes (KEGG) pathway enrichment analysis revealed that the two most significantly enriched pathways in BW4074 were alanine aspartate and glutamate metabolism, and arginine biosynthesis, while photosynthesis-antennae and photosynthesis were most enriched in BW35695. The KEGG pathway enrichment analysis supported the putative functional groupings data, which suggests that drought stress affects various biological processes in wheat leaves, particularly primary metabolism in BW4074 and photosynthesis in BW35695. Protein-protein interactions of the drought-responsive proteins were analysed using the Search Tool for the Retrieval of Interacting Genes/Proteins (STRING) database. The results showed that primary metabolism and protein synthesis were the main interacting functional groups for BW4074, while photosynthesis and protein synthesis were prominently interacting in BW35695. Photosynthesis-related proteins were significantly suppressed in BW35695, possibly as a strategy to reduce ROS-induced cell damage, while protein synthesis-related proteins were increased, possibly to enhance the biosynthesis of other stress-responsive proteins. Six drought-responsive proteins were selected from the iTRAQ data for quantitative real-time polymerase chain reaction (qRT-PCR) analysis. The gene expression results revealed that a *delta-1-pyrroline-5-carboxylate synthase (W5ACM8)* gene involved in proline biosynthesis significantly increased in BW4074, which correlated with the iTRAQ data. For

BW35695, all six target genes were not differentially expressed, possibly suggesting that the abundances of the proteins and transcripts differentially accumulate at different time points. These qRT-PCR results, call for multi-time point experimental designs for validating iTRAQ data. Overall, the study provides insight into the drought-responsive mechanisms of BW4074 and BW35695 wheat varieties. This information can serve as a reference in studies exploring the differences between plant varieties under drought stress conditions and assist in plant breeding programmes for improved drought resilience.

Keywords: Wheat; drought stress; proline; glycine betaine; reactive oxygen species; lipid peroxidation; antioxidants; proteomics; iTRAQ; gene expression analysis.

CHAPTER 1

GENERAL INTRODUCTION

1.1 Wheat origin, growth and importance

Wheat (*Triticum spp*.) is a C_3 cereal crop from the Poaceae family. It was first domesticated in the Fertile Crescent in the Middle East about 10,000 years ago and has since spread worldwide (Sarto *et al*., 2017; de Sousa *et al*., 2021; Iqbal *et al*., 2022). The earliest cultivated wheat species are einkorn (*Triticum monococcum* L.), emmer (*Triticum dicoccum*), and spelt (*Triticum spelta*). Currently, bread wheat (*Triticum aestivum* L.) and durum wheat (*Triticum durum*) are the two most cultivated wheat species (de Sousa *et al*., 2021; Iqbal *et al*., 2022). In terms of its production and consumption, bread wheat is regarded as an economically important cereal crop globally and is ranked second after maize (*Zea mays*), with a world production of 808 million tonnes in 2022 (Figure 1.1; FAOSTAT, 2023).

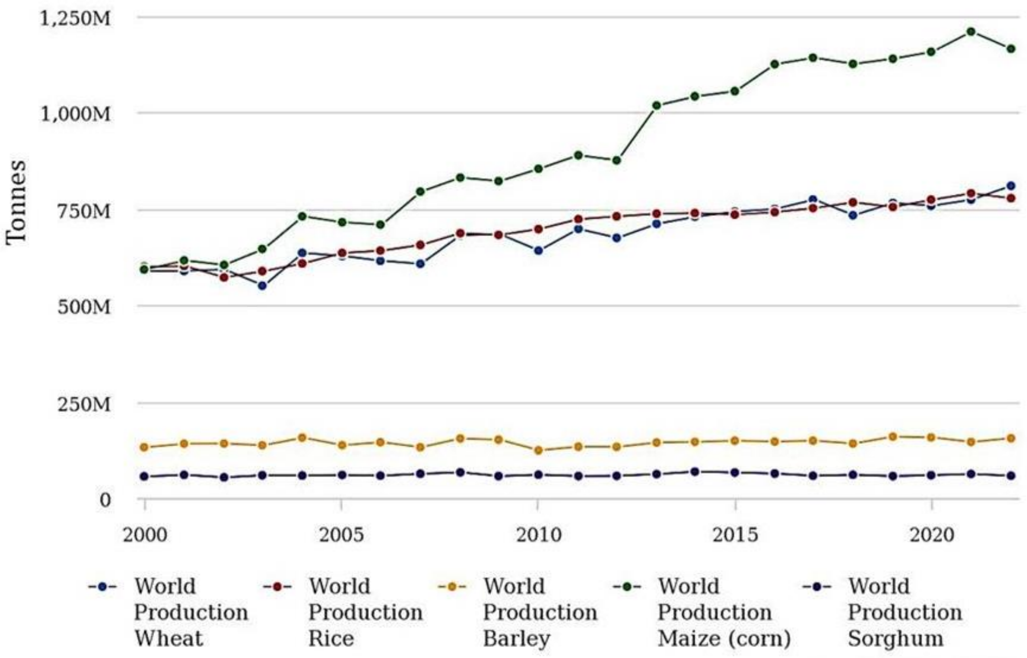

Figure 1.1: World cereal production (FAOSTAT, 2023).

Globally, the largest wheat-producing countries are China, India, and the Russian Federation (FAOSTAT, 2023). However, in the African continent, the most wheat-producing countries are Egypt and Ethiopia, followed by Algeria, Morocco, and South Africa. Furthermore, in South Africa, wheat is the second most grown cereal crop after maize, with an annual production of two million tonnes (FAOSTAT, 2023).

Wheat is primarily grown for human consumption, animal feed, and other uses including industrial biofuels (Khadka *et al*., 2020; Iqbal *et al*., 2022). Approximately 35% of the world's population relies on wheat as a staple food (Grote *et al*., 2021). It is predicted that the demand for wheat as a food item could increase twice as much as that for animal feed, particularly in Asian countries due to the increase in the world population (OECD-FAO, 2022). Wheat can be grown during the winter and summer seasons, and cultivars can be classified according to the growing seasons (Tadesse *et al*., 2019; de Sousa *et al*., 2021).

1.2 Effects of drought stress on crop yield and production

Abiotic stresses such as high salinity, extreme temperatures and drought stress have a negative impact on crop growth and yield (Athar *et al*., 2009; Fahad *et al*., 2017). However, drought remains the most significant constraint on crop productivity globally (Seleiman *et al*., 2021). Similar to crops such as maize and rice (*Oryza sativa*), wheat productivity is significantly affected by the harsh effects of drought stress (Ahmad *et al*., 2018; Bapela *et al*., 2022). Drought stress affects wheat growth throughout its developmental stages, with flowering and grain-filling stages being the most affected (Farooq *et al*., 2014; Sarto *et al*., 2017). Plants utilise a variety of physiological, biochemical and molecular responses to maintain growth and development during periods of limited water supply (Farooq *et al*., 2009; Sallam *et al*., 2019). Nevertheless, the response mechanisms may differ depending on the plant species or genotypes and the duration and intensity of the stress (Bray, 1997; Anjum *et al*., 2011; Moloi and Ngara, 2023). Studying drought responses in different genotypes or plant species can reveal distinct traits that enhance drought tolerance, which can be utilised to develop more resilient crops.

1.3 Problem statement

One of the primary goals of plant breeding programs is to enhance the stress tolerance of plant cultivars, however, breeding crops to withstand drought presents several challenges. Bapela and co-authors (2022) reviewed some of these challenges in wheat, which include limited research efforts that identify root and agro-physiological traits in selecting and improving wheat drought tolerance. Another notable challenge is identifying genes associated with drought stress tolerance and their expression as well as bridging the gap between research and applied crop breeding (Bapela *et al*., 2022). Plant breeders use a variety of ways to improve wheat drought tolerance, including physio-morphological trait-based approaches and genomics-assisted methodologies (Mwadzingeni *et al*., 2016; Khadka *et al*., 2020). Despite continuous efforts to enhance wheat drought stress tolerance, climatic models predict that the frequency and intensity of heat waves and drought episodes will increase due to climate change (IPCC, 2023). This will further negatively affect the yield and production of wheat, ultimately affecting global food security (Mbow *et al*., 2019).

The world population is currently at around 8.09 billion and is predicted to reach 9.7 billion by the year 2050, with a significant population growth expected in African countries (FAOSTAT, 2023). This growth in the global population will increase the demand for food by 2050, and it is predicted that the demand for wheat could increase by 60% worldwide (Tadesse *et al*., 2019; Bapela *et al*., 2022). Therefore, there is a greater need to develop high-yielding crops with increased water use efficiency as a strategy to increase food production under the changing climate. Working towards this goal requires more research efforts to gain insights into plant stress response mechanisms that plant breeders could employ to develop drought-tolerant crops. Therefore, integrating plant physiology with omics approaches such as transcriptomics, proteomics, and metabolomics is vital in unravelling plant responses to drought stress (Ghatak *et al*., 2017; Ngara *et al*., 2021; Singh *et al*., 2022; Zargar *et al*., 2022).

1.4 Research aim and objectives

This study aimed to comparatively analyse the morphological, physiological, biochemical, and molecular changes of two wheat varieties under drought stress conditions. The wheat varieties used were BW4074 (drought-susceptible) and BW35695 (drought-tolerant).

The objectives were to:

I. Evaluate the morphological, physiological and biochemical changes in the two contrasting wheat varieties in response to drought stress at seedling growth stages,

II. Perform a comparative leaf proteomic analysis on control and drought-stressed plants of the two wheat varieties using isobaric tag for relative and absolute quantitation (iTRAQ), and

III. Validate the expression of drought-responsive gene targets using quantitative real-time polymerase chain reaction.

1.5 Thesis outline

A brief outline of the thesis is provided below

Chapter 1: This chapter introduces wheat and the effects of drought stress on crop yield and production, as well as the aim and objectives of the study.

Chapter 2: This chapter is the literature review of the study.

Chapter 3: This experimental chapter compares the physiology and biochemistry of the two contrasting wheat varieties under drought stress conditions.

Chapter 4: This experimental chapter comparatively analyses the differential expressions of the leaf proteome in the two wheat varieties after 28 days of drought stress treatment.

Chapter 5: This experimental chapter analyses gene expression levels of the drought-responsive leaf proteins identified in the two wheat varieties

Chapter 6: This chapter presents the general discussion and conclusions of the experimental chapters and recommendations of the study.

CHAPTER 2

LITERATURE REVIEW

2.1 Plant response mechanisms to abiotic stresses

Plants require light, adequate water supply, optimum temperature and mineral nutrients for normal growth and development (Farooq *et al*., 2009; Taiz and Zeiger, 2012). However, during their life cycles, plants often encounter a range of abiotic stresses such as drought, salinity, extreme temperatures, chemical toxicity and nutrient deficiency that negatively affect their growth and development (Wang *et al*., 2003; Mahajan and Tuteja, 2005). In some crops, these abiotic stresses may cause extensive yield losses by more than 60% (Kopecká *et al*., 2023), subsequently reducing agricultural productivity (Mittler, 2006). In nature, abiotic stresses are often interconnected, causing general and/or specific effects on plants (Wang *et al.*, 2003). For example, individually, drought reduces plant growth by inducing osmotic stress and interfering with nutrient availability and uptake by roots (Chinnusamy *et al*., 2004; Salehi-Lisar and Bakhshayeshan-Agdam, 2016; Fahad *et al*., 2017). Salinity causes both osmotic stress and ion toxicity (Ashraf and Harris, 2004), while extreme temperatures may induce physiological drought (Duque *et al*., 2013).

Apart from inducing osmotic stress, drought, salinity and extreme temperatures also cause oxidative stress in plants (Choudhury *et al*., 2017). This happens as a result of the excessive production and accumulation of reactive oxygen species (ROS), which damage essential cellular components such as proteins, lipids and DNA (Sharma *et al*., 2012; Choudhury *et al*., 2017; Mittler *et al*., 2022). In addition, some abiotic stresses, such as drought and heat occur simultaneously in nature (Suzuki *et al*., 2014; Lamaoui *et al*., 2018; Zandalinas *et al*., 2018). Some studies have explored the effects of combined heat and drought stress on various crops such as wheat (*Triticum aestivum)* (Wang *et al*., 2010), sorghum (*Sorghum bicolor*) (Machado and Paulsen, 2001), and maize (*Zea mays*) (Hussain *et al*., 2019). These investigations revealed that subjecting crops to multiple stressors simultaneously has a greater detrimental effect on their growth, water relations, and productivity than each of the individual stresses (Machado and Paulsen, 2001; Wang *et al*., 2010; Hussain *et al*., 2019).

A transcriptomic study conducted on tobacco (*Nicotiana tabacum*) plants under a combination of drought and heat shock revealed that the plant's response to the combined stress was different from the responses to the individual stresses (Rizhsky *et al*., 2002). For instance, drought suppressed respiration and photosynthesis in the tobacco plants, while heat shock enhanced respiration but did not significantly alter photosynthesis. However, when the two stress factors were applied in combination, photosynthesis was suppressed and respiration enhanced (Rizhsky *et al*., 2002). In another study, Zhou *et al*. (2017) investigated the combined effect of heat and water scarcity on a common greenhouse tomato (*Solanum lycopersicum* L.) cultivar and two heat-tolerant tomato cultivars. Drought stress alone, or combined drought and heat stress treatments had similar impacts on plant growth and relative water content (RWC) across all the tomato cultivars. When the stresses were combined in the study, the plant responses were controlled by water deficit stress (Zhou *et al*., 2017).

Plants respond to environmental stresses by activating cellular responses through signalling pathways. These pathways transmit information resulting in physiological, molecular, and cellular changes (Knight and Knight, 2001; Mahajan and Tuteja, 2005; Zhu, 2016) as illustrated in Figure 2.1. Some of the cellular responses include the expression of stress-responsive genes and proteins, as well as the production and accumulation of compatible solutes and antioxidants (Vinocur and Altman, 2005). Antioxidants reduce excess levels of ROS to alleviate oxidative damage, while compatible solutes stabilise proteins and cell structures, and maintain cell turgor through osmotic adjustment (Krasensky and Jonak, 2015). Activation of the above-mentioned stress-response mechanisms ultimately re-establishes cellular homeostasis and plant survival (Vinocur and Altman, 2005).

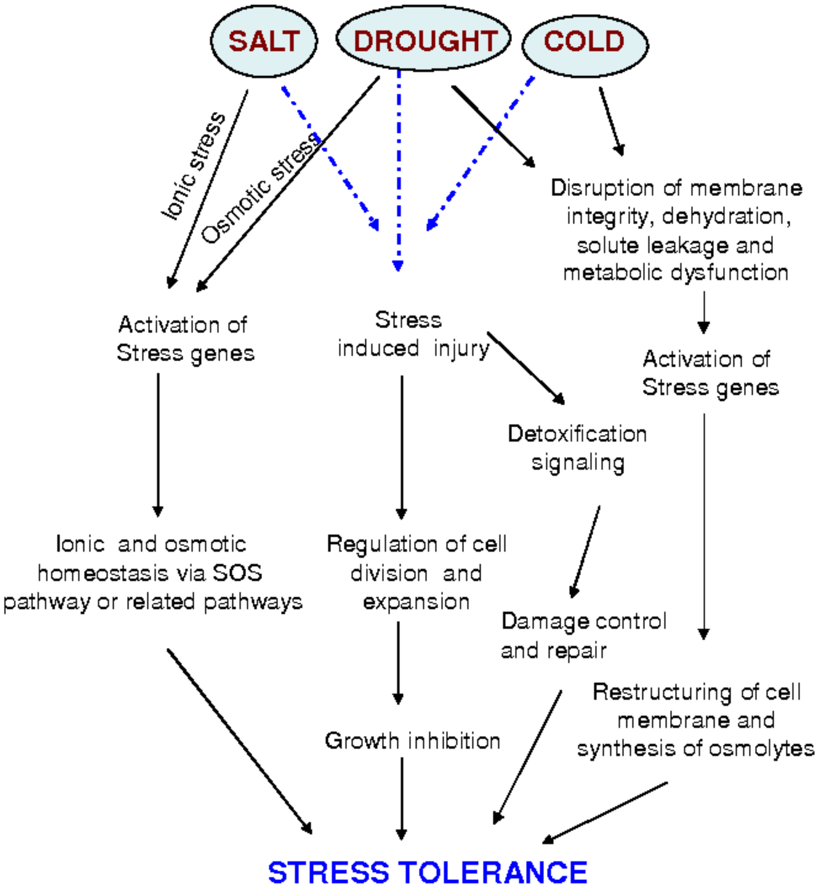

Figure 2.1: Pathways of plant responses to drought, salt and cold stresses. The effects of drought, salinity and cold stresses on plants trigger a range of response mechanisms such as the activation of stress-related genes and the accumulation of osmolytes, and antioxidants resulting in stress tolerance (Mahajan and Tuteja, 2005).

In the context of global warming and climate change (IPCC, 2023), as well as the increasing need for food for the growing population (Mirzabaev *et al.*, 2023), drought remains a major environmental factor affecting agricultural productivity worldwide. Therefore, there is a need to develop more drought-resilient crops to feed the growing world's population (Sugumar *et al*., 2024).

2.2 Drought stress and its effect on plants

Water is an important requirement for plant growth and development (Fang and Xiong, 2015). It is required for maintaining cell turgidity and growth, and for transporting nutrients and organic compounds throughout the plant (Bohnert *et al*., 1995). However, during their life cycles, plants are often faced with periods of water deficits (Chaves *et al*., 2009). In plants, water deficit stress, also referred to as drought stress, occurs when insufficient water supply interferes with the growth and development of plants (da Silva *et al*., 2013; Salehi-Lisar and Bakhshayeshan-Agdam, 2016). This stress also arises when the rate of transpiration exceeds the rate of water absorption by the roots (Bray, 1997; Seleiman *et al*., 2021).

Drought affects various aspects of a plant such as growth, yield, membrane integrity, pigment content, water relations and photosynthesis (Anjum *et al.*, 2011). The extent of such effects, however, depends on the intensity and duration of the stress, plant species, genotypes and developmental stages (Anjum *et al*., 2011; Moloi and Ngara, 2023), and whether the stress occurs simultaneously with other environmental stresses (Suzuki *et al*., 2014; Lamaoui *et al*., 2018). Drought stress inhibits the normal growth of a plant by reducing water uptake into the expanding cell and by altering cell wall properties (Cramer *et al*., 2011). Abid *et al*. (2018) studied the effects of water scarcity on drought-tolerant and drought-sensitive wheat cultivars over 10 days of stress treatment. The wheat plants were exposed to three different water regimes namely well-watered, moderate and severe drought stress, and analysed at the tillering and jointing growth stages. The drought-sensitive cultivar exhibited a significant reduction in plant growth, leaf water relations, membrane stability, and rate of photosynthesis compared to the drought-tolerant cultivar at the jointing stage during severe stress treatment (Abid *et al*., 2018).

In another study, Zeng *et al*. (2019) conducted a comparative proteomic analysis on two maize varieties subjected to 20% polyethylene glycol (PEG)-6000-induced osmotic stress treatment. The drought-sensitive maize variety also showed a substantial reduction in plant growth when compared to the drought-tolerant variety. Fadoul *et al*. (2018) reported that a 7-day drought stress treatment resulted in a significant increase in shoot and root length in the drought-tolerant sorghum genotype compared to the drought-sensitive one. Overall, while water scarcity can negatively affect plant development, the above-mentioned studies highlighted that drought-tolerant cultivars have a greater capacity to adapt to water-deficit conditions than their drought-sensitive counterparts.

Plant growth is controlled by various physiological, biochemical and molecular processes, and photosynthesis contributes substantially to the growth of a plant and its development (Ashraf and Harris, 2013). Nevertheless, like any other metabolic process, photosynthesis is negatively affected by drought (Ashraf and Harris, 2013; Hlahla *et al*., 2022). The process of photosynthesis can be disturbed as a result of a decrease in CO_2 assimilation due to diffusion limitations through the stomata (Chaves *et al*., 2009; Ashraf and Harris, 2013), or by a decrease in leaf expansion and the impairment of photosynthetic machinery due to osmotic and oxidative stress damage (Farooq *et al*., 2009). A decrease in the rate of photosynthesis was observed in drought-tolerant and sensitive wheat plants following water limitation as a result of decreased CO_2 assimilation (Abid *et al*., 2018). The reduction in CO_2 assimilation in plants under drought stress also leads to increased accumulation of ROS, which causes oxidative damage and subsequently affects plant growth (Ashraf, 2009; Laxa *et al*., 2019). These osmotic and oxidative effects of drought on plants trigger a variety of response mechanisms by the plants (Anjum *et al*., 2011).

2.3 Plant responses to drought stress

Plants have evolved a range of strategies to adapt to water deficit stress (Bartels and Sunkar, 2005). These adaptive strategies may be influenced by a variety factors such as the plant species, genotypes, growth stages, the degree and duration of drought stress, and whether the drought stress occurs simultaneously with other stressors (Bray, 1997; Suzuki *et al*., 2014). The current study focuses on the effects of drought stress on plants when applied individually. Therefore, this literature review mainly focuses on plant responses to drought stress alone.

Drought adaptive mechanisms can be morphological, physiological, biochemical and/or molecular in nature (Xiong and Zhu, 2002; Anjum *et al*., 2011). These mechanisms assist plants in sensing and responding to the stress, and in minimizing cellular damage as well as re-programming metabolic processes to sustain plant growth and developmental processes (Atkinson and Urwin, 2012). As such, some plants can escape, avoid or tolerate the effects of drought stress (Osmolovskaya *et al*., 2018; Seleiman *et al*., 2021) as illustrated in Figure 2.2. These response mechanisms are discussed in detail in the following sections.

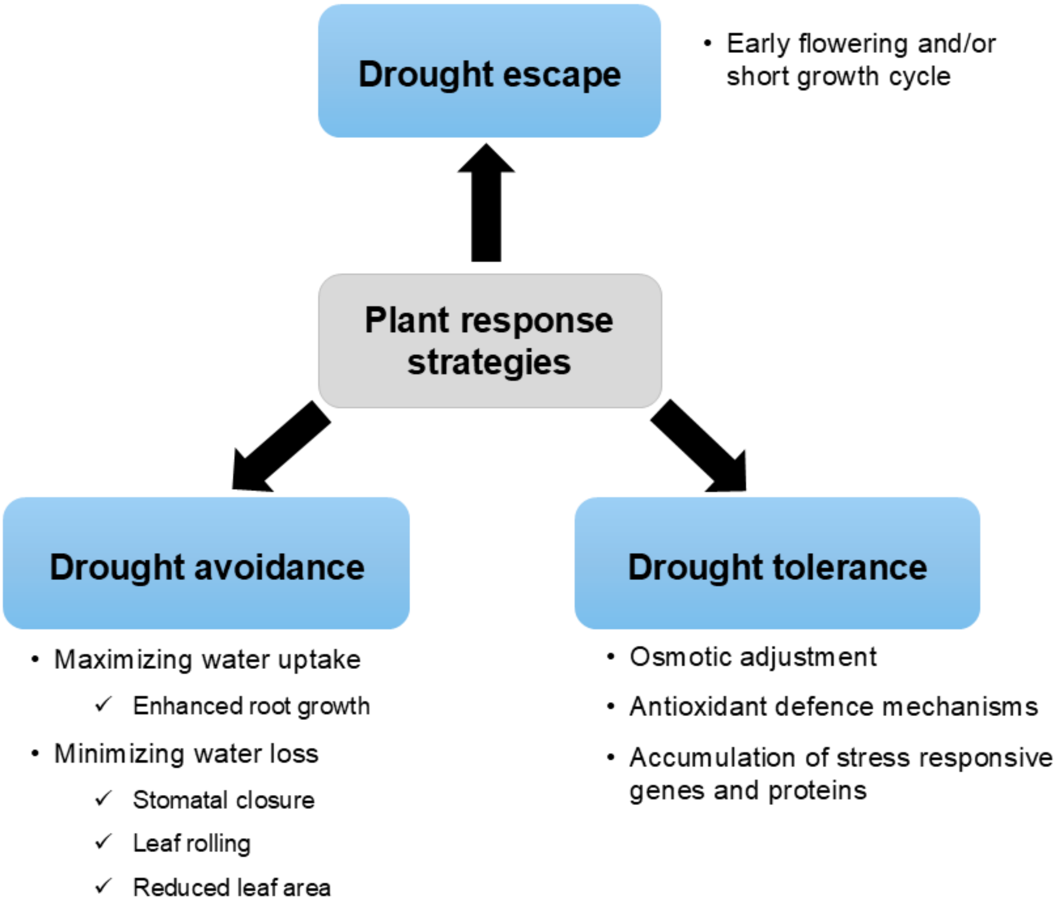

Figure 2.2: Adaptative strategies employed by plants under drought stress conditions (Adapted from Osmolovskaya *et al.*, 2018). Plants can cope with drought stress by flowering early or having a short growth cycle, reducing water loss or increasing water uptake, and activating a range of cellular responses.

2.3.1 Drought escape

Drought-escaping plants complete their life cycles during a short space of time before severe moisture stress occurs (Osmolovskaya *et al.*, 2018; Seleiman *et al.*, 2021). These plants mainly focus on their rapid growth and maturation, rather than investing in resistance mechanisms against drought stress that slows down growth (Verslues and Juenger, 2011). Drought escape is common in desert plants, such as ephemerals, which have a short life cycle and can produce seeds during the rainy season (Farooq *et al.*, 2009). A study conducted on field mustard

(*Brassica rapa*) plants in response to drought stress revealed that the plants were able to escape drought stress through early flowering (Franks, 2011). Early flowering in wheat (Shavrukov *et al*., 2017) and shorter life cycles of the short-duration sorghum varieties (Reddy *et al*., 2009) have been reported to reduce exposure of plants to drought stress and ultimately lead to increased crop production (Reddy *et al*., 2009; Shavrukov *et al*., 2017). However, in some cases, plants may need to use drought avoidance or tolerance mechanisms to survive periods of water scarcity (Shavrukov *et al*., 2017).

2.3.2 Drought avoidance

Drought avoidance occurs when plants maintain water uptake and reduce the rate of transpiration during periods of water deficits (Osmolovskaya *et al*., 2018; Seleiman *et al*., 2021). Water uptake is maintained through an extensive root system which also allows plants to extract nutrients from deep within the soil (Price *et al*., 2002; Shao *et al*., 2008). In rice (*Oryza sativa*), a deep rooting system is considered to be an important drought-avoidance mechanism (Price *et al*., 2002). Some plants, such as the wild watermelon (*Citrullus lanatus*) increase root growth during the early stages of drought to absorb water (Yoshimura *et al*., 2007). Sorghum also possesses an extensive root system that enables it to draw moisture from the receding water table during periods of water scarcity (Pavli *et al*., 2013). An increase in root and shoot length was observed in a drought-tolerant sorghum genotype after withholding water for 7 days (Fadoul *et al*., 2018). However, the drought-sensitive genotype exhibited a significant reduction in the same parameters (Fadoul *et al*., 2018). These findings suggest that increased root length in the drought-tolerant sorghum line enabled the plants to avoid soil moisture deficit (Fadoul *et al*., 2018).

Plants also utilise several mechanisms to reduce water loss under drought conditions. They close their stomata, roll their leaves, shed older leaves, and increase wax accumulation on leaf surfaces (Taiz and Zeiger, 2012; Fang and Xiong, 2015). Leaf rolling was reported as a sign of drought stress in a maize Korean inbred line, three days after withholding water (Kim *et al*., 2015). The maize plants were subjected to drought stress over 10 days and as the stress treatment progressed, the degree of leaf rolling became more pronounced in the water-deprived plants while in the well-watered plants, the leaf structure remained unchanged. These findings highlight the ability of maize plants to reduce transpiration water loss as the duration of the stress treatment increased (Kim *et al.,* 2015). Leaf senescence was also observed in sorghum as a mechanism to decrease the rate of transpiration (Stout and Simpson, 1978). Plants growing in dry areas also have xeromorphic adaptation traits such as smaller and thicker leaves, more epidermal trichomes, sunken stomata, and thicker cuticles which reduce transpiration (Fang and Xiong, 2015; Basu *et al*., 2016).

2.3.3 Drought tolerance

Drought tolerance occurs when plants sustain physiological activities during water deficit stress through the regulation of genes and metabolic activities (Farooq *et al*., 2009; Fang and Xiong, 2015). Some of the drought tolerance mechanisms of plants including osmotic adjustment, antioxidant defence mechanisms, and the expression of stress-related genes, proteins and metabolites are discussed below.

2.3.3.1 Osmotic adjustment

Osmotic adjustment is defined as the reduction of the osmotic potential due to the net accumulation of solutes in response to water deficit (Zhang *et al*., 1999). The maintenance of leaf turgor is essential to improve stomatal conductance for efficient intake of CO_2 (Farooq *et et* *al*., 2009) and enables plants to sustain higher photosynthetic and growth rates (Sanders and Arndt, 2012; Blum, 2017).

Plants accumulate a variety of organic and inorganic solutes in response to drought stress (Sanders and Arndt, 2012; Singh *et al*., 2015). Organic solutes, also referred to as compatible solutes, osmoprotectants or osmolytes, are low molecular weight, highly soluble compounds which are non-toxic even at higher concentrations (Ashraf and Foolad, 2007). These organic solutes include the amino acid proline, quaternary ammonium compounds such as glycine betaine, polyamines, sugars and sugar alcohols (Singh *et al*., 2015). Organic solutes not only protect plants by cellular osmotic adjustment but also through detoxification of ROS, protection of membrane integrity and stabilizing enzymes and other proteins (Ashraf and Foolad, 2007; Ghosh *et al*., 2022). Some of these osmolytes are briefly discussed in the following sections.

2.3.3.1.1 Proline

Proline is one of the most commonly synthesised amino acids in plant species such as wheat, barley (*Hordeum vulgare*), and sugar beet (*Beta vulgaris*) in response to various stress factors including drought (Delauney and Verma, 1993; Ashraf and Foolad, 2007; Ghosh *et al*., 2022). However, in their review, Ngara and Chivasa (2023) reported that proline accumulation does not always increase in all plants under heat or in combination with drought stress. The authors emphasized that the role of proline under drought and heat stress alone or in combination varies depending on the nature of the stress and the plant species (Ngara and Chivasa, 2023).

The current literature review mainly highlights proline accumulation in plants under drought stress. High levels of proline content were observed in the leaves of wheat (Marcek *et al*., 2019), maize (Saad-allah *et al*., 2022), barley (Harb *et al*., 2020), and in the leaves and sheaths of rice (Dien, *et al*., 2019) genotypes under drought stress compared to well-watered conditions. Although proline accumulation increased significantly in these cereal crops, the amount of proline content varied with genotype. Some genotypes had higher proline content compared to others, which could indicate better stress tolerance mechanisms. In a comparative study of two cereals, water deficit stress significantly increased proline content in the roots and leaves of maize and sorghum plants (Ali *et al*., 2023). However, a greater increase in proline content was noted in sorghum in both tissue types than in maize. The increase was more evident in the roots suggesting that sorghum was better able to reduce the water potential, thereby facilitating water uptake compared to maize (Ali *et al*., 2023). Based on the above-mentioned studies, it can be noted that proline accumulation varies among plant species and genotypes under water deficit conditions.

In a study conducted by Abid *et al*. (2018), osmotic adjustment occurred in the leaves of wheat cultivars following drought stress. However, a greater increase was observed in the drought-tolerant wheat cultivar than in the drought-sensitive one. The authors suggested that the increase in osmotic adjustment in both wheat cultivars could be a result of the high accumulation of proline and soluble sugars in the leaves. Proline also acts as a stabilizer of subcellular structures, a scavenger of free radicals, and a stress signalling molecule (Seki *et al*., 2007; Szabados and Savoure, 2010). Zeng *et al*. (2019) comparatively analysed the physiological and biochemical aspects in the roots of drought-sensitive and drought-tolerant maize varieties exposed to 20% PEG-6000-induced osmotic stress. Maize roots exhibited high levels of proline; however, the drought-tolerant variety maintained higher proline content accompanied with lower relative electrolyte leakage and reduced malondialdehyde (MDA) content. This possibly suggests that the drought-tolerant maize variety was able to stabilize cell membranes in the roots and reduce oxidative damage more effectively than the sensitive variety under drought (Zeng *et al*., 2019). In another study, proline accumulation in drought-stressed rice leaves was associated with drought tolerance in the rice cultivars (Pyngrope *et al*., 2013). However, the drought-tolerant rice cultivar exhibited higher amounts of proline content in the leaves compared to the drought-sensitive cultivar (Pyngrope *et al*., 2013).

2.3.3.1.2 Glycine betaine

Apart from proline, another osmolyte known to accumulate in plants is glycine betaine (Ashraf and Foolad, 2007) and has been reported in plants such as sorghum (Ogbaga *et al*., 2014; Goche *et al*., 2020), maize (Saad-allah *et al*., 2022), and wheat (Wang *et al*., 2010) under drought stress. Glycine betaine plays a role in osmotic adjustment and protection of the thylakoid membrane against osmotic and oxidative stresses, thus maintaining high photosynthetic efficiency (Ashraf and Foolad, 2007). Goche *et al*. (2020) evaluated glycine betaine content in contrasting sorghum varieties under water deficit conditions. The study revealed that water deficit stress significantly increased glycine betaine content in the leaves and roots of the two sorghum varieties. Furthermore, the results showed a higher accumulation of glycine betaine in the roots of the sorghum varieties than in leaves, with the drought-tolerant variety exhibiting the highest glycine betaine content than the drought-susceptible variety (Goche *et al*., 2020).

Prajapat and co-workers (2018) also evaluated the accumulation of glycine betaine in cotton (*Gossypium hirsutum* L.) genotypes following drought stress. Both cotton genotypes also exhibited increased levels of glycine betaine in leaves and roots under drought stress conditions. In the study, high levels of glycine betaine were observed in leaves than in roots, with the drought-tolerant genotype also having a higher content than the drought-susceptible genotype (Prajapat *et al*., 2018). The increased accumulation of glycine betaine indicates that drought-tolerant cultivars of different plant species can synthesize higher osmolyte content required for osmotic adjustment, thus protecting cellular components under water deficit conditions.

Although glycine betaine may play a role in osmoregulation in plants under drought stress, some plants such as rice, tobacco, and Arabidopsis (*Arabidopsis thaliana*) naturally do not accumulate glycine betaine (Rhodes and Hanson, 1993). Furthermore, glycine betaine synthesis can be significantly low in some plants under stress conditions, therefore, other studies explored its effectiveness in plants during exogenous application. A study conducted by Shehzadi *et al*. (2019) found that foliar application of 100 mM glycine betaine on oat (*Avena sativa* L.) cultivars subjected to drought stress resulted in increased endogenous levels of glycine betaine and proline in the leaves. Administering exogenous glycine betaine on the oat plants also led to a reduction in H_2O_2 levels and enhanced the activity of superoxide dismutase in the leaves of both cultivars and maintained the redox balance. However, no significant differences were observed in the accumulation of the antioxidant between the two oat cultivars (Shehzadi *et al*., 2019). Similar results were observed in drought-stressed maize plants exposed to 3 mM glycine betaine solution (Pei *et al*., 2022) and winter wheat plants exposed to 50 mM (Ahmed *et al*., 2019). In winter wheat, exogenous glycine betaine application resulted in higher RWC, membrane stability, chlorophyll content and gas exchange properties (Ahmed *et al*., 2019). The above-mentioned studies suggest that applying glycine betaine exogenously could be a useful strategy for enhancing the tolerance of plants to drought stress.

2.3.3.1.3 Inorganic solutes

Osmotic adjustment also occurs due to the accumulation of inorganic solutes, such as sodium, potassium and calcium (Chen and Jiang, 2010), which regulates the osmotic potential of the vacuole to maintain turgor pressure (Fang and Xiong, 2015). A study on barley reported that osmotic adjustment in leaves was achieved due to the accumulation of potassium, sodium, soluble sugars and proline in response to drought stress (Mejri *et al*., 2016). Wu *et al*. (2014) also reported that potassium, sodium and soluble sugars were major contributors to osmotic adjustment in shoots of sugar beet cultivars in response to drought stress. These studies highlight the importance of inorganic solutes, sugars and proline in enhancing plant resilience to drought stress.

2.3.3.2 Antioxidant defence mechanisms

Upon exposure to drought, plants also experience oxidative stress (Farooq *et al*., 2009), which results from an imbalance in the production and accumulation of ROS, and the antioxidant defence systems within cell compartments (Apel and Hirt, 2004). These ROS include single oxygen, superoxide anion, hydroxyl radicals and hydrogen peroxide and may damage lipids, proteins and DNA (Apel and Hirt, 2004; Gill and Tuteja, 2010). High accumulation of ROS has been observed in leaves, shoots and roots of crops such as wheat (Huseynova *et al*., 2015; Amoah and Seo, 2021), sorghum (Nxele *et al*., 2017), maize (Chen *et al*., 2016; Zheng *et al*., 2020), rice (Pyngrope *et al*., 2013), and cassava (*Manihot esculenta*) (Zhu *et al*., 2020) in response to drought stress.

Amoah and Seo (2021) conducted a comparative analysis between four wheat genotypes subjected to drought stress treatment for 5, 10 and 15 days. The wheat genotypes used were Geumgangmi, PL 337, PL 371 and PL 257. Upon exposure to drought stress, high levels of H_2O_2 content were observed in leaves of all wheat genotypes as the duration of the stress increased. However, the results showed variations in H_2O_2 content in the leaves of the genotypes, with Geumgangmi having higher levels of H_2O_2, thus exhibiting increased sensitivity to the imposed stress than the other genotypes (Amoah and Seo, 2021). In another comparative study, rice cultivars also showed increased production and accumulation of $O_2^{\cdot -}$ and H_2O_2 in shoots and $HO^{\cdot}$ in both roots and shoots following progressive levels of water deficit stress (Pyngrope *et al*., 2013). In the study, the drought-sensitive rice cultivar exhibited higher ROS accumulation than the tolerant cultivar (Pyngrope *et al*., 2013).

The lipid damage caused by ROS can be observed by high MDA content in the respective plant tissues (Sharma *et al*., 2012). As such, MDA is widely used as a biomarker for lipid peroxidation in plants under stress (Ayala *et al*., 2014). Rezayian *et al*. (2018) investigated the oxidative damage of cell membranes in leaves of canola (*Brassica napus* L.) cultivars under drought stress conditions. The cultivars used, Sagirol and RG00S3 exhibited differences in drought tolerance. Upon exposure to water limitation, an increase in MDA content was observed in both cultivars, however, the level of MDA was lower in RGS003. The authors suggested that the low MDA content in RGS003 might have been a result of higher antioxidant activities and that RGS003 was better able to protect membrane structures than Sarigol under drought (Rezayian *et al*., 2018). In another comparative study, two soybean (*Glycine max*) varieties were subjected to 5, 10 and 20% PEG-6000-induced osmotic stress in a time-course experiment for 7 days (Zhou *et al*., 2022). The results indicated a gradual increase in MDA content in both soybean varieties as the intensity and duration of the stress progressed. However, the level of MDA was significantly lower in the drought-resistant variety compared to the drought-sensitive variety, possibly due to the observed higher total antioxidant capacity in the drought-resistant variety (Zhou *et al*., 2022). Overall, these studies highlight that the effects of drought-induced oxidative stress were more prominent in the sensitive cultivars than the tolerant ones.

To minimise the damage caused by ROS, plants use a wide range of enzymatic and non-enzymatic antioxidants (Bhatnagar-Mathur *et al*., 2008). The enzymatic antioxidants include superoxide dismutase, catalase, ascorbate peroxidase, glutathione peroxidase, monodehydroascorbate reductase, dehydroascorbate reductase and glutathione reductase, while non-enzymatic antioxidants include ascorbate, glutathione, carotenoids and tocopherols (Gill and Tuteja, 2010; Dumanović *et al*., 2021). The degree to which enzymatic antioxidant activities increase under drought stress conditions varies between plant species, cultivars, and on the severity and duration of the stress (Reddy *et al*., 2004; Tardieu *et al*., 2018).

Abid *et al*. (2018) reported that the drought-sensitive wheat cultivar exhibited a lower capacity to increase and maintain antioxidant enzyme activity in leaves under drought stress compared to the drought-tolerant wheat cultivar. Conversely, the drought-tolerant cultivar exhibited higher enzyme activities of superoxide dismutase, catalase and ascorbate peroxidase in response to the drought stress . The authors suggested that the tolerant cultivar’s ability to activate antioxidant mechanisms reduced drought-induced oxidative damage in leaves and enhanced drought tolerance (Abid *et al*., 2018). Another comparative study reported that the activities of superoxide dismutase significantly increased in the leaves of a drought-tolerant soybean variety when subjected to gradual water limitation, resulting in reduced formation of MDA (Xu *et al*., 2023).

2.3.3.3 Abscisic acid and drought stress-related genes

During drought stress conditions, plants produce abscisic acid (ABA), a stress hormone that plays a key role in the activation of stress-responsive genes and other physiological responses (Agarwal and Jha, 2010; Todaka and Takahashi, 2019). Briefly, the pyrabactin resistance/like/regulatory components of ABA receptors (PYR/PYL/RCAR) bind to ABA and inhibit type 2 protein phosphatases (PP2C), thus triggering the activation of sucrose nonfermenting-1-related protein kinases (SnRKs) which activates downstream transcription factors to induces ABA responses (Danquah *et al*., 2014; Takahashi *et al*., 2018; Yao *et al*., 2021). However, some genes are expressed through an ABA-independent signalling pathway (Yoshida *et al*., 2014; Yao *et al*., 2021) as illustrated in Figure 2.3. In the ABA-independent pathway, dehydration-responsive element (DRE)-binding Protein 2A (DREB2A) binds to the DRE to activate stress-responsive gene expression (Agarwal and Jha, 2010).

The stress-responsive genes are categorized into two groups based on their product functions. The first category includes proteins that regulate signal transduction and gene expression (Shinozaki and Yamaguchi-Shinozaki, 2007). These proteins include various transcription factors, protein kinases, protein phosphatases, enzymes involved in phospholipid metabolism, and other signalling molecules such as calmodulin-binding proteins (Shinozaki and Yamaguchi-Shinozaki, 2007; Kumar *et al.*, 2018). Transcription factors are regulatory proteins that modulate the expression of specific genes (Singh and Laxmi, 2015). Examples of transcription factors include the ABA-responsive element (ABRE), ABRE-binding protein (AREB), C-repeat-binding factor (CBF), dehydration-responsive element (DRE), DRE-binding protein (DREB), and early responsive to dehydration (ERD) (Agarwal and Jha, 2010).

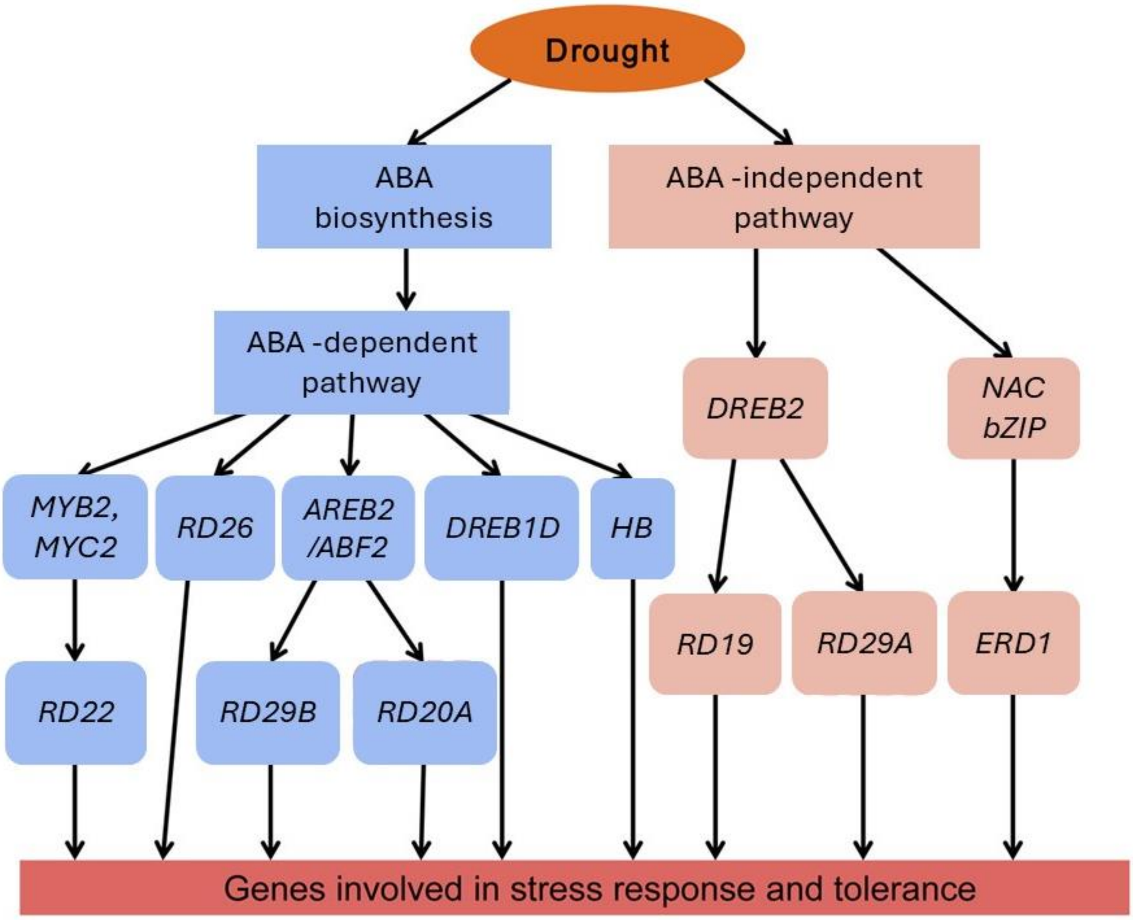

Figure 2.3: Transcriptional regulatory networks in response to drought stress through ABA-dependent and ABA-independent pathways. Components in the blue blocks represents the ABA-dependent pathway whereas, those in the pink blocks represents the ABA-independent pathway. ABA signalling and ABA-independent signalling pathways triggers various transcription factors including ABRE-binding protein (AREB), ABRE binding factor (ABF), myelocytomatosis (MYC), myeloblastosis (MYB), dehydration-responsive element binding genes (DREBs), and basic leucine zip- per (bZIP). These transcription factors regulate gene expression process involved in plant growth, metabolism, and stress responses. Stress inducible genes in these pathways include a responsive to dehydration (RD) gene and an early responsive to dehydration 1(ERD1) gene (adapted from Huang *et al*., 2021).

The second group of gene products includes proteins that function in stress response, and include late embryogenesis-abundant (LEA) proteins, enzymes for osmolyte biosynthesis, ROS detoxification enzymes, ubiquitination-related enzymes and proteases (Shinozaki and Yamaguchi-Shinozaki, 2007). Guo *et al*. (2009), conducted a transcriptomic analysis on leaves of a drought-sensitive (Moroc9-75) and two drought-tolerant (Martin and HS41-1) barley genotypes after a 13-day drought stress treatment. The study used microarray and quantitative real-time polymerase chain reaction (qRT-PCR) to identify genes that were differentially expressed in the three genotypes in response to drought. The results of the study revealed distinct gene expression patterns in these three genotypes, with Martin and HS41-1 having 144 and 66 differentially expressed genes respectively, whereas Moroc9-75 had 53. Moreover, the two drought-tolerant genotypes had 17 genes with similar expression patterns. These 17 genes encoded proteins that improve drought tolerance by regulating stomatal closure, ROS detoxification, osmotic adjustment, and membrane and protein stabilization under drought stress. The findings suggest that the two drought-tolerant barley genotypes, were able to protect their cellular components under drought stress better than the drought-sensitive genotype (Guo *et al*., 2009).

In another transcriptome study, Zheng *et al*. (2020) investigated gene expression patterns in the roots of two inbred maize lines of using qRT-PCR and Illumina RNA sequencing technologies. Plants of both maize lines were subjected to drought stress for 24, 48, and 72 hours. The results of the study indicated that at all three time points, the drought-tolerant genotype had more differentially expressed genes (DEGs) than the sensitive genotype. The authors hypothesized that the higher number of DEGs at the 72-hour time point indicated that the long-term stress treatment had triggered internal mechanisms to cope with water scarcity. The identified DEGs at 72 hours were involved in ROS scavenging processes, as well as metabolism of secondary compounds, fatty acid and hormones (Zheng *et al*., 2020). Similar drought transcriptomic studies have also been extensively reviewed by Ngara *et al*. (2021), highlighting differential gene expression patterns between sorghum varieties with contrasting drought phenotypes.

Apart from ABA signalling pathways, there are other chemical signalling molecules that activate stress-responsive networks under stress conditions. These include ROS (Mittler *et al*., 2022), calcium (Ca^{2+}) (Knight and Knight, 2001), nitric oxide (Lau *et al*., 2021), Ca^{2+} regulated proteins and mitogen-activated protein kinase (MAPK) cascades (Danquah *et al*., 2014), which have been extensively reviewed elsewhere (Knight and Knight, 2001; Danquah *et al*., 2014; Lau *et al*., 2021; Mittler *et al*., 2022) and will not be discussed in this literature review. An in-depth analysis of these diverse signalling pathways and their effects in plants requires a systems biology approach that relies on cutting-edge techniques such as genomics, transcriptomics, proteomics, and metabolomics (Cramer *et al*., 2011; Jogaiah *et al*., 2013; Thanmalagan *et al*., 2022; Zargar *et al*., 2022). These omics technologies provide a comprehensive understanding of the molecular mechanisms that occur during drought stress and will be instrumental in the development of plants that can thrive in adverse conditions (Ngara *et al*., 2021; Zargar *et al*., 2022). Various omics studies continue to broaden our understanding of adaptive responses in diverse crops under water deficit conditions (Ngara *et al*., 2021; Rakkammal *et al*., 2022; Thanmalagan *et al*., 2022; Zargar *et al*., 2022). The current study mainly utilised a proteomics approach to investigate the differential protein expression patterns in the leaves of two wheat varieties with contrasting drought phenotypes under drought stress.

2.4 Proteomics

Proteomics is a large-scale analysis of proteins within an organism, tissue or cell (Kellner, 2000; Graves and Haystead, 2002). Qualitative and quantitative protein expressions can be analysed through a variety of approaches, from gel-based to non-gel-based methods (Chen and Harmon, 2006; Zargar *et al*., 2016; Tan *et al*., 2017), which are briefly discussed below.

2.4.1 Gel-based proteomic methods

Gel-based proteomic approaches involve protein separation through gel electrophoresis and protein identification by mass spectrometry (MS) (Kellner, 2000; Zargar *et al*., 2016; Tan *et al*., 2017). This approach includes one and two dimensional sodium dodecyl-polyacrylamide gel electrophoresis (1D and 2D SDS-PAGE), as well as two-dimensional differential gel electrophoresis (2D-DIGE) (Kellner, 2000). In one dimensional gel electrophoresis, proteins are separated solely based on their molecular weight (Abdallah *et al*., 2012). However, this approach faces challenges when identifying individual proteins in complex mixtures as proteins of the same mass are recognized at the same spot on the gel, resulting in a mixed signal (Owen *et al*., 2014).

To overcome limitations of the 1D gel electrophoresis, the 2D SDS–PAGE method is used (Wu *et al*., 2006). This method separates proteins using a two-step process, firstly, based on charge using isoelectric focusing, and then by molecular weight using SDS-PAGE (Chandramouli and Qian, 2009; Magdeldin *et al*., 2014; Lilley and Dupree, 2018). Two-dimensional gel electrophoresis allows thousands of proteins to be separated in a single gel (Magdeldin *et al*., 2014; Lilley and Dupree, 2018). After gel electrophoresis, stains such as coomassie brilliant blue, silver stain or fluorescent dyes are used to detect the separated proteins (Steinberg, 2009). Protein spots of interest are then excised from the gel and subjected to in-gel digestion using trypsin (Magdeldin *et al*., 2014). The resulting peptide fragments are then analysed using MS (Hurkman and Tanaka, 2007; Magdeldin *et al*., 2014; Zargar *et al*., 2016).

A combination of 2D SDS–PAGE and MS analysis has been widely used to identify numerous differentially expressed proteins in leaf and root tissues of crops such as wheat (Faghani *et al*., 2015; Michaletti *et al*., 2018; Moosavi *et al*., 2020), rice (Ali and Komatsu, 2006), soybean

(Xu *et al*., 2006; Alam *et al*., 2010), barley (Kausar *et al*., 2013; Chmielewska *et al*., 2016), maize (Kim *et al*., 2015; Li *et al*., 2019), sugar beet (Wang *et al*., 2017), and sorghum (Li e*t al*., 2020) under drought stress conditions. However, 2D SDS-PAGE has its own limitations, for instance, 2D gel electrophoresis is limited in its ability to separate proteins with extreme isoelectric points and/or molecular weights, hydrophobic membrane proteins and low abundant proteins (Oeljeklaus *et al*., 2009; Magdeldin *et al*., 2014). Moreover, 2D gels are at times non-reproducible due to gel-to-gel variation between experiments (Oeljeklaus *et al*., 2009; Magdeldin *et al*., 2014; Lilley and Dupree, 2018).

Some of these drawbacks such as gel-to-gel variations can be overcome by using a modified version of 2D gel electrophoresis called 2D-DIGE (Zargar *et al*., 2016). With 2D-DIGE, two or three protein samples can be separated on the same gel after labelling the protein samples with distinct cyanaine-based fluorescent dyes called Cy2, Cy3, and Cy5. These dyes are spectrally distinct but matched for charge and mass, which makes them ideal for comparative analysis (Monteoliva and Albar, 2004; García-Descalzo *et al*., 2012). By labelling the samples in this way, differences in protein abundance between the samples can be analysed with better accuracy in a single gel thus minimizing variability between the gels (Monteoliva and Albar, 2004; Wu *et al*., 2006; García-Descalzo *et al*., 2012). Some proteomic studies in barley (Ashoub *et al*., 2013) and sorghum (Jedmowski *et al*., 2014) exposed to drought stress have used 2D-DIGE for the separation of proteins prior to MS analysis.

Figure 2.4 illustrates an overview of the 2D-DIGE proteomic method from sample processing to protein identification by mass spectrometry. Briefly, in workflow A (Figure 2.4), two protein samples are labelled with fluorescent dyes, Cy3 or Cy5, then pooled and electrophoresed on a single 2D gel. The protein spot patterns are shown by illuminating the gel alternately with Cy3 and Cy5 excitation wavelengths. Thereafter, a software is used to analyse the 2D images and finally the differentially expressed protein spots are excised and identified by mass spectrometry.

In workflow B (Figure 2.4), the two protein samples are also labelled with either Cy3 or Cy5 and a pooled internal standard is labelled with Cy2. The pooled internal standard contains equal amounts of the two samples. Thereafter, the three protein samples are pooled and electrophoresed on a single 2D gel. The protein spot patterns are viewed by illuminating the gel alternately with Cy3, Cy2 and Cy5 excitation wavelengths. The 2D gel are then analysed using a software and the internal standard is used for normalization, prior to spot excision and then MS identification .

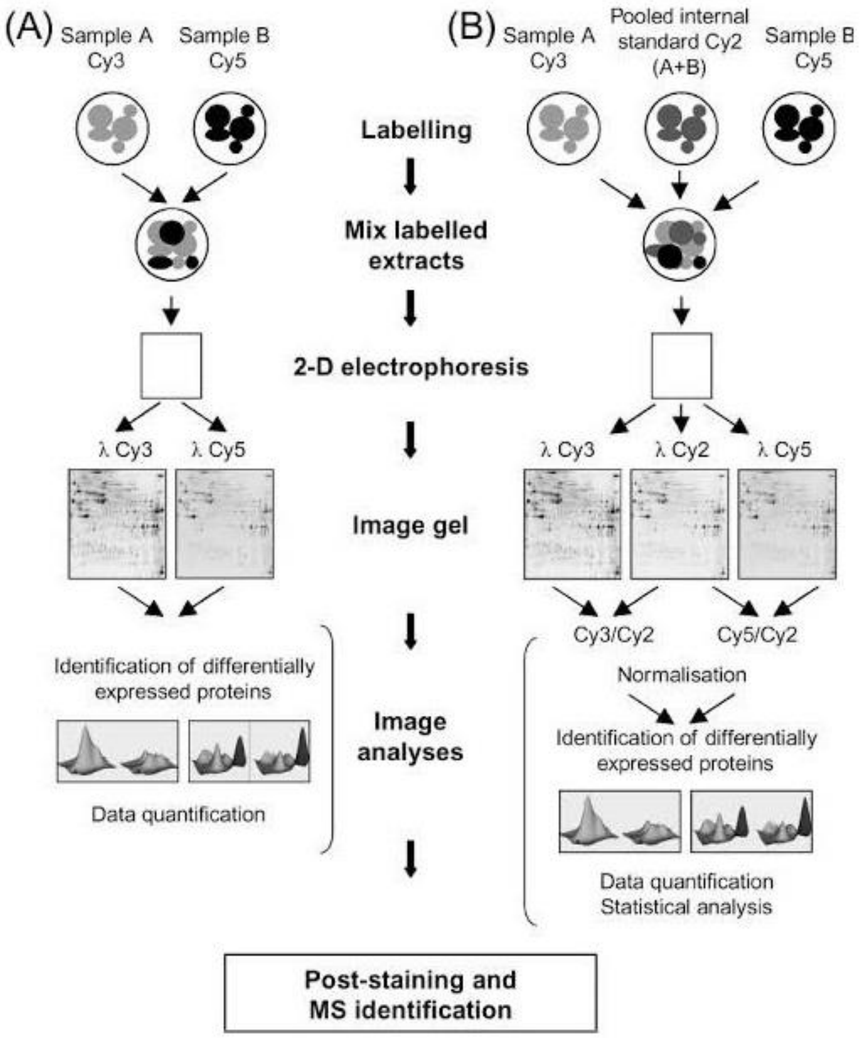

Figure 2.4: A schematic overview of the 2D-DIGE proteomic method. (A) shows workflow of labelling protein samples with Cy3 and Cy5 dyes while (B) shows workflow of labelling protein samples with Cy3, Cy5 dyes and a pooled internal standard Cy2 dye. The samples are pooled and resolved on a 2D gel. The gels are subsequently stained and imaged and finally proteins are identified using mass spectrometry (Monteoliva and Albar, 2004).

Despite the ability of 2D-DIGE to reduce certain 2D gel-based limitations in protein separation, some of the membrane proteins tend to precipitate during isoelectric focusing which then requires the use of non-gel based methods (Lilley and Dupree, 2018).

2.4.2 Gel-free proteomic approaches

Gel-free proteomic techniques involve the separation of proteins using liquid chromatography (LC) coupled with protein identification by MS (Abreu *et al*., 2013) and are classified as label-based or label-free methods (Zargar *et al.*, 2016). Label-free methods use multi-dimensional capillary LC coupled with electrospray ionisation (ESI) tandem MS for the separation and identification of peptides (Tan *et al*., 2017). On the other hand, label-based methods involve chemical or metabolic labelling of proteins or peptides (Zargar *et al*., 2016). Chemical labelling techniques include isotope-coded affinity tag (ICAT), isotope-coded protein labelling (ICPL), tandem mass tags (TMT), and isobaric tag for relative absolute quantitation (iTRAQ). The metabolic labelling techniques include stable isotopic labelling with amino acids in cell culture (SILAC) and culture-derived isotope tags (CDITs) (Abdallah *et al*., 2012; Aslam *et al*., 2017).

Briefly, in the isotope-coded affinity tag method, proteins are labelled with either the light or heavy version of the ICAT reagent, pooled, and then subjected to proteolytic digestion. The resulting peptides are isolated using avidin affinity chromatography and analysed using multidimensional liquid chromatography with MS/MS (Abdallah *et al*., 2012). Another similar method is the ICPL, which is a modified form of ICAT (Zargar *et al*., 2016). The ICPL method uses the N-hydroxysuccinimide (NHS) chemistry to label amino groups and lysine in proteins or peptides. This method also involves a post-digest ICPL technique to label peptides after digestion. The labelled peptides are then separated and analysed using MS for protein identification and quantification (Abdallah *et al*., 2012; Zargar *et al*., 2016). While the above-mentioned methods use isotopic labelling, TMT and iTRAQ use isobaric tags to label peptides. The iTRAQ method labels peptides with either 8-plex or 4-plex isobaric tags at their N-terminus and side chain amine groups, then mixed and digested before being separated through high-performance liquid chromatography, and analysed using MS (Zargar *et al*., 2016, Aslam *et al*., 2017; Chen *et al*., 2021). Tandem mass tags also label peptides similar to the iTRAQ method, however, it has a higher multiplexing capability of up to 16 samples (Chen *et al*., 2021).

For the *in vivo* SILAC metabolic labelling method, cell samples are specifically cultured using a stable isotopically tagged amino acid. Once cultivated, these samples are combined prior to protein extraction to minimize technical variation, lysed, digested then separated via chromatographic fractionation and analysed using MS/MS (Abdallah *et al*., 2012). These gel-free methods have been reported to overcome some drawbacks of the gel-based methods, however, they also have some limitations of their own which have been extensively reviewed (Abdallah *et al*., 2012; Zargar *et al*., 2016; Aslam *et al*., 2017; Chen *et al*., 2021; Sivanich *et al*., 2022). Among the gel-free methods, isobaric tag labelling methods offer more advantages through multiplexing, which greatly increases sample throughput and quantitative accuracy (Chen *et al*., 2021; Sivanich *et al*., 2022). The current study utilised the iTRAQ method to quantify drought-responsive leaf proteins of two wheat varieties with contrasting drought phenotypes and this method is briefly discussed in the next section.

2.4.2.1 The iTRAQ method

The iTRAQ method is a mass spectrometry-based quantitative technique in which different protein samples can be quantified simultaneously (Zargar *et al*., 2016; Aslam *et al*., 2017; Chen *et al*., 2021). Figure 2.5 below illustrates an iTRAQ workflow where samples are extracted, digested with trypsin and labelled with different isobaric tags. The protein samples are then mixed, separated by liquid chromatography and identified by MS. Thereafter, the relative quantification of proteins is conducted by comparing the intensities of ions observed on the mass spectra (Aggarwal and Yadav, 2016).

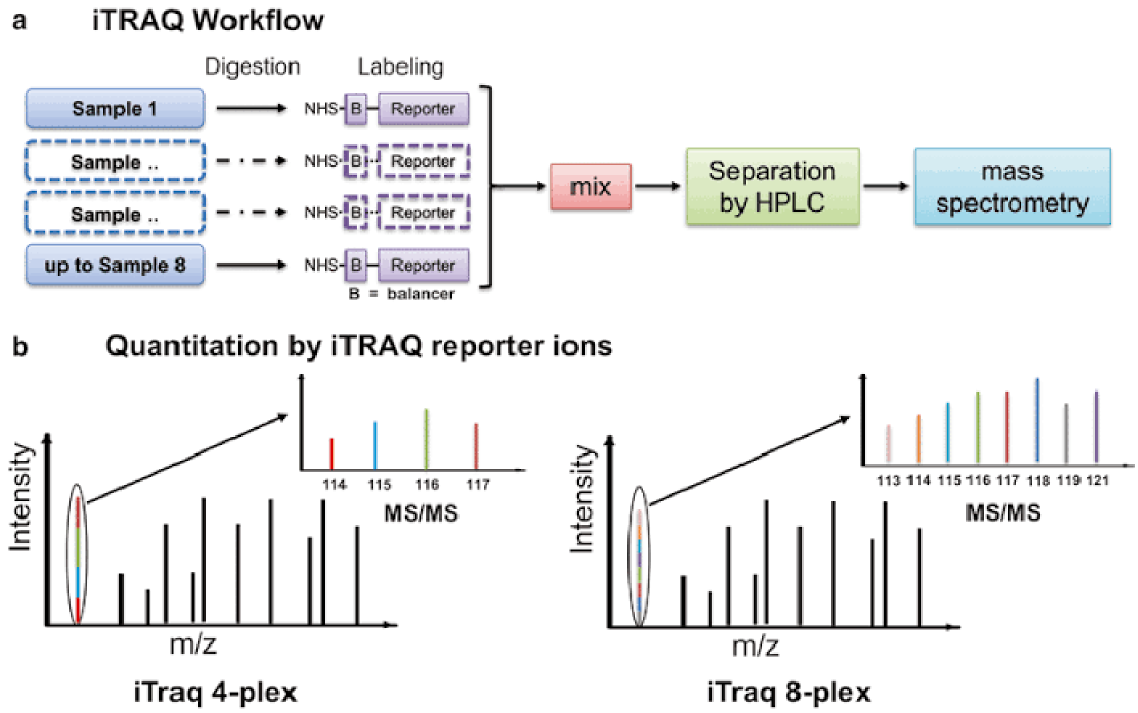

Figure 2.5: A schematic summary of the iTRAQ method. (A) shows protein samples being isolated, digested and the peptides are modified using an N-hydroxysuccinimide (NHS) ester derivative. The modified peptides are then labelled using 4 or 8-plex iTRAQ tags, separated by high-performance liquid chromatography (HPLC) and identified by mass spectrometry. (B) shows the reporter ions of differential masses being released from peptide during tandem mass spectrometry (MS/MS) to give sample-specific quantitation of a particular peptide (Aggarwal and Yadav, 2016).

The iTRAQ method is highly sensitive and identifies a range of proteins such as those with high molecular weight, those that are too acidic or basic and low abundant proteins, which can be problematic for 2D gel electrophoresis (Sur, 2013). The iTRAQ method has been used to comparatively analyse protein changes between varieties with contrasting drought phenotypes in crops such as wheat (Ford *et al*., 2011), maize (Zeng *et al*., 2019; Li *et al*., 2021), soybean (Ji *et al*., 2016), and sorghum (Goche *et al*., 2020). However, the proteomic approach is generally more expensive compared to other proteomic techniques which limits its application in most quantitative proteomic studies (Bowser and Robinson, 2023). Nevertheless, the use of this isobaric-based technique has contributed substantially towards our knowledge on molecular responses of plants to drought including those of agriculturally important cereals.

2.5 Cereal proteomics under drought stress

Cereal proteomics studies continue to provide insights into the molecular mechanisms of plant responses to drought stress (Barkla, 2016; Ghatak *et al*., 2017). Ghatak *et al*. (2017) reviewed leaf and root proteomic studies of cereals such as wheat, rice, maize, barley, pear millet (*Pennisetum glaucum*) and sorghum, and provided a comprehensive and comparative overview of proteome changes observed in these crops in response to drought stress. The authors reported that there are variations in protein changes observed between the control and stressed plants, cultivars and plant species in response to drought. The review also highlighted that comparative proteomic analyses between genotypes under drought stress is important in generating information of drought response mechanism which can be used in breeding programmes to develop more drought tolerant crops (Ghatak *et al*., 2017).

Goche *et al*. (2020) conducted a comparative proteomic analysis on the root tissue of two sorghum genotypes with contrasting phenotypes. Sorghum plants were grown on potting soil for 21 days and water was withheld for 8 days. Root total soluble proteins were extracted and quantified using the iTRAQ method and MS. The study reported an up-regulation of drought-responsive proteins involved in signal transduction, and defence/detoxification-related proteins, while those involved in metabolic processes were largely downregulated in the two sorghum varieties following water limitation stress. The study also highlighted that the drought-tolerant variety controlled protein degradation by up-regulating protease inhibitors and down-regulating peptidases, while peptidases were upregulated in the susceptible variety (Goche *et al*., 2020). Overall, the study reported contrasting proteome expression patterns between sorghum varieties and that the drought-tolerant variety showed better drought tolerance compared to the drought-susceptible variety by accumulating proteins responsible for regulating protein degradation.

In light of the contrasting proteomic results of proteolysis-related proteins observed in different sorghum varieties by Goche *et al*. (2020), Moloi and Ngara (2023) reviewed the differences in protein expression of proteases and protease inhibitors induced by drought in contrasting varieties of cereals, including sorghum, rice, wheat, and barley. The review revealed that drought-susceptible varieties exhibited increased proteolytic activity, whereas drought-tolerant genotypes expressed more protease inhibitors to protect proteins from degradation. The authors also suggested that the upregulation of protease inhibitors in tolerant cultivars could serve as a marker for drought tolerance in some cereals. However, further studies are needed to further explore the roles of protein degradation under drought stress (Moloi and Ngara, 2023).

Li *et al*. (2021) also conducted an iTRAQ-based proteomic comparison of the leaf proteome of two maize varieties with varying levels of drought tolerance. The maize varieties were grown in soil and subjected to a drought stress treatment for 7 days. Based on the physiological data, the drought-tolerant maize variety performed better than the sensitive variety in terms of photochemical efficiency and antioxidant enzyme activity. The authors then analysed the leaf proteome and observed that the upregulated proteins were associated with photosynthesis, antioxidants/detoxifying enzymes, molecular chaperones, and metabolic enzymes in the drought-tolerant maize variety. The study also showed an increase in the accumulation of proteins responsible for repairing photosystem II and photoprotection, which improved the photochemical capacity in the drought-tolerant maize variety. In the drought-sensitive maize variety, molecular chaperones and sucrose production pathways were induced, but they failed to fully protect the damaged photosystem. Overall, the study highlighted the interaction between physiological and molecular mechanisms in maize plants, particularly the tolerant variety, after mild drought stress (Li *et al*., 2021). Furthermore, comparative analyses of diverse plant varieties reviewed in the current study revealed distinct responses to drought stress, highlighting their unique strategies for resilience and adaptability.

CHAPTER 3

COMPARATIVE MORPHO-PHYSIOLOGICAL AND BIOCHEMICAL RESPONSES OF WHEAT VARIETIES TO DROUGHT STRESS

3.1 Introduction

Wheat (*Triticum aestivum*) is a commonly grown cereal crop that is widely used for human consumption (Sarto *et al*., 2017). However, drought stress adversely affects all stages of its development (Farooq *et al*., 2014), posing a threat to food security. Due to the expected increase in the frequency and severity of drought episodes in many parts of the world as a result of climate change (Nelson *et al*., 2009; IPCC, 2023), there is a need to enhance our understanding of plant drought responses. The information obtained will be beneficial to plant breeding initiatives in developing drought-resistant crops capable of withstanding the adverse impacts of drought (Passioura, 2012).

Drought stress limits crop growth and development by negatively affecting various physiological and biochemical processes including photosynthesis, respiration, ion uptake and translocation, and nutrient metabolism (Jaleel *et al*., 2009; Anjum *et al*., 2011). When exposed to limited water supply, plants produce and accumulate abscisic acid (ABA), which leads to stomatal closure and reduced transpiration (Lim *et al*., 2015). A study conducted on wild (*Hordeum spontaneum)* and cultivated (*Hordeum vulgare*) barley genotypes revealed increased levels of ABA under water deficit conditions (Bandurska and Stroiński, 2003). Both genotypes had higher ABA content in the leaves and roots under moderate and severe drought stress compared to their respective controls (Bandurska and Stroiński, 2003). Under moderate conditions, ABA accumulated earlier in the roots of both genotypes than in the leaves. However, under severe stress, ABA accumulated much earlier in the leaves of both genotypes compared to the roots. The early accumulation of ABA in the roots under moderate stress probably served as a stress signal to regulate stomatal behaviour in the leaves. Under severe stress, the wild genotype had significantly higher leaf ABA concentration and lower leaf dehydration than the cultivated genotype. The authors higlighted that increased levels of ABA in the leaves of the wild genotype under severe drought conditions could improve the plant's water retention ability (Bandurska and Stroiński, 2003).

Xu *et al*. (2023) also conducted a comparative study between two soybean (*Glycine max* L.) varieties subjected to gradual water deficit stress. The results revealed that as the duration of the stress increased, the ABA content in the leaves also increased (Xu *et al*., 2023). The drought-tolerant variety also exhibited higher levels of ABA in the leaves compared to the drought-susceptible variety. Additionally, the drought-tolerant variety had reduced stomatal conductance resulting in reduced transpiration, a higher relative water content (RWC) and an enhanced water use efficiency (Xu *et al*., 2023).

Nonetheless, drought-induced stomatal closure can reduce carbon dioxide (CO_2) uptake, affecting photosynthesis (Farooq *et al*., 2009), and cause an increase in the production and accumulation of reactive oxygen species (ROS) (Laxa *et al*., 2019). High levels of ROS such as superoxide anion (O_2^-), hydrogen peroxide (H_2O_2) and singlet oxygen ($^1O_2$) can damage proteins, lipids, and nucleic acids, ultimately leading to plant cell death (Gill and Tuteja, 2010; Sharma *et al*., 2012). The extent of oxidative cell damage in plants can be assessed by measuring the amount of malondialdehyde (MDA), a biomarker of lipid peroxidation (Ayala *et al*., 2014). High MDA content in sorghum (*Sorghum bicolor*) (Nxele *et al*., 2017) and wheat (Naderi *et al*., 2020) has been associated with increased ROS levels during drought stress. Comparative studies conducted on cultivars with contrasting drought phenotypes also revealed that ROS-induced cell damage is more prominent in drought-sensitive genotypes than drought-tolerant ones (Khanna-Chopra and Selote, 2007; Kusvuran and Dasgan, 2017; Naderi *et al*., 2020; Zheng *et al*., 2020). These studies also suggest that the drought-tolerant genotypes possess greater protective mechanisms against oxidative stress than the drought-susceptible genotypes.

To detoxify ROS, plants accumulate a range of enzymatic and non-enzymatic antioxidants (Apel and Hirt, 2004; Ahmad *et al*., 2010; Sharma *et al*., 2012). Detoxification of some ROS may depend on the simultaneous action of several antioxidants. For example, superoxide dismutase (SOD) catalyses the dismutation of O_2^- into O_2 and H_2O_2. Catalase (CAT) converts the H_2O_2 into water and O_2, and peroxidases (APX and GPX) scavenge H_2O_2 to water (Ahmad *et al*., 2010). Moreover, plants accumulate osmolytes and osmoprotectants such as proline, which also act as scavengers of ROS, contribute towards osmotic adjustment and stabilise proteins and protein complexes in the chloroplast and cytosol (Hare and Cress, 1997; Szabados and Savouré, 2010). Crops such as barley, sorghum and wheat increased the accumulation of antioxidant activities and proline in the leaves and roots following water limitation possibly to protect cellular components against the osmotic and oxidative effects of drought (Mejri *et al*., 2016; Abid *et al*., 2018; Goche *et al*., 2020).

Several studies have compared wheat cultivars with different levels of drought tolerance to evaluate their physiological and biochemical responses to drought stress to gain a better understanding of the plant’s responses to drought (Singh *et al*., 2012; Nasirzadeh *et al*., 2021; Wang *et al*., 2022; Dashtaki *et al*., 2023). Wang *et al*. (2022) investigated the physiological and biochemical responses of wheat cultivars subjected to drought stress treatment for 6, 12 and 18 days. As the drought stress treatment progressed, the drought-susceptible cultivar had more growth reduction compared to the drought-tolerant cultivar. The MDA content in the leaves of the susceptible cultivar also increased more than that of the drought-tolerant cultivar. Conversely, the drought-tolerant wheat cultivar exhibited higher levels of SOD activity, proline and soluble sugars content in the leaves than the susceptible cultivar, possibly indicating better stress tolerance (Wang *et al*., 2022).

Akter *et al*. (2023) also conducted a comparative study on wheat varieties subjected to drought stress at different developmental stages. The results indicated that the drought-tolerant variety accumulated higher levels of proline, soluble sugars, and chlorophyll, while the drought-sensitive variety had higher electrolyte leakage and MDA levels. The above-mentioned studies suggest that drought-tolerant varieties of various plant species are better equipped to withstand water deficit stress than their drought-sensitive counterparts.

This chapter aimed to comparatively analyse the morphological, physiological and biochemical changes between two wheat varieties with contrasting drought phenotypes to better understand their diverse drought response mechanisms. The wheat varieties used in this study are non-commercial varieties and might provide a wider range of genetic diversity. This could potentially uncover mechanisms that are not present in current commercial wheat varieties.

3.2. Materials and methods

3.2.1 Plant material

Six wheat (*Triticum aestivum*) varieties were used in preliminary experiments of this study to select two with contrasting drought phenotypes for the main experiments. The wheat seeds were obtained from the International Maize and Wheat and Improvement Centre (CIMMYT), Mexico and were bulked up by Dr. Nemera Shargie at the Agricultural Research Council

(ARC)-Grain Crops Institute (GCI), Potchefstroom, South Africa, during the 2017-2018 rainy season. A list of the wheat varieties and their drought phenotypes is shown in Table 3.1.

Table 3.1: Wheat varieties used in the study.

Variety	Phenotypic trait
BW4074	Drought-susceptible
BW4113	Drought-susceptible
BW34025	Drought-susceptible
BW33909	Drought-tolerant
BW35695	Drought-tolerant
BW35697	Drought-tolerant

3.2.2 Screening wheat varieties for drought tolerance

3.2.2.1 Seed germination, growth, and drought stress treatment

Seeds of wheat varieties BW4074, BW4113, BW34025, BW33909, BW35695 and BW35697 were placed on moist paper towels in Petri dishes, wrapped in foil and incubated in a growth chamber (Model: GC-539DH, Already Enterprise Inc., Tapei, Taiwan) for six days. The growth chamber was set up with a temperature range of 18/15 °C day and night. After six days, germination was measured by counting the sprouting seedlings.

The wheat seedlings were then transplanted in plastic pots with a volume of 552.5 cm^3 (10 cm top diameter × 6.5 cm bottom diameter × 8.5 cm height), filled with potting soil (Culterra, Muldersdrif, South Africa). The potting soil was saturated with 40 ml of Nitrosol Nutrient solution [Envirogreen (Pty) Ltd., Braamfontein, South Africa], and the pots were allowed to drain for two hours before transplanting the seedlings. Twelve seedlings per wheat variety were transplanted in each plastic pot and the potted plants were placed in a growth chamber with day and night temperatures of 18/15 °C under a 16-hour photoperiod. The growth chamber used OSRAM L18W/640 light bulbs that provide 1200 lumens. The plants were watered every two days with 40 ml of distilled water and allowed to grow until they were 13 days old with two fully expanded leaves. The plants were then thinned to ten plants per pot prior to drought stress treatment.

Drought stress was initially induced on 14-day-old plants by withholding water for 14 days while the control group received water throughout the experiment. Following the stress treatment period, growth and physiological parameters such as RWC and relative shoot water loss (RSWL) were measured to assess the effect of water limitation on wheat plants. No significant differences in the measured parameters were observed between the control and drought-treated plants. Therefore, the stress treatment duration was extended to 28 days, while visually assessing morphological differences between the control and drought-stressed plants. After the 28 days of stress treatment, growth and physiological measurements were conducted.

3.2.2.2 Measurement of leaf relative water content

Leaf RWC was estimated on day 28 of water limitation using a method described by Barrs and Weatherley (1962). On day 28 of the stress treatment, the third oldest leaf from the control and drought-stressed plants was harvested and used for determining the RWC. The measurements were carried out using five biological replicates. The leaves were removed from the plants and immediately weighed to determine the fresh weight (FW). Thereafter, the leaf samples were submerged in 50 ml Falcon tubes containing distilled water and incubated for 24 hours at 4 °C. After incubation, the leaves were blotted dry with a paper towel and weighed to determine the turgid weight (TW). The leaf samples were then oven-dried for 48 hours at 60 °C to estimate the dry weight (DW). A formula described by Barrs and Weatherley (1962) was used to calculate the RWC.

$$\mathrm{RWC} = \frac{\mathrm{FW} - \mathrm{DW}}{\mathrm{TW} - \mathrm{DW}} \times 100$$

RWC = relative water content, FW = fresh weight, DW = dry weight, and TW = turgid weight.

3.2.2.3 Measurement of relative shoot water loss

Relative shoot water loss was estimated following the 28 days of drought stress as described by Rahman *et al*. (2000). Shoots of the control and drought-treated wheat plants were separated from the roots and immediately weighed to determine the fresh weight (FW). The shoots were left at room temperature for 6 hours and weight measurements were taken every hour to determine the wilted weight (WW). After six hours, the shoots were oven-dried at 60 °C for 48 hours to determine the dry weight (DW). The RSWL measurements were conducted using five biological replicates and calculated using the following equation as described by Rahman *et al*. (2000).

$$\mathrm{RSWL} = \frac{\mathrm{FW} - \mathrm{WW}}{\mathrm{DW}}$$

RSWL = relative shoot water loss, FW = fresh weight, WW = wilted weight, and DW = dry weight.

3.2.2.4 Measurements of growth parameters

Growth parameters were also measured after 28 days of drought stress treatment. Shoot and root lengths were measured in centimetres for both control and drought-stressed plants. Shoot length was measured from the base of the shoot to the tip of the longest leaf, while the root length was measured from the base of the shoot to the tip of the longest root. Thereafter, fresh shoot and root weight measurements were recorded, and the shoots and roots were oven-dried at 60 °C for 48 hours to determine the dry weights. Five biological replicates per treatment group and tissue type were used for the growth measurements.

Based on the RWC, RSWL and growth measurements results, varieties BW4074 and BW35695 were selected for use in morpho-physiological, biochemical and leaf proteome analysis under drought stress conditions.

3.2.3 Drought stress treatment of BW4074 and BW35695 wheat varieties

Wheat varieties BW4074 (an improved cultivar that is drought-susceptible) and BW35695 (a drought-tolerant breeder's line) were grown and exposed to drought stress as described in Section 3.2.2.1. On days 0, 14 and 28 of drought stress treatment, leaf and root samples were harvested and stored at -80 °C for subsequent use in physiological, biochemical, proteome and gene expression analyses.

3.2.3.1 Soil moisture content measurements

Soil moisture content (SWC) was measured using a gravimetric method as previously described (Vineeth *et al.*, 2016), with minor modifications. On days 14 and 28 of drought stress, measurements of soil moisture content were carried out to assess the level of soil moisture deficit. Three replicates of soil samples from the control and water-deprived pots were weighed to determine the wet weight (WW), then oven-dried at 105 °C for 48 hours to obtain the dry weight (DW). The soil moisture content was calculated following the formula:

$$\mathrm{SWC} = \frac{\mathrm{WW} - \mathrm{DW}}{\mathrm{DW}} \times 100$$

SWC = soil water content, WW = wet weight and DW = dry weight.

3.2.3.2 Leaf relative water content and growth parameters

The comparison between the control and drought-stressed plants after 14 days of stress treatment previously revealed no significant differences in leaf RWC and growth measurement. Therefore, the leaf RWC and growth measurement were only conducted on day 28 of drought stress treatment. Leaf RWC was estimated as described in Section 3.2.2.2 with four biological replicates for both treatment groups per wheat variety. The growth parameters were measured as described in Section 3.2.2.4 using three biological replicates per treatment per wheat variety.

3.2.3.3 Estimation of chlorophyll and carotenoid content

A modified extraction method using dimethyl sulfoxide (DMSO) (Hiscox and Israelstam, 1979) was used to estimate chlorophyll a and b and carotenoid content in the wheat plants. Frozen leaf tissue was sampled by measuring 100 mg of the third oldest leaf at days 0, 14 and 28 of drought stress. Three biological replicates per treatment per wheat variety were taken at each sampling time point and stored at -80 °C. The frozen leaf tissue was cut into pieces, mixed with 20 ml of DMSO and incubated in a water bath for three hours at 65 °C. Following the incubation period, the samples were pulse vortexed and their absorbance was measured at 480, 649 and 665 nm using a JENWAY 7300 spectrophotometer (Bibby Scientific Ltd., Staffordshire, UK) with DMSO as a blank solution. A formula described by Wellburn (1994) was used to calculate chlorophyll a, b and carotenoid content.

$$\text{Chlorophyll a } (\mu g/ml) = 12.19(A_{665nm}) - 3.45(A_{649nm})$$

$$\text{Chlorophyll b } (\mu g/ml) = 21.99(A_{649nm}) - 5.32(A_{665nm})$$

$$\text{Carotenoid: } [1000A_{480nm} = 2.14\text{Chl-a} - 70.16\text{Chl-b}]/220$$

Chl-a = Chlorophyll a; Chl-b = Chlorophyll b

3.2.3.4 Estimation of superoxide anion content in leaf and root tissues

Superoxide anion content in wheat leaves and roots of wheat plants was estimated using a modified method (Gokul *et al.*, 2021). Measurements of superoxide anion content were conducted on day 28 of drought stress treatment. Briefly, 50 mg of fresh leaf and 100 mg of fresh root tissue were harvested and submerged in 1.5 ml Eppendorf tubes containing 50 mM potassium phosphate buffer, pH 7.0 containing 10 mM potassium cyanide (KCN), 80 µM nitroblue tetrazolium (NBT) and 10 mM H_2O_2. The samples were incubated at room temperature for 20 minutes and then homogenised using micro pestles to extract the superoxide anion present in the samples. Thereafter, the samples were centrifuged at 13 000 × *g* for 5 minutes and the absorbance was measured at 600 nm using a JENWAY 7300 spectrophotometer. All centrifugation steps in this study were done at room temperature unless stated otherwise. Three biological replicates were used per treatment and tissue for each wheat variety. The superoxide anion content was determined using the extinction coefficient of 12.8 $mM^{-1}cm^{-1}$.

3.2.3.5 Estimation of hydrogen peroxide content in leaf and root tissues

A modified method described by Gokul *et al*. (2021) was used to estimate the concentration of H_2O_2 in wheat leaves and roots following 28 days of drought stress treatment. Three biological replicates were prepared for the control and drought-stressed plants per wheat variety. Leaf and root samples per treatment group were separately ground in liquid nitrogen. Subsequently, 100 mg of the powdered samples were weighed and transferred into 1.5 ml Eppendorf tubes. Thereafter, 500 µl of 6% (w/v) trichloroacetic acid (TCA) was added to each sample, vortexed and centrifuged at 15 000 × *g* for 10 minutes. The leaf and root test samples were prepared by mixing 93.8 µl of the TCA extract with 187.5 µl 20 mM dipotassium phosphate (pH 5) and 375 µL 500 mM potassium iodide in 2ml plastic cuvettes. Hydrogen peroxide standards were also prepared in 2 ml plastic cuvettes in triplicates as indicated in Appendix, Table A1.1. The standards and test samples were incubated at room temperature for 20 minutes and the absorbance was measured at 390 nm using a JENWAY 7300 spectrophotometer. The H_2O_2 standards were used to plot a standard curve which was then used to estimate the H_2O_2 content of the wheat plants.

3.2.3.6 Lipid peroxidation in leaf and root tissues

The TCA extracts mentioned in Section 3.2.3.5 were also used to conduct a lipid peroxidation assay. A modified method by Gokul *et al*. (2021) was used to assess lipid peroxidation in wheat leaf and root samples by measuring the malondialdehyde (MDA) content. Three biological replicates were used for each tissue sample per treatment and wheat variety. A total of 300 µl of the TCA extract was transferred into a 1.5 ml Eppendorf tube and mixed with 450 µl of 0.5% (w/v) thiobarbituric (TBA) prepared in 20% TCA. The mixture was vortexed and incubated at 90 °C for 20 minutes and then cooled on ice for 10 minutes. The mixture was centrifuged at 10 000 × *g* for 5 minutes, and the absorbance was measured at 532 and 600 nm on a JENWAY 7300 spectrophotometer using 0.5% (w/v) TBA as a blank solution. The absorbance at 600 nm was subtracted from the absorbance at 532 nm to correct for non-specific turbidity. The MDA concentrations were calculated using a molar extinction coefficient of 155 $mM^{-1}cm^{-1}$.

3.2.3.7 Enzymatic antioxidant activity assays

3.2.3.7.1 Protein extraction and quantification for antioxidant activity assays

Frozen leaf and root samples harvested on day 28 of drought stress treatment were ground using ice-cold mortar and pestles. A 100 mg of each powdered tissue sample from the control and drought-stressed plants was transferred into 2 ml Eppendorf tubes. The samples were homogenised with 500 µl of extraction buffer [40 mM phosphate buffer (pH 7.4), 1 mM ethylenediaminetetraacetic acid (EDTA) and 5% (w/v) polyvinylpyrrolidone (PVP)] and centrifuged for 5 minutes at 9 000 × *g.* After centrifugation, the supernatant was collected into a 1.5 ml Eppendorf tube and stored at -20℃ prior to protein quantification and antioxidant activity assays.

Protein concentrations were quantified using a Bradford assay (Bradford, 1976) with minor modifications as described by Ngara (2009). Bovine serum albumin (BSA) standards were prepared in 2 ml plastic cuvettes in duplicates from a 1 mg/ml BSA stock solution. The BSA standards were prepared by mixing BSA with 10 µl of 0.1 M hydrochloric acid (HCl), 80 µl of distilled water and extraction buffer to make it 100 µl. Protein samples were also prepared in 2 ml plastic cuvettes in duplicates by separately mixing 2 µl of each of the leaf and root protein extracts with 8 µl of extraction buffer, 10 µl of 0.1 M HCl and 80 µl of distilled water. Thereafter, BSA standards and protein samples were mixed with 900 µl of Protein Assay Dye Reagent Concentrate (BIO-RAD, Hercules, California, USA) diluted at a ratio of 1:4 and incubated for 5 minutes at room temperature. The absorbance was recorded at 595 nm using a JENWAY 7300 spectrophotometer with the 0 mg/ml BSA standard solution as a blank. A standard curve was plotted using the BSA standards to calculate the protein concentrations of the leaf and root samples.

3.2.3.7.2 Superoxide dismutase activity assay

The activity of SOD in wheat leaves and roots was determined using a method by Gokul *et al.* (2021) with minor modifications. Three biological replicates were used per treatment and wheat variety for leaf and root samples. The reaction mixture was prepared in 2 ml plastic cuvettes with a total volume of 800 µl. Each reaction mixture contained the 10 µl enzyme extract, 300 µl 20 mM phosphate buffer (pH 7.8), 100 µl 0.1 mM NBT, 100 µl 0.5 µM riboflavin, 100 µl 10 mM methionine, 800 µl 0.1 mM EDTA and the volume was made up to 800 µl using distilled water. The mixtures were incubated at room temperature for 20 minutes while exposed to light (LED lights) for the reaction to occur. A light-dependent reaction with riboflavin and NBT generates superoxide radicals, which are detoxified by SOD, allowing for the measurement of SOD activity. After incubation, the absorbance was recorded at 560 nm using a JENWAY 7300 spectrophotometer. A blank solution was prepared with all the components of the reaction mixture except the enzyme extract. One unit of SOD activity was defined as the amount of enzyme that inhibited 50% of NBT photo-reduction.

3.2.3.7.3 Ascorbate peroxidase activity assay

A modified method described by Moloi and van der Merwe (2021) was used to measure APX activity in wheat leaves and roots following 28 days of drought stress. A 1 ml reaction mixture was prepared in quarts cuvettes. The reaction mixture contained 530 µl 50 mM potassium phosphate buffer (pH 7.0), 150 µl 0.5 mM ascorbate, 50 µl 0.1 mM EDTA, 70 µl leaf enzyme extract and 200 µl 0.1 mM H_2O_2. The same components were prepared with 50 µl root enzyme extract to make a final volume of 1 ml. The reduction in absorbance was measured using a UV-visible spectrophotometer (Cary 100 Bio, Varian, Australia) at 290 nm for 2 minutes at 20 °C. The blank solution contained all reagents except for the enzyme extract. The APX activity was calculated using an extinction coefficient of 2.8 $mM^{-1}cm^{-1}$. Three biological replicates were used of each tissue type, per treatment and wheat variety.

3.2.3.7.4 Guaiacol peroxidase activity assay

Guaiacol peroxidase (GPX) activity was determined using a modified method as described by Moloi and van der Merwe (2021). Briefly, a reaction mixture for the leaf sample consisted of 505 µl 80 mM phosphate buffer (pH 5.5), 100 µl 50 mM guaiacol, 50 µl 20 mM H_2O_2, 5 µl leaf extract and 340 µl distilled water to make a final volume of 1 ml. For the root samples, 2 µl enzyme extract was used with similar reaction mixture components as the leaf samples to have a final volume of 1 ml. The leaf and root samples were prepared in 2 ml plastic cuvettes. Three biological replicates were used per treatment and wheat variety. A blank solution containing all reagents except for the enzyme was used. An increase in absorbance was measured at 470 nm with a UV-visible spectrophotometer (Cary 100 Bio) for 3 minutes 30 °C. An extinction coefficient of 26.6 mM^{-1} cm^{-1} was used to calculate the GPX activity in the wheat plants.

3.2.3.8 Sample preparation for osmolyte content analysis

Osmolyte content analysis was conducted using three biological replicates for leaf and root tissue samples. The samples were harvested on days 0, 14 and 28 of drought stress treatment. Leaf discs (1 cm) were cut off from the second leaf of the control and drought-treated plants on day 0 because the third leaf was still emerging. However, for days 14 and 28, the samples were obtained from the third leaf because the second leaf was chlorotic on day 14 in some plants in the drought stress treatment pots. For the roots, 50 mg of ground tissue samples were used. To each sample, 65 µl of 0.25 N HCl was added, pulse vortexed and incubated on a heat block at 60 °C for 5 minutes. The samples were centrifuged at 21 300 × *g* for 10 minutes, and 50 µl of the supernatant was collected and stored at -20 °C before being couriered to Durham University (UK) for proline and glycine betaine content analysis.

3.2.3.8.1 Proline content analysis

Hydrophilic Interaction Liquid Chromatography-Mass Spectrometry (HILIC-MS) was used to analyse proline content in the leaves and roots of both wheat varieties. The chromatography separation was performed on Waters Acquity UPLC BEH Amide (1.07 µm 1.0×100 mm) guard column as previously described (Prinsen *et al*., 2016: Goche *et al*., 2020). A volume of 2 µl for leaf and root samples, diluted at 1:100 was injected in solvent A, 85% acetonitrile (MeCN) + 10 mM ammonium formate, 0.15% formic acid and the temperature of the column was maintained at 40 °C. Proline standards were prepared from 0.005-12 µM in solvent A. Chromatography separation was carried out at a flow rate of 0.2 ml/minute using a gradient of solvent B (85:15 H_2O: MeCN+ 10 mM ammonium formate and 0.15% formic acid). The initial concentration was 0% and increased to 100% from 10 to 12 minutes, thereafter, reduced to 0% at 12.1 minutes. The total run time was 18 minutes. The column was connected to a Sciex 6500 Qtrap mass spectrometer with ESI operated in positive ionisation mode and the MRM mode transition was 116-70.

3.2.3.8.2 Glycine betaine content analysis

The HILIC method was also used to analyse leaf and root glycine betaine content (Prinsen *et al*., 2016; Goche *et al*., 2020). The chromatography separation for this analysis was performed on a Supelco Ascentis Express HILIC 2.1 x 150 mm column. The column temperature was maintained at 30 °C and the volume of sample injected was 2 µl. The samples were diluted at a ratio of 1:100 in solvent A (85% acetonitrile (MeCN) + 10 mM ammonium formate, 0.15% formic acid). The standards were also prepared in solvent A from 0.1-5 µM and 5-30 µM across two calibration curves. The chromatography separation was carried out at a flow rate of 0.4 ml/minute using a gradient of solvent B (85:15 H2O: MeCN+ 10 mM ammonium formate and 0.15% formic acid). The concentration of the solvent started at 0% and increased to 100% after

7 to 10 minutes, thereafter, the gradient decreased to 0% and the total run time was 15 minutes. The column was connected to a Sciex 6500 Qtrap mass spectrometer with ESI operated in positive ionisation mode and the MRM mode transition were 118.1>58.10 and 118.1>59.2. The quantitation was carried out using the quantitation wizard Sciex Analyst 1.7.1.

3.2.3.9 Statistical analysis

The Student's *t*-test and analysis of variance (ANOVA) with a Tukey-Kramer post-test were used to compare the means of the morpho-physiological and biochemical results at a 5% level of significance. A three-way ANOVA was performed in cases where there were three factors, stress type (control and drought stress), duration of stress treatment (across the different sampling times), and wheat genotypes (drought-susceptible and drought-tolerant). All the data analyses were conducted using the GraphPad Prism software version 8.0.2.263.

3.3 Results

3.3.1 Screening wheat varieties for drought tolerance

3.3.1.1 Leaf relative water content (RWC) and relative shoot water loss (RSWL)

A reduction in leaf RWC was observed after day 28 of drought stress treatment across five of the wheat varieties (BW4074, BW4113, BW34025, BW33909, and BW35695) when compared to their respective controls (Figure 3.1A). Among the six wheat varieties, the drought-tolerant varieties BW35695, BW33909, and BW35697 maintained higher RWC values at 71%, 82%, and 85%, respectively. However, the drought-susceptible varieties, BW34025, BW4074, and BW4113, had lower RWC values at 46%, 61%, and 66%, respectively, in response to drought stress.

Shoot water loss was also evaluated to analyse the plants' capacity to retain water (Figure 3.1B). The results indicated that over a six-hour period, the drought-susceptible varieties BW34025, BW4074, and BW4113 as well as one drought-tolerant variety BW33909 lost water at a faster rate than the two drought-tolerant varieties, BW35695 and BW35697. Overall, the 28 days of drought stress treatment negatively affected the plant water status of the wheat varieties.

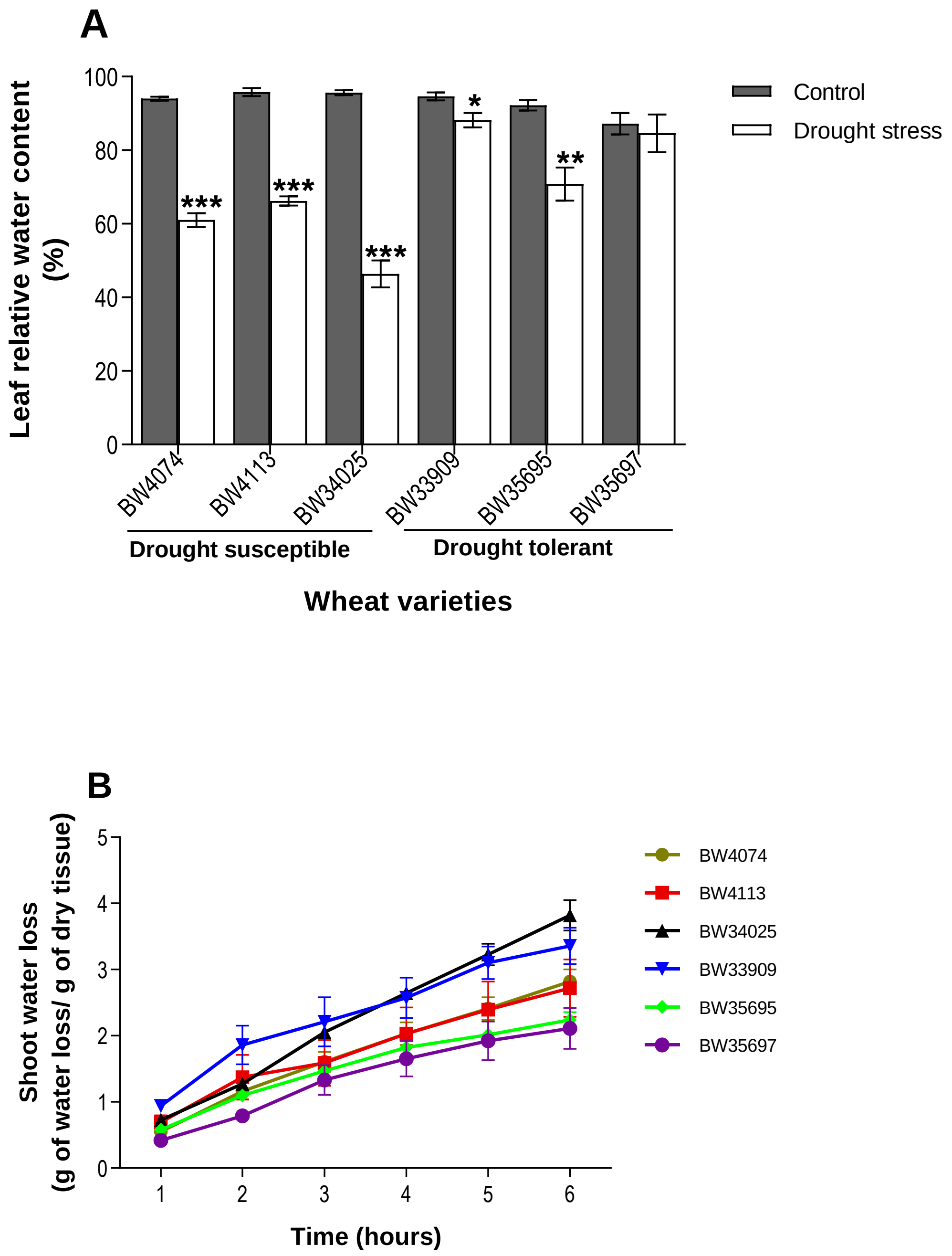

Figure 3.1: The effects of drought stress on leaf relative water content and relative shoot water loss of wheat plants. (A) shows the RWC while (B) shows the RSWL. Plants were grown for 14 days, and drought stress was induced by withholding water for 28 days while control plants were well-watered. The RWC was estimated on the third leaf of the control and drought-stressed plants. Data presented as mean ±SE (*n* = *4*) for RWC and (*n* = *5*) for RSWL. *, ** and *** = significance between control and drought-stressed samples of RWC at $p \leq 0.05$, 0.01, and 0.001, respectively according to a Student's *t*-test.

3.3.1.2 Effects of drought stress on wheat growth

The 28 days of drought stress significantly reduced shoot fresh weight of five wheat varieties BW4113, BW34025, BW33909, BW35695 and BW35697 (Figure 3.2A). On the other hand, drought-treated BW4074 and BW35695 plants exhibited a 51.2% and 53.6% reduction, respectively, in root fresh weight compared to their controls (Figure 3.2C). In contrast, the root dry weight significantly increased in the drought-treated BW4074 samples (Figure 3.2D). No significant differences in shoot length were observed after 28 days of stress treatment in all wheat varieties (Figure 3.2E). However, the root length of BW4113 and BW33909 drought-treated plants was significantly increased relative to the controls (Figure 3.2F).

The drought-susceptible BW4074 and drought-tolerant BW35695 wheat varieties were selected for subsequent use in comparative physiological and biochemical analyses. The selection of these two wheat varieties to use in the entire project was based on the RWC, RSWL (Figures 3.1A and B), growth measurements (Figure 3.2) results and the availability of seeds.

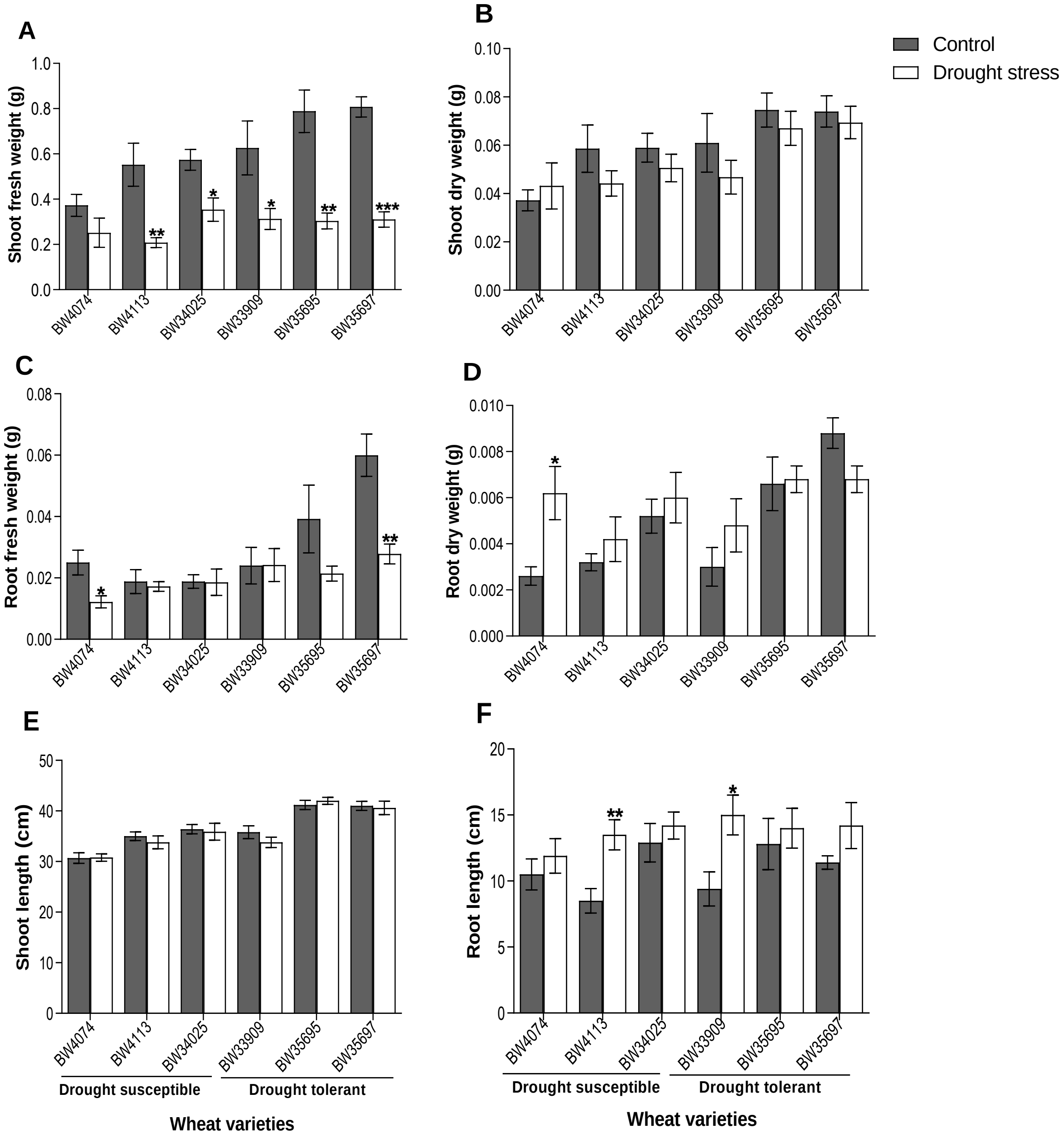

Figure 3.2: Effects of drought stress on the growth of different wheat varieties. Shoot fresh weight (A), shoot dry weight (B), root fresh weight (C), root dry weight (D), shoot length (E) and root length (F). Plants were grown for 14 days. Drought stress was induced by withholding water for 28 days while control plants were well-watered. Data presented as mean ± SE (*n* = 5). *, ** and *** = significance between control and drought-stressed samples at $p \leq 0.05$, 0.01, and 0.001, respectively according to a Student's *t*-test.

3.3.2 Drought stress treatments on BW4074 and BW35695 wheat varieties

To evaluate the differential effects of water deprivation on wheat varieties with contrasting drought phenotypes, a 28-day drought stress treatment was imposed on the plants. Generally, drought stress negatively affected the growth of BW4074 (drought-susceptible) and BW35695 (drought-tolerant) wheat plants (Figure 3.3). The wheat plants showed signs of wilting on day 16 of drought stress treatment and by day 28, the first and second oldest leaves of the drought-stressed plant were chlorotic.

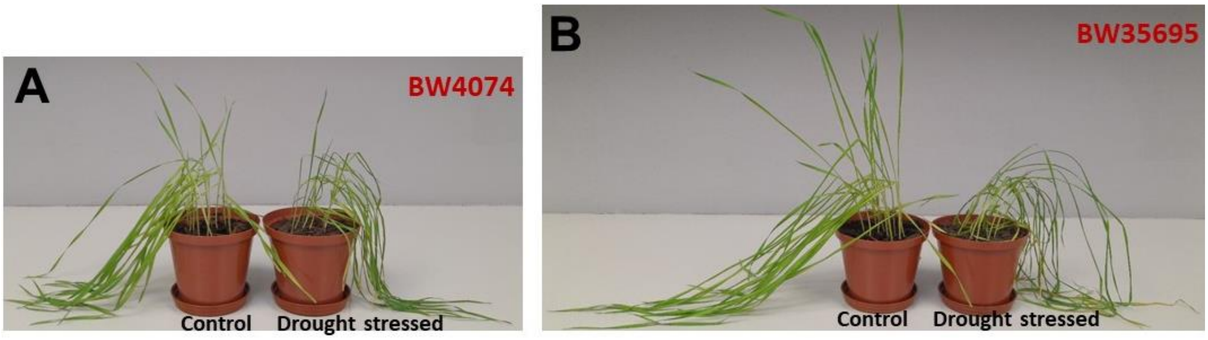

Figure 3.3: The effect of drought stress on wheat growth. Picture (A) shows the control and drought-stressed BW4074 (drought-susceptible), while (B) shows the control and drought-stressed BW35695 (drought-tolerant) wheat varieties 28 days after stress treatment. Drought stress was induced on 14-day-old plants by withholding water, while control plants were well-watered.

3.3.2.1 Soil moisture content measurements

The soil moisture content of the drought-stressed pots decreased significantly relative to the controls (Figure 3.4). On day 14 of drought stress treatment, the soil moisture of BW4074 water-deprived pots decreased to 76% while for BW35695, the reduction was 77%. By the 28th day of drought stress treatment, the soil moisture content for BW4074 decreased to 53% and 59% for BW35695. However, no significant differences in soil moisture content were observed between the two wheat varieties at each time point, suggesting no difference in water utilisation between the varieties.

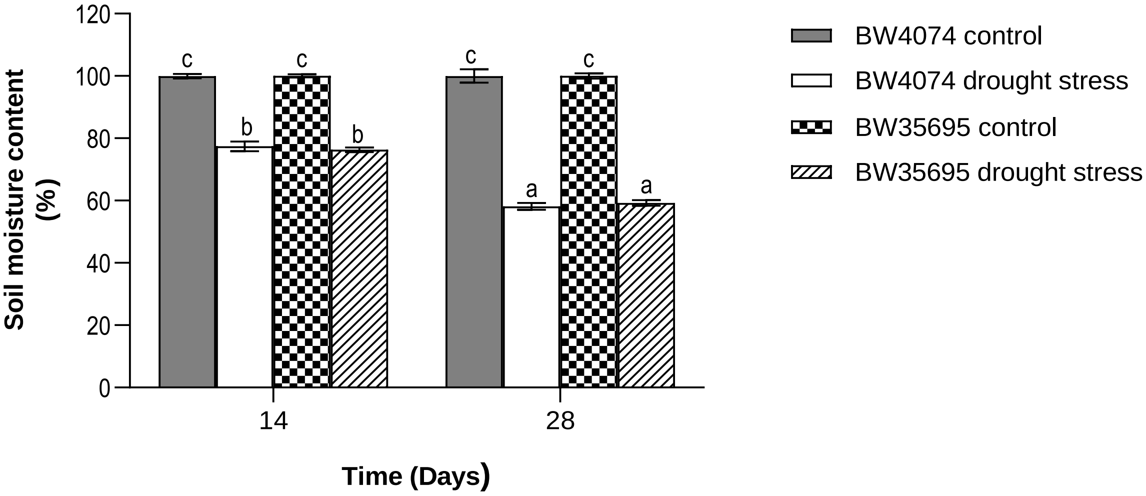

Figure 3.4: Soil moisture content at different time points of drought stress. Drought stress was induced by withholding water for 28 days. Soil samples were measured on days 14 and 28 of drought stress treatment using the gravimetric method. Data presented as mean ± SE (*n* = 3). Bars with different letters represent statistical significance at $p \leq 0.05$ according to ANOVA (Tukey-Kramer test).

3.3.2.2 Leaf relative water content

The 28 days of drought stress resulted in a decrease in the leaf RWC in both wheat varieties when compared to their respective controls (Figure 3.5). The RWC of the drought-stressed plants declined by 22% for BW4074 and 12% for BW35695 compared to their respective controls. However, a significant decrease was only observed in the drought-susceptible BW4074. In contrast, the drought-tolerant variety maintained a higher RWC compared to the susceptible variety suggesting its greater water retention capacity.

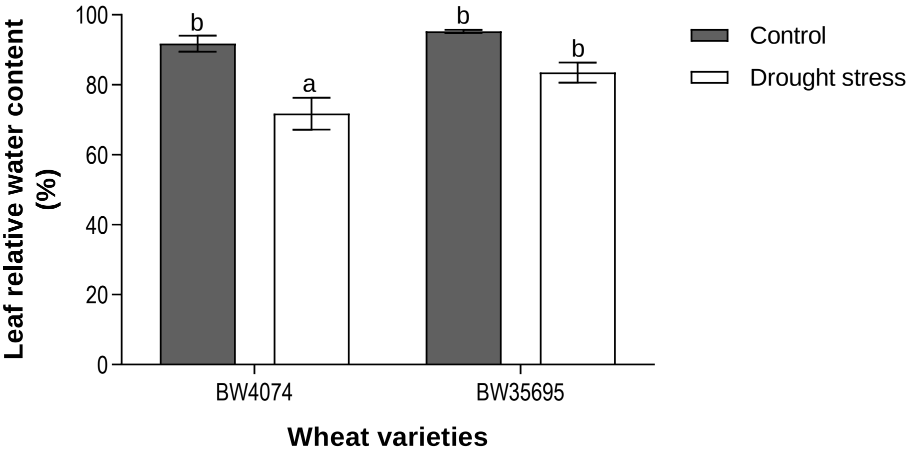

Figure 3.5: The effects of drought stress on leaf relative water content of wheat plants. Plants were grown for 14 days, and drought stress was induced by withholding water for 28 days. RWC measurements were taken on the third leaf of both the control and drought-stressed plants. Data presented as mean ± SE (*n = 4*). Bars with different letters represent statistical significance at $p \leq 0.05$ according to ANOVA (Tukey-Kramer test).

3.3.2.3 Effects of drought stress on wheat growth parameters

The shoot and root growth parameters of BW4074 and BW35695 wheat varieties were measured following 28 days of drought stress (Figure 3.6). Both wheat varieties exhibited a decline in shoot fresh weight following the drought stress treatment, with BW35695 showing a significant decrease of 61.5% (Figure 3.6A). However, the shoot dry weight was not significantly different (Figure 3.6B). Root fresh and dry weight results showed no significant changes between the controls and drought-stressed plants in both varieties (Figures 3.6C and D). Similarly, shoot and root lengths of drought-treated plants did not differ significantly from their respective controls (Figures 3.6E and F).

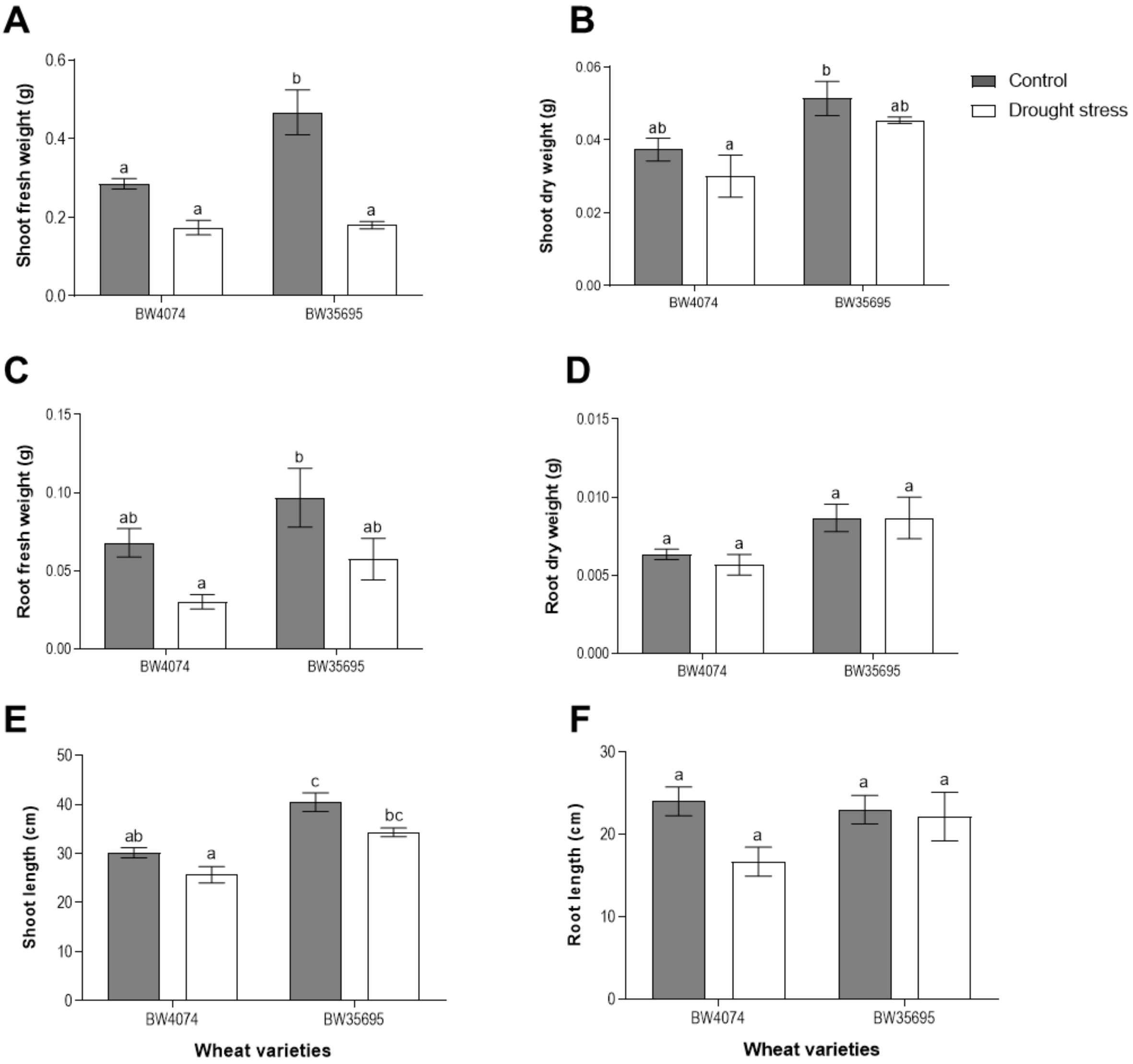

Figure 3.6: Effects of drought stress on the growth of wheat plants. Shoot fresh weight (A), shoot dry weight (B), root fresh weight (C), root dry weight (D), shoot length (E) and root length (F). Plants were grown for 14 days, and drought stress was induced by withholding water for 28 days. Data presented as mean ± SE (*n* = 3). Bars with different letters represent statistical significance at $p \leq 0.05$ according to ANOVA (Tukey-Kramer test).

3.3.2.4 Chlorophyll and carotenoid content measurements

At days 0, 14, and 28 of drought stress treatment, leaf chlorophyll and carotenoid content were estimated in both BW4074 and BW35695 wheat varieties. Significant changes in the contents of the photosynthetic pigments were observed only after 28 days of drought stress in both wheat varieties (Figure 3.7). Notably, BW35695 demonstrated a remarkable increase of 92% and 50% in chlorophyll a as well as carotenoid content, respectively, compared to control plants, while BW4074 did not exhibit any significant changes in the same parameters (Figures 3.7A and C). On the other hand, chlorophyll b content increased by 49% and 91% in BW4074 and BW35695, respectively, but there were no significant differences between the two wheat varieties (Figure 3.7B).

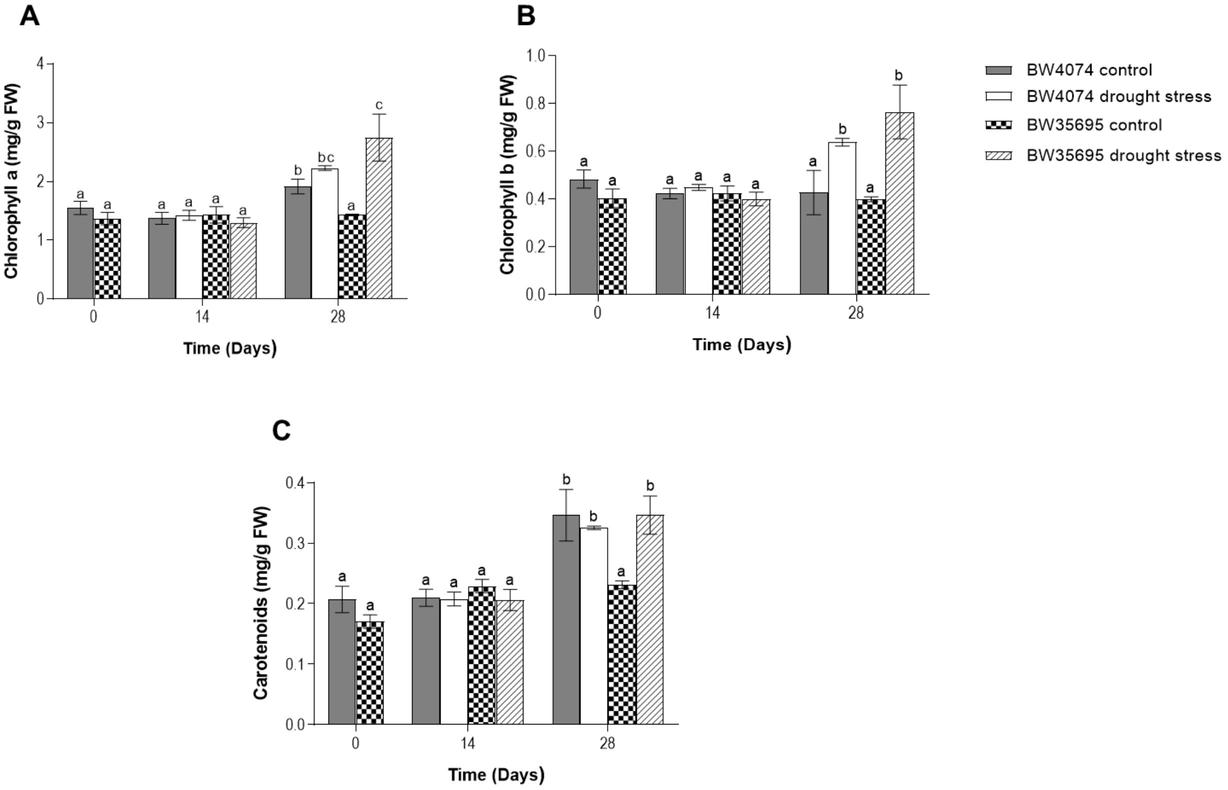

Figure 3.7: Effects of drought stress on chlorophyll and carotenoid content in leaves of wheat plants. Chlorophyll a (A), chlorophyll b (B) and carotenoid (C) content of BW4074 and BW35695 wheat varieties. Plants were grown for 14 days, and drought stress was induced by withholding water for 28 days. Data presented as mean ± SE (*n* = 3). Bars with different letters represent statistical significance at $p \leq 0.05$ according to ANOVA (Tukey-Kramer test).

3.3.2.5 Reactive oxygen species content analysis

The levels of H_2O_2 and superoxide anion were estimated in the leaves and roots of BW4074 and BW35695 wheat varieties after 28 days of withholding water (Figure 3.8). The results showed non-significant increases in superoxide anion content in the leaves of both wheat varieties (Figure 3.8A). However, the superoxide anion content in the roots remained unchanged for BW36595 and a non-significant increase in BW4074 was observed (Figure 3.8B). In contrast, drought stress significantly increased the levels of H_2O_2 in the roots of BW4074 and BW35695 by 38% and 62% respectively, compared to the controls (Figure 3.8D). However, in the leaves, only BW4074 exhibited a 37% significant increase in H_2O_2 content, while that of BW35695 remained unchanged (Figure 3.8C).

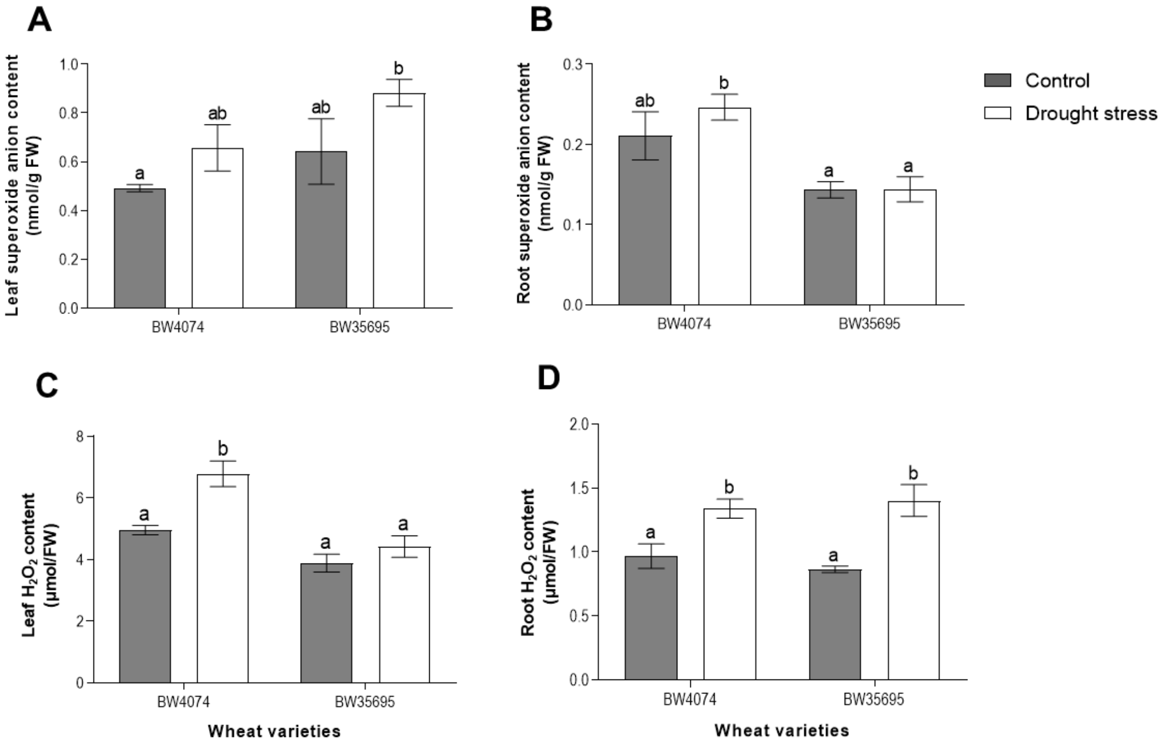

Figure 3.8: Effects of drought stress on ROS accumulation in wheat plants. Leaf and root superoxide anion content (A and B) and leaf and root hydrogen peroxide content (C and D). Plants were grown for 14 days, and drought stress was induced by withholding water for 28 days. Data presented as mean ± SE (*n* = 3). Bars with different letters represent statistical significance at $p \leq 0.05$ according to ANOVA (Tukey-Kramer test).

3.3.2.6 Lipid peroxidation analysis

Lipid peroxidation was estimated by measuring the MDA content in the roots and leaves of BW4074 and BW35695 wheat varieties at day 28 of drought stress (Figure 3.9). The results showed a significant increase in MDA content by 118% and 172% in the leaf and root tissues of BW4074, respectively, compared to the controls (Figure 3.9A and B). In contrast, the MDA content significantly increased by 60% in the roots of BW35695 (Figure 3.9B), while in the leaves a 64% non-significant increase was observed in BW35695 (Figure 3.9A). These results highlight greater membrane lipid damage in the drought-susceptible BW4074 than the drought-tolerant BW35695.

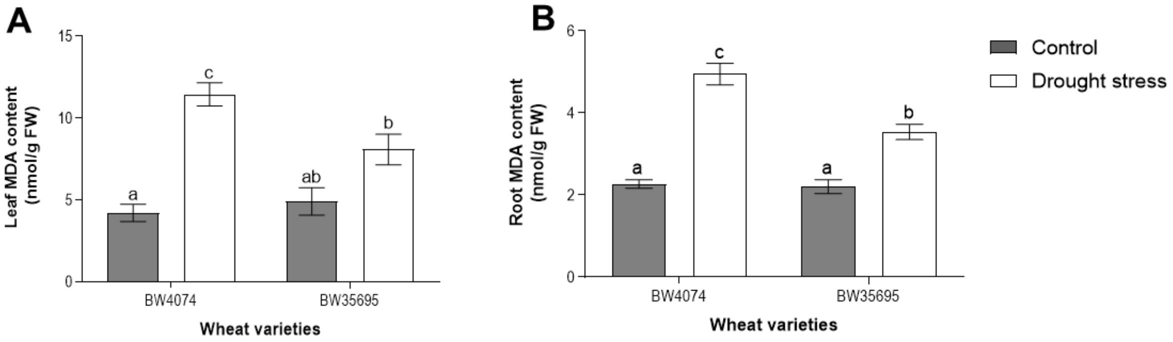

Figure 3.9: The effects of drought stress on MDA content in wheat plants. Leaf MDA content (A) and root MDA content (B) of BW4074 and BW35695 wheat varieties. Plants were grown for 14 days, and drought stress was induced by withholding water for 28 days. Data represent ± SE (*n* = 3). Bars with different letters represent statistical significance at $p \leq 0.05$ according to ANOVA (Tukey-Kramer test).

3.3.2.7 Antioxidant activities in wheat plants

The activities of SOD, APX and GPX in leaf and root tissues of wheat plants were estimated after 28 days of withholding water (Figure 3.10). A 191% significant increase in SOD activity was observed in the leaves of BW35695, while a non-significant decrease was observed in BW4074 following the drought stress treatment (Figure 3.10A). In addition, in the roots, SOD activity decreased significantly by 42% in BW4074 drought-treated samples but remained unchanged in BW35695 following the drought stress treatment (Figure 3.10B).

Guaiacol peroxidase activity increased by 98% in the leaves of BW35695 following 28 days of water limitation (Figure 3.10C). However, a non-significant increase was observed in GPX activity in the roots of BW35695 (Figure 3.10D). The GPX activity in the drought-stressed leaves and roots of BW4074 showed a non-significant increase relative to their controls (Figures 3.10C and D). Ascorbate peroxidase activity showed no significant changes in BW4074 drought-stressed leaf and root samples when compared to their respective controls (Figures 3.10E and F). However, the roots of BW35695 showed a non-significant increase in APX following the drought stress treatment (Figure 3.10F).

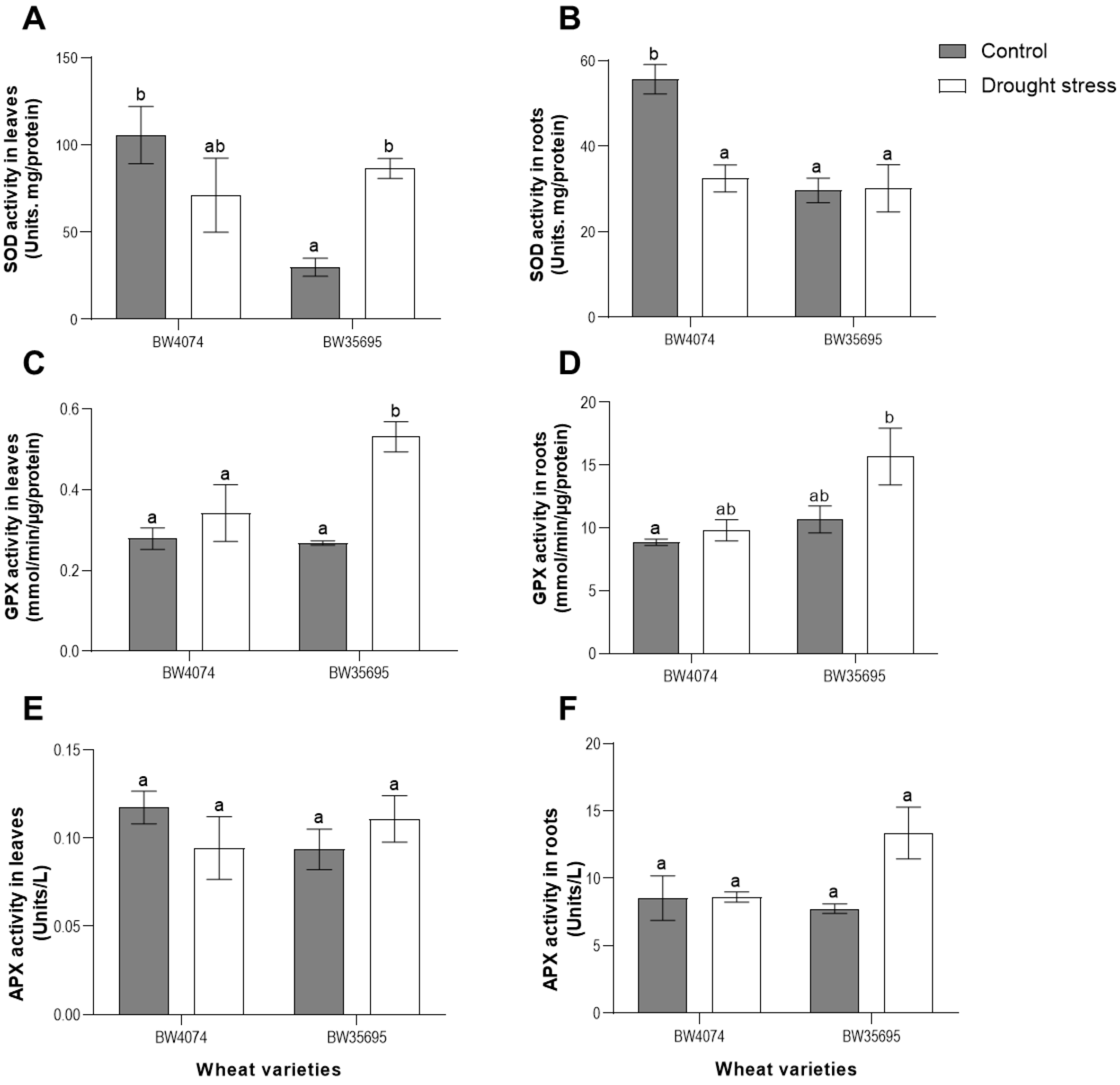

Figure 3.10: The effect of drought stress on enzymatic antioxidant activity in wheat plants. (A) and (B) show SOD activity, (C) and (D) show GPX activity, while (E) and (F) show APX activity in the leaf and root of BW4074 and BW35695 wheat varieties. Plants were grown for 14 days, and drought stress was induced by withholding water for 28 days. Data represent ± SE (*n* = 3). Bars with different letters represent statistical significance at $p \leq 0.05$ according to ANOVA (Tukey-Kramer test).

3.3.2.8 Proline and glycine betaine content analysis

The proline and glycine betaine content in the leaves and roots of BW4074 and BW3595 wheat varieties was estimated on days 0, 14, and 28 of drought stress treatment (Figure 3.11). There was no significant difference in the levels of proline in the leaves and roots of both varieties on days 0 and 14 after withholding water. However, on day 28, the drought-stressed leaf and root samples of BW35695 had a significant increase in the levels of proline relative to the controls (Figures 3.11A and B). The drought-susceptible variety BW4074 also had a significant increase in proline, but only in the roots (Figure 3.11B). A significant increase in glycine betaine content was only observed in the roots of BW4074. The drought-tolerant variety exhibited a significant increase in the levels of glycine betaine in both leaves and roots, while the drought-susceptible variety showed a significant increase in glycine betaine content only in the roots (Figures 3.11C and D). These results suggest that the accumulation of the osmolytes was tissue specific and varied between the wheat varieties in response to drought stress.

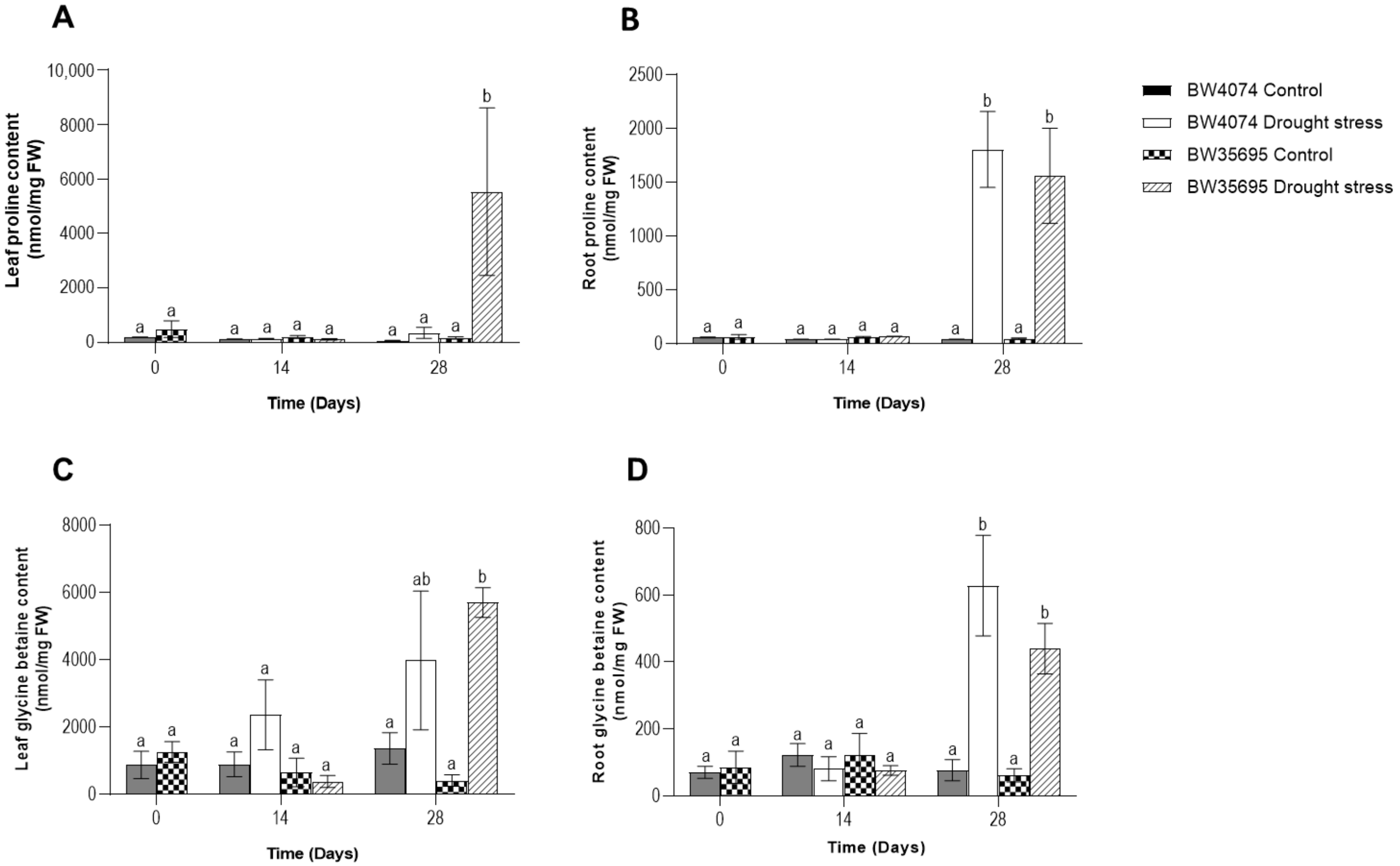

Figure 3.11: Effects of drought stress on proline and glycine betaine content in wheat plants. Leaf and root proline content (A and B) and leaf and root glycine betaine content (C and D) of BW4074 and BW35695 wheat varieties. Plants were grown for 14 days, and drought stress was induced by withholding water for 28 days. Data presented as mean ± SE (n = 3). Bars with different letters represent statistical significance at $p \leq 0.05$ according to (ANOVA Turkey test).

3.4 Discussion

This current study screened six wheat varieties, that are drought-susceptible (BW4074, BW4113, BW34025) and drought-tolerant (BW33909, BW35695, and BW35697) (Table 3.1) to select two varieties with contrasting drought phenotypes for the main experiments. A 28-day drought stress experiment revealed that the water status of the wheat varieties was negatively affected relative to the control plants. However, the drought-tolerant varieties BW33909, BW35695 and BW35697 maintained a higher RWC when compared to the drought-susceptible counterparts BW4074, BW4113 and BW34025 (Figure 3.1A). These results suggest that the drought-tolerant varieties had a better water retention capacity than the drought-susceptible wheat varieties. Similarly, other wheat studies reported differential responses in leaf RWC between different genotypes following drought stress (Sultan *et al*., 2012; Liwani *et al*., 2018; Marcek *et al*., 2019). These studies revealed that the drought-tolerant cultivars maintained a higher RWC under drought stress conditions ensuring that cells remain hydrated for optimum metabolic functions (Qiao *et al*., 2024). The differences in the genotypes' capacity to retain water under drought stress conditions were also observed in the relative shoot water loss results of the six wheat varieties (Figure 3.1B). Drought-tolerant varieties, BW35695 and BW35697, showed a greater capacity to retain water longer than the drought-susceptible varieties. Furthermore, the 28-day stress treatment significantly hindered shoot growth across five of the wheat cultivars (Figure 3.2A). Overall, the 28 days of drought stress treatment significantly affected the wheat plants in terms of water status and growth, with the drought-susceptible varieties exhibiting more pronounced effects compared to the drought-tolerant varieties.

Based on the results of the drought stress screening experiments as well as the availability of seeds, wheat varieties BW4074 (drought-susceptible) and BW35695 (drought-tolerant) were selected for the main drought stress experiments. The wheat varieties were subjected to the same drought stress conditions for 28 days. To gauge the level of drought stress in the potted plants, the soil moisture content of the control and water-deprived plants was measured using a gravimetric method (Vineeth *et al.*, 2016). The results revealed that drought stress significantly reduced the soil moisture content for both wheat varieties at 14 and 28 days of stress treatment (Figure 3.4). However, no differences in water utilisation were observed between the wheat varieties at both time points. The imposed water deficit stress was equivalent to mild and moderate drought stress conditions (Samarah, 2005; Bai *et al*., 2006) on days 14 and 28 of the stress treatment, respectively. Due to the observed reduction in soil moisture content, the leaf RWC of the two wheat varieties at day 28 of drought stress treatment was assessed. The leaf RWC decreased in both BW4074 and BW35695 wheat varieties following water limitation stress (Figure 3.5A). However, BW35695 maintained a higher RWC compared to BW4074, possibly to keep the cell hydrated and continue with metabolic activities under drought stress conditions. The observed results are in agreement with other comparative wheat studies which analysed leaf RWC between drought-susceptible and tolerant cultivars under drought stress conditions (Faghani *et al*., 2015; Nasirzadeh *et al*., 2021; Akter *et al*., 2023). These studies also highlighted that a plant’s ability to conserve water under drought stress may be a mechanism that allows the continuation of metabolic activities needed for growth (Faghani *et al*., 2015; Nasirzadeh *et al*., 2021; Akter *et al*., 2023).

Chlorophyll plays an essential role in light harvesting processes and serves as an electron transfer cofactor during photosynthesis (Melkozernov and Blankenship, 2006). According to Anjum *et al*. (2011), a decrease in chlorophyll content under drought stress conditions is considered a symptom of oxidative stress. Plants such as chickpea (*Cicer arietinum* L.) (Mafakheri *et al*., 2010), sunflower (*Helianthus annuus* L.) (Ghobadi *et al*., 2013), maize (*Zea* *mays*) (Chen *et al*., 2016) and wheat (Saeidi *et al*., 2017) exhibit a decrease in chlorophyll a, b and total chlorophyll following water limitation stress. Contrary to the above-mentioned studies, in the current study, drought stress resulted in an increase in chlorophyll a and carotenoid content for BW35695 following 28 days of drought stress (Figure 3.7A and C), while chlorophyll b increased in both wheat varieties (Figure 3.7B). These findings indicate that the drought-tolerant variety enhances the accumulation of the photosynthesis pigments in response to drought stress.

Rahbarian *et al*. (2011) also observed an increase in chlorophyll a, b and carotenoid content in drought-susceptible and tolerant chickpea genotypes under water deficit conditions during early flowering and podding stages. However, in this chickpea study, a drought-susceptible genotype MCC448 had the highest chlorophyll a, b and carotenoid content under drought stress in all developmental stages. Conversely, Pirzad *et al*. (2011) observed varying levels of chlorophyll a, b and total chlorophyll in chamomile (*Matricaria chamomilla* L.) plants at four different irrigation regimes. The results revealed that chlorophyll content increased under mild drought stress conditions but decreased at severe drought stress (Pirzad *et al*., 2011).

Based on the above-mentioned studies as well as the results of the current study, it is evident that chlorophyll content may not necessarily be reduced following water limitation and may vary depending on the plant species, cultivar and plant's ability to tolerate the imposed stress. In the current study, chlorophyll a and b and carotenoid levels significantly increased in BW35695, while chlorophyll b significantly increased in BW4074. The observed increase in carotenoid content in BW35695 (Figure 3.7C) could also be associated with the role of carotenoids in protecting plants from the damaging effects of increased ROS accumulation (Farooq *et al*., 2009). Higher levels of carotenoids were also reported in the leaves of another drought-tolerant wheat cultivar (Abid *et al*., 2018). The authors suggested that the carotenoids might have an important role in restraining ROS accumulation in the chloroplasts via photoprotection of the photosystem (Abid *et al*., 2018).

Abiotic stressors such as drought often disrupt the balance between the production, accumulation and detoxification of ROS. This disruption leads to an increase in the production and accumulation of ROS, which results in the oxidative damage of lipids, proteins, nucleic acids and cell membranes (Gill and Tuteja, 2010; Sharma *et al*., 2012). In this study, the level of H_2O_2 increased significantly in the leaves BW4074 and the roots of both varieties, following drought stress (Figure 3.8C and D). Similar results were obtained in leaves of drought-tolerant and susceptible wheat cultivars subjected to long-term soil drought stress (Huseynova *et al*., 2015).

Due to the observed increase in H_2O_2 accumulation, the MDA content was measured to assess the potential cellular damage in wheat plants under drought stress conditions. Malondialdehyde content can be used as a proxy for plant cell damage (Ayala *et al*., 2014). Both wheat varieties had elevated MDA contents in leaves and roots after withholding water for 28 days (Figure 3.9A and B). However, the drought-susceptible variety had a higher MDA content in both tissues compared to BW35695 possibly indicating the greater levels of oxidative damage caused by increased H_2O_2 levels in BW4074 (Figure 3.8C and D). These findings suggest that the drought-susceptible wheat variety may be more vulnerable to oxidative damage than the tolerant variety. Similar to the current study, other comparative studies also reported significant differences in the accumulation of MDA in the leaves of drought-susceptible and tolerant/resistant wheat (Marcińska *et al*., 2013; Abid *et al*., 2018; Naderi *et al*., 2020), maize (Anjum *et al*., 2016) and common bean (*Phaseolus vulgaris* L.) (Kusvuran and Dasgan, 2017) varieties under drought stress. The lower MDA content observed in drought-tolerant varieties in the above-mentioned studies and the current one implies that these genotypes have a higher antioxidant capacity than their drought-susceptible counterparts under drought stress conditions.

The high antioxidant capacity of BW35695 was noted from the significant increase in SOD activity in the leaves following 28 days of drought stress (Figure 3.10A). However, in the roots of BW35695, SOD activity remained unchanged (Figure 3.10B). Similar to the current study, other drought-tolerant wheat varieties exhibited higher levels of SOD activity in leaves and shoots under drought stress conditions (Naderi *et al*., 2020; Nasirzadeh *et al*., 2021; Wang *et al*., 2022). In contrast, the drought-susceptible variety BW4074 exhibited a decrease in SOD activity in the leaves and roots under drought stress conditions (Figure 3.10A and B). The decrease in SOD activity may be related to reduced synthesis or enhanced degradation of the enzyme (Huseynova, 2012). Another comparative wheat study also reported a significant decrease in SOD activity in the leaves of drought-sensitive wheat cultivars (Huseynova, 2012). Overall, the SOD activity results of the two wheat varieties suggest that BW35695 was able to protect cellular components from oxidative stress by catalysing the dismutation of O_2^- to H_2O_2 and molecular oxygen (O_2).

Ascorbate and guaiacol peroxidases function in the detoxification of hydrogen peroxide (Gill and Tuteja, 2010). In this study, BW35695 exhibited a significant increase in GPX activity in drought-stressed leaves, while BW4074 showed no change (Figure 3.10C). Other comparative studies also observed increased levels of GPX activity in leaves of drought-tolerant wheat varieties (Huseynova *et al*., 2015; Naderi *et al*., 2020; Dashtaki *et al*., 2023). Similarly, after drought stress treatment, APX activity was also increased in BW35695 roots, however the increase was not statistically significant (Figure 3.11F). The above-mentioned studies and the current one suggest that the observed increase in SOD and GPX in the drought-tolerant varieties could indicate the ability of these varieties to detoxify O_2^- and H_2O_2 and protect cellular components from oxidative damage. Increased antioxidant activities help to improve plant performance under stress conditions by scavenging excess ROS.

Plants also accumulate proline, a compatible solute known to scavenge singlet oxygen and reduce photodamage in the thylakoid membranes under drought stress conditions (Reddy *et al*., 2004). Proline also acts as an osmoprotectant under drought stress conditions (Ashraf and Foolad, 2007). In the current study, proline content increased significantly in the leaves of BW35695 and roots of both varieties after 28 days of drought stress treatment (Figure 3.11A and B). Similarly, increased levels of proline were observed in the leaf tissue of a drought-tolerant wheat genotype under different water regimes (Dashtaki *et al*., 2023). Moreover, the drought-tolerant genotype had an increased amount of proline under severe stress conditions as compared to the sensitive genotype (Dashtaki *et al*., 2023). The high accumulation of proline possibly indicates that drought-tolerant varieties were better able to protect cellular components under drought conditions. Glycine betaine, another compatible solute which also functions in osmotic adjustment and osmoprotection was significantly increased in the leaves of BW35695 and roots of both wheat varieties (Figures 3.11C and D). High levels of glycine betaine have also been reported in the leaves and roots of drought-tolerant varieties of cotton (*Gossypium hirsutum* L) (Prajapat *et al*., 2018) and sorghum (Goche *et al*., 2020). The increased accumulation of both osmolytes in the drought-tolerant wheat variety BW35695 indicates that this variety can better protect cellular components under water deficit conditions than the drought-susceptible variety.

3.5 Conclusion

The morpho-physiological and biochemical analyses revealed different response mechanisms between the wheat varieties following drought stress treatment. The drought-tolerant variety, BW35695 maintained plant water status, increased the levels of photosynthetic pigments and accumulated high levels of osmolytes and antioxidant capacity. Overall, the drought-tolerant variety, BW35695 better tolerated the effects of moderate drought stress as compared to the drought-susceptible variety, BW4074.

CHAPTER 4

COMPARATIVE LEAF PROTEOMIC ANALYSIS BETWEEN WHEAT VARIETIES IN RESPONSE TO DROUGHT STRESS

4.1 Introduction

Abiotic stress factors affect plant proteomes, resulting in changes in protein abundance, cellular localization, post-transcriptional and post-translational modifications, protein interactions, and biological functions (Kosová *et al*., 2018). Numerous researchers have used gel-based and gel-free proteomic methods to analyse protein expressions in plants under diverse stress conditions (Zargar *et al*., 2016; Tan *et al*., 2017; Jan *et al*., 2023). In particular, cereal proteomic studies continue to shed light on how plants adapt to drought stress at the molecular level with a focus on developing drought-tolerant crops (Barkla, 2016; Ghatak *et al*., 2017). Furthermore, plant proteomic studies comparing varieties with contrasting levels of drought tolerance can offer deeper insights into the molecular basis of the different drought phenotypes. Such studies often reveal common and unique drought stress-responsive proteins between the varieties, which may be valuable to plant breeders in their efforts to produce more stress-tolerant plants (Ghatak *et al*., 2017).

Yu *et al*. (2016) conducted a comparative leaf proteome analysis using two-dimensional (2D) gel electrophoresis on two soybean (*Glycine max* L.) genotypes subjected to mild (70-75 % of soil moisture content) and severe (40% of soil moisture content) drought stress. The study found that severe drought resulted in a higher number of differentially expressed proteins compared to mild stress. The drought-responsive proteins were related to energy metabolism and photosynthetic functions, defence response and protein metabolism. Furthermore, the drought-tolerant genotype exhibited a greater ability to scavenge reactive oxygen species

(ROS) compared to the sensitive genotype, with increased levels of ROS detoxification proteins like superoxide dismutase and ascorbate peroxidase being identified. The results suggest that the drought-tolerant soybean genotype was more effective at preventing oxidative damage to cellular components and maintaining redox equilibrium (Yu *et al*., 2016).

Zeng and co-workers (2019) also evaluated differential protein expressions in the roots of two maize (*Zea mays*) varieties subjected to 20% polyethylene glycol (PEG)-6000. The study used the isobaric tags for relative and absolute quantitation (iTRAQ) gel-free method to compare protein expressions of the two maize varieties. Drought-responsive root proteins in the drought-tolerant variety were mainly associated with the ribosome pathway, glycolysis/gluconeogenesis pathway, and amino sugar and nucleotide sugar metabolism. In the drought-sensitive variety, the root proteins were mainly associated with the phenylpropanoid biosynthesis pathway, starch and sucrose metabolism. The drought-tolerant maize variety also had an up-regulation of peroxidases compared to the drought-sensitive variety, which corresponded with observed high levels of non-enzymatic antioxidant activity in the drought-tolerant variety (Zeng *et al*., 2019).

As indicated by the above-mentioned studies, proteomic techniques have been used to unravel plant molecular changes under drought stress. The current chapter used the iTRAQ method to comparatively investigate the differential leaf protein expression patterns of two wheat varieties, BW4074 (drought-susceptible) and BW35695 (drought-tolerant) under drought stress.

4.2 Materials and methods

4.2.1 Leaf protein extraction and quantification

Total soluble leaf proteins were extracted from BW4074 and BW35695 wheat varieties as previously described (Ngara, 2009). Four biological replicates were used for control and drought-stressed leaf samples. Briefly, leaf samples harvested on day 28 of drought stress treatment were stored at -80 °C. The frozen leaf material was ground to a fine powder using sterile frozen mortars and pestles. Approximately 1 g of the powdered leaf material was transferred into 2 ml Eppendorf tubes and homogenised with 10% (w/v) trichloroacetic acid (TCA). The mixture was briefly vortexed and centrifuged at 21 130 × *g* for 10 minutes to pellet the leaf material. All centrifugation steps in this study were done at room temperature unless stated otherwise. The supernatant was discarded, and the pellet was washed three times with ice-cold 80% (v/v) acetone while centrifuging at 21 130 × *g* for 10 minutes. The pellet was then air-dried at room temperature before adding urea extraction buffer [9 M urea, 2 M thiourea and 4% 3-(3-Cholamidopropyl) dimethylammonio]-1-propanesulfonate (CHAPS)] in a 1:1.5 ratio of pellet to buffer. The samples were vigorously vortexed overnight and then centrifuged at 21 130 × *g* for 10 minutes. The supernatant containing leaf total soluble protein was collected and stored at -20 °C. The concentrations of the leaf protein extracts were determined using a modified Bradford assay as described in Section 3.2.3.7.1 with the urea extraction buffer as the diluent.

4.2.2 One-dimensional (1D) sodium dodecyl sulfate-polyacrylamide gel electrophoresis (SDS-PAGE)

The quantified leaf protein extracts from both wheat varieties were visually analysed on a 1D SDS-PAGE as described by Laemmli (1970). The gels were prepared on 1 mm thick glass plates using the Mini-PROTEAN® Tetra Cell gel casting system (BIO-RAD, Hercules, California, USA) according to the manufacturer’s instructions. Resolving gels of 12% (v/v) and stacking gels of 5% (v/v) were prepared as indicated in Appendix, Table A1.2.

Protein samples were prepared at a ratio of 1:1 with 2X sample buffer [100 mM Tris-HCL pH 6.8, 200 mM (w/v) DTT, 4% (w/v) SDS, 20% glycerol and a pinch of bromophenol blue] in a 1.5 ml Eppendorf tube. The mixture was pulse vortexed, centrifuged, and incubated on a heat block for 5 minutes at 100 °C. The denatured protein samples and a P77045 Unstained Protein Standard, Broad Range (New England Biolabs Inc., Massachusetts, USA) were loaded into the gels. Gel electrophoresis was carried out using electrode running buffer [25 mM Tris, 192 mM glycine, 0.1% (w/v) SDS] on a Mini PROTEAN Tetra Cell (BIO-RAD) using a Basic PowerPac (BIO-RAD). The gels were run at 100 V for 30 minutes before increasing the voltage to 150 until the bromophenol blue dye began running out of the gel plates.

After gel electrophoresis, the gels were stained with three Coomassie Brilliant Blue (CBB) R-250 staining solutions. The gels were first placed in warm Coomassie I [0.025% (w/v) CBB R-250, 10% (v/v) glacial acetic acid and 25% (v/v) propan-2-ol] followed by Coomassie II [0.003% (w/v) CBB R-250, 10% (v/v) glacial acetic acid and 10% (v/v) propan-2-ol] for 30 minutes each with gentle shaking. Lastly, the gels were stained with Coomassie III [0.003% (w/v) CBB R-250 and 10% (v/v) glacial acetic acid] while shaking overnight. Thereafter, the gels were immersed in a destaining solution [40% (v/v) acetic acid and 10% (v/v) glycerol] while shaking until the gel background was clear. The gels were scanned and documented using a Molecular Imager Gel Doc™ XR+ with Image Lab™ software version 5.2.1 (BIO-RAD, Hercules, USA).

4.2.3 Acetone precipitation of protein samples

Leaf protein extracts were precipitated with 80% (v/v) acetone and placed on a bench top for 2 hours before incubating at -20 °C overnight. After incubation, the samples were centrifuged at 21 300 × *g* for 10 minutes, and the supernatant was carefully discarded. The protein pellets were washed twice with ice-cold 80% (v/v) acetone while centrifuging at 21 300 × *g* for 10 minutes. Thereafter, 100 µl of ice-cold 80% (v/v) acetone was added to the protein pellets and sent to Durham University in the United Kingdom for iTRAQ and mass spectrometry analyses. The iTRAQ data analysis and bioinformatics of the identified drought-responsive leaf proteins were done at the University of the Free State, Qwaqwa Campus.

4.2.4 iTRAQ and liquid chromatography-mass spectrometry (LC-MS) analyses

4.2.4.1 Sample preparation for iTRAQ analysis

An iTRAQ method as previously described by Goche *et al.* (2020) was followed to analyse BW4074 and BW35695 wheat leaf protein samples. The acetone-precipitated leaf protein samples were re-solubilised in appropriate buffers before iTRAQ analysis. Briefly, the leaf protein precipitate in acetone were centrifuged at 15 000 × *g* for 5 minutes, and the supernatant was discarded. Thereafter, the protein pellets were air-dried at room temperature, resuspended in 100 µl urea buffer and centrifuged at 15 000 × *g* for 10 minutes. Thereafter, the supernatant was collected and quantified using the Bradford assay (Section 3.2.3.7.1). To visually analyse the protein quality, the protein samples were electrophoresed on a 12% (v/v) SDS polyacrylamide gel (Section 4.2.2).

4.2.4.2 iTRAQ sample labelling

The iTRAQ sample labelling was carried out on four biological replicates of control and drought-stressed leaf protein samples of each wheat variety. For each leaf sample, 10 µg of protein was used for iTRAQ labelling. Briefly, the leaf protein samples were acetone precipitated overnight at -20 °C, centrifuged for 10 minutes at 15 000 × *g* and air-dried. The air-dried protein samples were resolubilised using an iTRAQ Reagent-Multiplex Buffer Kit (Applied Biosystems Sciex, Redwood City, USA), following the manufacturer's instructions. A 2.5 µl denaturant solution was added to each pellet and incubated at 60 °C for an hour. Thereafter, 47.5 µl of dissolution buffer was added, and the samples were vortexed for 20 minutes and centrifuged at 15 000 × *g* for 10 minutes. The supernatant was collected and reduced with 1 µl tris (2-carboxyethylphosphine) (TCEP).

The samples were alkylated with 0.5 µl methyl-methane-thiol-sulfonate (MMTS), vortexed, and incubated at room temperature for 10 minutes. After incubation, the protein samples were digested using a 1:10 (w/w) trypsin (Promega, Madison, USA) overnight at 37 °C. The samples were vacuum-dried and resuspended in MilliQ water, and the pH was adjusted to 7.5 using the dissolution buffer. The samples were then labelled using an 8-plex iTRAQ reagent kit (AB Sciex) following the manufacturer's instructions. Four biological control replicates of each wheat variety were labelled using molecular weight tags 113, 114, 115, and 116, while the drought-stressed samples were labelled with 117, 118, 119, and 121. After labelling, the control and drought stress samples of each wheat variety were pooled into one tube, briefly vortexed and centrifuged before redistributing into two tubes before being vacuum-dried.

4.2.4.3 iTRAQ sample clean-up

Sample clean-up was conducted as described by Goche *et al.* (2020) using Hydrophilic Interaction Liquid Chromatography (HILIC) SPE cartridges (PolyLC Inc.). These cartridges contained 300 mg of 12 µm polyhydroxyethyl-A, used to remove unincorporated labels and buffer salts. The cartridges were first equilibrated by adding 4 x 3 ml releasing solution (5%

acetonitrile (ACN), 30 mM ammonium formate pH 3.0), followed by 4 x 3 ml binding solution (85% ACN, 30 mM ammonium formate pH 3.0). The dried iTRAQ-labelled peptides were dissolved in 75 µl of 3% ACN, 0.1% formic acid (FA), followed by the addition of 150 µl 0.3 M ammonium formate, pH 3. The pH of the mixture was checked and trifluoroacetic acid (TFA) was used to adjust the pH to 3.0. The solution was clarified by centrifuging at 10 000 × *g* for 10 minutes and then combined with 1 275 µl of ACN. The 1.5 ml sample was transferred to the SPE cartridge, and the flow-through was retained and passed through a second time. The column was rinsed twice with 2 ml of the binding solution, and the peptides were then eluted using 2 x 1 ml releasing solutions. The eluate was freeze-dried and resuspended in a solution containing 3% ACN and 0.1% FA for liquid chromatography-mass spectrometry analysis.

4.2.4.4 LC-MS analysis

Liquid chromatography-mass spectrometry was performed following a method described by Goche *et al*. (2020). A TripleTOF 6600 mass spectrometer (AB Sciex) linked to an Eksigent 425 LC system via a Sciex Nanospray III source was used for the LC-MS analysis. Peptides originating from 5 µg of protein were used for each LC-MS run and the chromatographic separations of peptides utilised a trap and elute method. Samples were washed on a Triart C18 guard column 1/32", 5 µm, 5 x 0.5 mm (YMC) acting as a trap, and online separation of peptides was performed on a TriArt C18 1/32", 3 µm, 150 x 0.3 mm column (YMC) over 87 minutes at a flow rate of 5 µl/minute. Two buffers were prepared, buffer A (0.1% FA in water) and buffer B (0.1% FA in ACN). Sequential linear gradients of 3 to 5% B over 2 minutes, 5 to 30% buffer B over 66 minutes, 30 to 35 % B over 5 minutes and 35 to 80% B over 2 minutes were followed by a 3-minute column wash in 80% B. Return to 3% B was over 1 minute before column re-equilibration for 8 minutes. Data-dependent top-30 MS-MS acquisition, with collision energy adjusted for iTRAQ-labelled peptides, was initiated immediately for 85 minutes. Precursor-ion scans (400 to 1600 m/z) of 250 ms enabled the selection of up to 30 multiply-charged ions (>500 cps) for collision-induced dissociation fragmentation and MS/MS spectrum acquisition (m/z 100-1500) for 50 ms. A cycle time of 1.8 seconds and a rolling precursor exclusion of 15 seconds was applied to limit multiple fragmentation of the same peptide. Spectrometer data was acquired using the Analyst TF 1.7.1 instrument control and data processing software (AB Sciex).

4.2.4.5 Mass spectra data analysis

A method previously described by Goche *et al.* (2020) was used to analyse the mass spectra data. Protein identification and quantification was performed by processing the raw data files against a TrEMBL database sequences (downloaded July 2022) of *Triticum aestivum* using the ProteinPilot™ 5.0.1 version 4895 software, incorporating the Paragon Algorithm 5.0.1.0.4874 (AB Sciex). An iTRAQ 8-plex peptide-labelled Paragon method, for tryptic peptides with iodoacetamide cys-modification and data acquired on a TripleTOF 6600 spectrometer, was used. Label bias correction was applied to the data and the 'Thorough ID' and 'Run False Discovery Rate Analysis' options were selected, with the Detected Protein Threshold set at 0.05 (10%) [Unused ProtScore (conf)]. Peptide and protein tables were exported from ProteinPilot for manual data processing and filtering. A minimum threshold of 1.3 at a 95% confidence interval was established for each identified peptide, and a minimum score threshold of 2.0 at a 99% confidence interval was established for protein identification. All proteins were identified based on at least a single peptide.

The abundance of each drought-responsive leaf protein was calculated as a ratio to the 113-tagged control sample in each wheat variety. The average ratios for all control and drought-stressed samples were also calculated. The fold-change in protein expression was denoted by the ratio of the control average to the drought-stressed average. Downregulated proteins were denoted with a negative sign, where the drought stress sample averages were the numerators with the control averages as the denominators. A Student's *t*-test was conducted to compare control and drought-stressed samples at a confidence level of 95%.

4.2.5 Bioinformatics analysis of differentially expressed proteins

The UniProt database http://www.uniprot.org (The UniProt Consortium, 2023) was used to determine the biological processes, molecular functions, and cellular components of the drought-responsive leaf proteins. Family names of the identified proteins were determined using the InterPro database http://www.ebi.ac.uk/interpro/ (Paysan-Lafosse *et al*., 2023). A pathway enrichment analysis on the Kyoto Encyclopedia of Genes and Genomes (KEGG) database http://bioinformatics.sdstate.edu/go/ (Kanehisa and Goto, 2000) was used to analyse the functions of the drought-responsive proteins using gene IDs as input data. A False discovery rate was calculated using the Benjamini-Hochberg method.

Protein-protein interaction networks of the drought-responsive proteins were predicted using the Search Tool for Retrieval of Interacting Genes/Proteins (STRING) version 12.0 database https://string-db.org/ (Szklarczyk *et al*., 2023). The STRING network parameters were selected as follows: (i) Full STRING network (the edges indicate both functional and physical protein associations), (ii) Confidence edge, (iii) Active interaction sources (Textmining, Experiments, Databases, Co-expression, Neighbourhood, Gene fusion and Co-occurrence) and (iv) Confidence score was 0.4.

4.3 Results

4.3.1 One-dimensional leaf protein profiles of BW4074 and BW35695 wheat plants

Total soluble leaf proteins extracted from the control and drought-stressed wheat samples were visually analysed on Coomassie Brilliant Blue-stained 1D gels to evaluate the quantity and quality of the samples. Figure 4.1 shows the leaf protein expression patterns of the control and drought-stressed samples of the two wheat varieties. The results showed good quality of the leaf extracts in both wheat varieties. It was observed that in BW35695, there was an up-regulation (red-arrows) of proteins between the molecular range of 15 and 20 kDa and a down-regulation (blue-arrow) around 40 kDa. In contrast, BW4074, protein expression patterns were relatively similar between the control and drought-stressed samples.

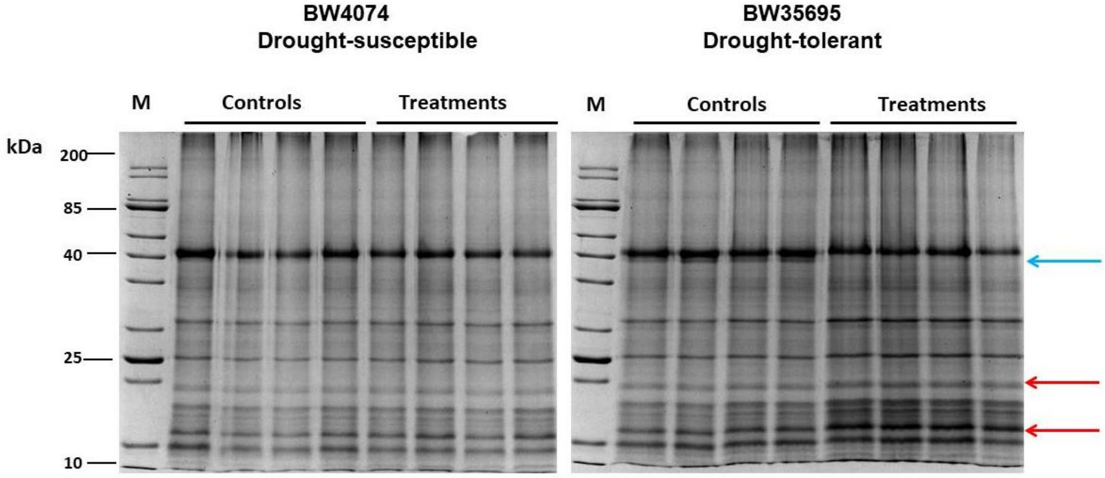

Figure 4.1: Leaf proteomes of BW4074 and BW35695 wheat varieties analysed on a 1D gel. Each 12% (v/v) SDS-PAGE gel was loaded with 10 µg of the leaf protein. Lane M in both gels represents the protein molecular weight marker (kDa). The first four lanes of each gel are the control biological replicate leaf protein extracts, followed by the drought-stressed biological replicate leaf protein extracts. The gels were stained with Coomassie Brilliant Blue and scanned using a Molecular Imager Gel Doc™ XR+ with Image Lab™ Software version 5.2.1 (BIO-RAD).

4.3.2 iTRAQ analysis of drought-responsive wheat leaf proteins

Following a visual comparison of protein expressions in control and drought-stressed leaf samples (Figure 4.1), 10 µg of protein from each leaf sample of BW4074 and BW35695 was used for iTRAQ analysis and protein identification. Four biological replicate samples were labelled with the iTRAQ molecular weight tags, separated, and identified using LC-MS analysis (Section 4.2.4). A total of 1062 and 882 leaf proteins were positively identified in BW4074 and BW35695 wheat varieties, respectively. Out of the 1062 positively identified proteins in BW4074, 69 were differentially expressed in response to drought stress at a 95% significance level (Table 4.1). For BW35695, 110 of the 882 positively identified proteins were responsive to drought stress treatment (Table 4.1). Furthermore, in BW4074, 41 (59%) proteins were upregulated whilst 28 (41%) were downregulated. For BW35695, 58 (53%) proteins were upregulated, while 52 (47%) were downregulated. A summary of the proteome data is shown in Table 4.1. From the sets of differentially expressed proteins (Table 4.1), nine were common to both wheat varieties, while 60 and 101 were unique to BW4074 and BW35695, respectively (Figure 4.2). Of the nine common proteins, six were upregulated while three were downregulated in both wheat varieties.

Table 4.1: Summary of wheat leaf protein counts obtained from the iTRAQ data.

Wheat variety	Positively identified proteins	Drought-responsive proteins	Upregulated proteins	Downregulated Proteins
BW4074	1062	69	41	28
BW35695	882	110	58	52

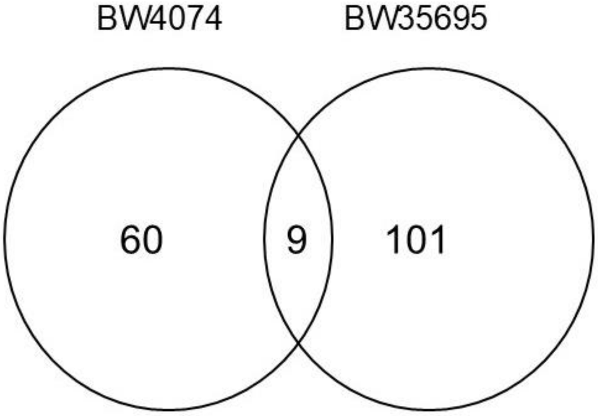

Figure 4.2: A Venn diagram showing the number of drought-responsive leaf proteins of two wheat varieties. BW4074 is the drought-susceptible variety while BW35695 is drought-tolerant.

The UniProt and InterPro databases were used to retrieve Gene Ontology (GO) data and protein family names of the drought-responsive proteins, and the information was used to functionally group the proteins. The GO terms, protein family names, and the putative functional categories of the drought-responsive proteins are shown in Tables 4.2 and 4.3 for BW4074 and BW35695 wheat varieties, respectively.

Table 4.2: List of drought-responsive leaf proteins of the drought-susceptible wheat variety BW4074 identified using iTRAQ and LC-MS/MS.

No.[a]	Accession[b]	Protein name	Scor[c]	% Cov[d]	Seq. Pep[e]	Ratio[f]	SD[g]	p-value[h]	Gene ontology analysis[i]			Family name[j]
									P	F	C	
Primary metabolism												
11	A0A3B6MJZ2	5-methyltetrahydropteroyltriglutamate-homocysteine S-methyltransferase OS=*Triticum aestivum*	38.07	30.26	20	1.47	0.07	1.59E-04	Methionine biosynthetic process	Methyltransferase activity	None	Cobalamin-independent methionine synthase
71	A0A3B6DM57	Lipoxygenase OS=*Triticum aestivum*	46.66	24.49	25	1.22	0.09	5.04E-03	Fatty acid biosynthetic process	Oxidoreductase activity	None	Lipoxygenase, plant
104	A0A3B6GPF7	Glutamate decarboxylase OS=*Triticum aestivum*	12.57	18.16	8	1.29	0.12	6.48E-03	Glutamate metabolic process	Glutamate decarboxylase activity	Cytosol	Glutamate decarboxylase
106	A0A3B6U5R3	Acid phosphatase OS=*Triticum aestivum*	13.55	25.71	8	1.44	0.18	1.87E-02	None	Acid phosphatase activity	None	Acid phosphatase, plant
147	A0A3B6JRZ2	Apyrase OS=*Triticum aestivum*	10.46	12.1	5	1.36	0.29	4.90E-02	Nucleoside diphosphate catabolic process	Nucleoside diphosphate phosphatase activity	Membrane	Nucleoside phosphatase GDA1/CD39
202	A0A3B6C6N3	Beta-amylase OS=*Triticum aestivum*	8.08	11.66	4	-1.27	0.07	1.31E-02	Polysaccharide catabolic process	Beta-amylase activity	None	Glycosyl hydrolase, family 14B plant
235	A0A3B6QIZ3	S-adenosylmethionine synthase OS=*Triticum aestivum*	7.28	9.898	5	1.35	0.09	2.99E-03	S-adenosylmethionine biosynthetic process	Methionine adenosyltransferase activity	Cytosol	S-adenosyl methionine synthetase
268	A0A3B6H4R5	2-hydroxyacyl-CoA lyase OS=*Triticum aestivum*	6.44	8.377	3	1.39	0.11	1.36E-02	Fatty acid alpha-oxidation	Thiamine pyrophosphate binding	Peroxisome	TPP-binding domain-containing protein HACL1-like
417	A0A3B6QKI8	GDSL esterase/lipase OS=*Triticum aestivum*	4	13.67	2	-1.86	0.22	1.29E-02	None	Hydrolase activity, acting on ester bonds	None	GDSL lipase/esterase-like, plant
431	A0A1D5URN5	Fibronectin type III-LIKE domain-containing protein OS=*Triticum aestivum*	3.97	4.534	2	-1.55	0.08	2.99E-02	Xylan catabolic process	Xylan 1,4-beta-xylosidase activity	Extracellular region	Beta-D-xylosidase
588	A0A077RPJ4	Tryptophan synthase OS=*Triticum aestivum*	2.19	10.85	2	-1.67	0.19	4.51E-02	Tryptophan biosynthetic process	Tryptophan synthase activity	Cytosol	Tryptophan synthase, alpha chain
664	Q45NB2	Glutamine synthetase OS=*Triticum aestivum*	17.88	39.11	15	-1.68	0.26	3.75E-02	Glutamate biosynthetic process	Glutamine synthetase activity	Cytoplasm	Glutamine synthetase

741	A0A3B6FGE7	Enoyl reductase (ER) domain-containing protein OS=*Triticum aestivum*	2	7.062	1	1.89	0.41	2.32E-02	None	Oxidoreductase activity	None	Medium-chain dehydrogenase/ reductase
760	A0A3B6DHI0	Glutamate dehydrogenase OS=*Triticum aestivum*	2	2.691	1	-2.08	0.19	4.52E-02	Glutamate catabolic process	Glutamate dehydrogenase activity	Mitochondrion	Glutamate dehydrogenase
871	W5ACM8	Delta-1-pyrroline-5-carboxylate synthase OS=*Triticum aestivum*	1.73	1.676	1	1.52	0.24	3.17E-02	Proline biosynthetic process	Glutamate-5-semialdehyde dehydrogenase activity	Cytoplasm	Delta-l-pyrroline-5-carboxylate synthetase
1013	A0A3B6MSL2	Aminocyclopropanecarboxylate oxidase OS=*Triticum aestivum*	1.1	4.389	1	1.58	0.36	2.09E-02	None	Oxidoreductase activity	None	Plant 2-oxoglutarate-dependent oxidoreductases
Protein synthesis/folding/degradation												
22	W5CXB0	Heat shock 70 kDa protein, mitochondrial OS=*Triticum aestivum*	27.46	22.81	14	1.12	0.04	4.01E-02	Protein refolding	Unfolded protein binding	Cytoplasm	Heat shock protein 70 family
167	Q5I7L1	Ribosomal protein L13a OS=*Triticum aestivum*	9.56	22.82	5	1.18	0.06	1.57E-02	Translation	Structural constituent of ribosome	Ribosome	Large ribosomal subunit protein uL13, eukaryotic/archaeal
242	Q5I7K4	Ribosomal protein L17 OS=*Triticum aestivum*	7.12	25	4	1.19	0.10	1.99E-02	Translation	Structural constituent of ribosome	Ribosome	Large ribosomal subunit protein uL14
251	E2F3W4	Small ribosomal subunit protein uS8c OS=*Triticum aestivum*	6.89	23.08	4	-1.19	0.04	3.21E-03	Translation	Structural constituent of ribosome	Ribosome	Small ribosomal subunit protein uS8
271	A0A3B6MTE3	Peptidylprolyl isomerase OS=*Triticum aestivum*	6.3	18.92	3	1.28	0.15	3.72E-02	None	Peptidyl-prolyl cis-trans isomerase activity	None	Peptidyl-prolyl cis-trans isomerase FKBP18-like
390	W5I1R7	30S ribosomal protein S3, chloroplastic OS=*Triticum aestivum*	4.06	13.22	2	1.63	0.18	8.04E-03	Translation	Structural constituent of ribosome	Ribosome	Small ribosomal subunit protein uS3
465	A0A3B6TJK6	Small ribosomal subunit protein uS10 domain-containing protein OS=*Triticum aestivum*	3.54	12.26	2	1.64	0.40	2.86E-02	Translation	Structural constituent of ribosome	Ribosome	Small ribosomal subunit protein uS10
467	A0A3B6A2M8	50S ribosomal protein L12, chloroplastic OS=*Triticum aestivum*	3.49	13.97	2	-1.38	0.12	2.42E-02	Translation	Structural constituent of ribosome	Ribosome	Large ribosomal subunit protein bL12
507	W5H9B7	Peptidyl-prolyl cis-trans isomerase OS=*Triticum aestivum*	3	13.3	2	-1.57	0.21	3.52E-02	Protein folding	Peptidyl-prolyl cis-trans isomerase activity	Cytoplasm	Cyclophilin-type peptidyl-prolyl cis-

												trans isomerase/CLD
683	A0A2X0SLI3	40S ribosomal protein S6 OS=*Triticum aestivum*	4.65	11.6	2	1.94	0.33	4.09E-02	Translation	Structural constituent of ribosome	Ribosome	Small ribosomal subunit protein eS6-like
869	W5D1B3	Trigger factor ribosome-binding bacterial domain-containing protein OS=*Triticum aestivum*	1.77	4.4	1	-1.47	0.20	4.54E-02	Protein folding	Peptidyl-prolyl cis-trans isomerase activity	None	Trigger factor
1014	W5D1D3	30S ribosomal protein S20, chloroplastic OS=*Triticum aestivum*	2.17	3.191	1	-1.27	0.08	2.50E-02	Translation	Structural constituent of ribosome	Ribosome	Small ribosomal subunit protein bS20
1050	A0A3B6QHV4	Anion-transporting ATPase-like domain-containing protein OS=*Triticum aestivum*	0.84	3.275	1	-1.68	0.25	2.63E-02	Post-translational protein targeting to ER membrane	ATP hydrolysis activity	GET complex	Arsenical pump ATPase, ArsA/GET3
1210	A0A3B6HY00	Sigma 54 modulation/S30EA ribosomal protein C-terminal domain-containing protein OS=*Triticum aestivum*	7.26	20.13	6	1.29	0.20	4.50E-02	Negative regulation of translation elongation	Ribosomal small subunit binding	Cytosolic small ribosomal subunit	Ribosome hibernation promoting factor, long/plastid
Defence/ROS detoxification												
143	Q96123	Superoxide dismutase [Cu-Zn] OS=*Triticum aestivum*	10.63	46.77	10	1.32	0.07	1.06E-03	Removal of superoxide radicals	Superoxide dismutase activity	Chloroplast	Superoxide dismutase (Cu/Zn) / superoxide dismutase copper chaperone
148	A0A3B6HMK6	Glutathione reductase OS=*Triticum aestivum*	10.49	17.45	7	1.94	0.66	4.69E-02	Cell redox homeostasis	Glutathione-bisulfide (NADPH) reductase activity	Cytoplasm	Glutathione reductase
295	A7VL25	Group3 late embryogenesis abundant protein OS=*Triticum aestivum*	5.9	18.08	3	1.38	0.07	3.02E-02	None	None	None	None predicted
395	O82715	Pathogenesis related protein-1.2 OS=*Triticum aestivum*	4.04	21.97	4	-1.29	0.02	2.53E-03	Response to biotic stimulus	None	Extracellular space	Venom allergen 5-like
418	A0A3B6CH98	Peroxidase OS=*Triticum aestivum*	4	7.038	2	-1.48	0.10	2.23E-02	Response to oxidative stress	Peroxidase activity	Extracellular region	Plant peroxidase
427	S6AWC2	Cold induced 16 OS=*Triticum aestivum*	4.06	13.29	2	1.68	0.42	4.43E-02	Regulation of abscisic acid biosynthetic process	None	None	Nodulin-related protein1/2
512	H9NAV6	Superoxide dismutase [Cu-Zn] OS=*Triticum aestivum*	2.95	13.16	1	1.45	0.34	4.82E-02	Removal of superoxide radicals	Superoxide dismutase activity	None	Superoxide dismutase (Cu/Zn) / superoxide

												dismutase copper chaperone
811	A0A3B6TKC6	Monodehydroascorbate reductase (NADH) OS=*Triticum aestivum*	2.16	5.357	2	1.32	0.16	3.66E-02	None	Oxidoreductase activity	Cytoplasm	FAD-dependent oxidoreductases and apoptosis regulators
937	D8L9B5	Putative PDI-like protein OS=*Triticum aestivum*	1.46	2.955	1	-2.57	0.11	1.11E-02	Response to endoplasmic reticulum stress	Protein-disulfide reductase activity	Endoplasmic reticulum lumen	Protein disulfide isomerase A6
Energy												
5	A0A3B5Z298	Phosphoglycerate kinase OS=*Triticum aestivum*	49.11	39.26	30	-1.51	0.22	4.29E-02	Glycolytic process	Phosphoglycerate kinase activity	Cytosol	Phosphoglycerate kinase family
49	A0A3B6FUA0	Fructose-bisphosphate aldolase OS=*Triticum aestivum*	20.09	35.57	14	1.71	0.27	2.64E-03	Glycolytic process	Fructose-bisphosphate aldolase activity	Cytosol	Fructose-bisphosphate aldolase, class I
68	A0A3B6TBB9	Ferredoxin--NADP reductase, chloroplastic OS=*Triticum aestivum*	15.94	30.11	13	-2.02	0.31	1.77E-02	Photosynthesis	Ferredoxin-NADP+ reductase activity	Chloroplast	Ferredoxin-NADP reductase
81	A0A3B6KSW8	Glyceraldehyde-3-phosphate dehydrogenase OS=*Triticum aestivum*	23.65	32.21	22	-1.68	0.18	4.84E-02	Glucose metabolic process	Glyceraldehyde-3-phosphate dehydrogenase activity	None	Glyceraldehyde-3-phosphate dehydrogenase, type 1
96	A0A3B6QKY1	Aconitate hydratase OS=*Triticum aestivum*	14.01	9.026	7	1.26	0.16	4.17E-02	Citrate metabolic process	Aconitate hydratase activity	Cytosol	Aconitase/Iron-responsive element-binding protein 2
165	A0A3B6QBJ3	Acetyltransferase component of pyruvate dehydrogenase complex OS=*Triticum aestivum*	9.67	7.38	6	-1.42	0.15	2.45E-02	Acetyl-CoA biosynthetic process from pyruvate	Acetyltransferase activity	Cytoplasm	Dihydrolipollysine-residue acetyltransferase component of pyruvate dehydrogenase complex
175	A0A3B6LW58	Glucose-1-phosphate adenylyltransferase OS=*Triticum aestivum*	9.36	12.55	5	1.21	0.09	3.34E-02	Starch biosynthetic process	Glucose-1-phosphate adenylytransferase activity	Chloroplast	Glucose-1-phosphate adenylytransferase
182	A0A3B6TJ01	Pyruvate dehydrogenase E1 component subunit beta OS=*Triticum aestivum*	8.87	16.12	5	1.43	0.16	4.63E-02	Acetyl-CoA biosynthetic process from pyruvate	Pyruvate dehydrogenase activity	Pyruvate dehydrogenase complex	Pyruvate dehydrogenase E1 component subunit beta
252	A0A3B6RKE8	Glyceraldehyde-3-phosphate dehydrogenase OS=*Triticum aestivum*	20.62	34.2	17	1.33	0.20	3.54E-02	Glucose metabolic process	Glyceraldehyde-3-phosphate dehydrogenase activity	Cytosol	Glyceraldehyde-3-phosphate dehydrogenase, type 1

274	A0A3B6QKZ9	ATP synthase delta chain, chloroplastic OS=*Triticum aestivum*	6.34	32.4	6	-1.27	0.08	8.97E-03	ATP biosynthetic process	Proton-transporting ATP synthase activity, rotational mechanism	Membrane	ATPase OSCP/delta subunit
518	A0A3B6MR18	Phosphoenolpyruvate carboxylase OS=*Triticum aestivum*	4.8	2.366	2	1.37	0.23	4.38E-02	Tricarboxylic acid cycle	Phosphoenolpyruvate carboxylase activity	Cytosol	PEPCase type 1
537	P69415	Photosystem I iron-sulfur center OS=*Triticum aestivum*	2.86	19.75	3	-1.46	0.19	3.80E-02	Photosynthesis	4 iron, 4 sulfur cluster binding	Photosystem I	Photosystem I protein PsaC
701	A0A3B6BY66	Dihydrolipoyllysine-residue succinyltransferase OS=*Triticum aestivum*	2.04	4.684	1	-1.61	0.18	3.67E-02	Tricarboxylic acid cycle	Dihydrolipoyllysine-residue succinlytransferase activity	Mitochondrion	Dihydrolipoamide succinyltransferase
773	Q35980	30 kDa subunit of complex I NADH dehydrogenase OS=*Triticum aestivum*	2	3.833	1	-1.24	0.05	1.10E-02	Electron transport chain	NADH dehydrogenase (ubiquinone) activity	Mitochondrion	None predicted
1089	A0A3B6EQ45	Uncharacterized protein OS=*Triticum aestivum*	0.74	3.712	2	1.28	0.12	2.73E-02	Pentose-phosphate shunt	Transaldolase activity	Cytoplasm	Transaldolase type 2
1371	A0A3B6BZB5	Transketolase OS=*Triticum aestivum*	4.85	1.42	2	-1.88	0.04	1.89E-02	Pentose-phosphate shunt	Transketolase activity	Cytosol	Transketolase, bacterial-like
Transcription												
470	A0A3B6LSN3	MBD domain-containing protein OS=*Triticum aestivum*	3.44	5.684	2	1.36	0.20	3.57E-02	Transcription regulation	DNA binding	Nucleus	Methyl-CpG binding domain-containing protein 10/11
454	A0A3B6LV22	H15 domain-containing protein OS=*Triticum aestivum*	11.01	18.97	6	1.50	0.19	4.14E-03	Negative regulation of DNA recombination	Nucleosomal DNAbinding	Nucleus	Linker histone H1/H5
1051	A0A3B6A3G3	Hyaluronan/mRNA-binding protein domain-containing protein OS=*Triticum aestivum*	0.84	4.011	1	1.99	0.59	2.54E-02	None	RNA binding	Nucleus	RNA binding protein HABP4/SERBP1-like
Secondary metabolism												
174	A0A3B6QF91	Phenylalanine ammonia-lyase OS=*Triticum aestivum*	9.34	10.65	5	1.39	0.09	5.53E-03	L-phenylalanine catabolic process	Phenylalanine ammonia-lyase activity	Cytoplasm	Phenylalanine ammonia-lyase
184	A0A3B6IV90	CN hydrolase domain-containing protein OS=*Triticum aestivum*	8.75	16.38	4	1.10	0.04	1.26E-02	Oxaloacetate metabolic process	Omega-amidase activity	None	Carbon-nitrogen hydrolase superfamily
510	A0A3B6C785	Zeta-carotene desaturase OS=*Triticum aestivum*	2.93	4.401	2	-1.50	0.18	4.20E-02	Carotenoid biosynthetic process	Oxidoreductase activity	Chloroplast	Zeta-carotene desaturase

742	A0A3B6DPV0	AB hydrolase-1 domain-containing protein OS=*Triticum aestivum*	2	5.764	1	-1.78	0.07	3.66E-02	None	Catalytic activity	None	Epoxide hydrolase-like
Cell structure												
636	A0A3B6SEK0	Cyanobacterial aminoacyl-tRNA synthetase CAAD domain-containing protein OS=*Triticum aestivum*	2.05	10.76	2	-1.87	0.19	2.29E-02	None	None	Chloroplast thylakoid membrane	Protein curvature thylakoid I
Unclear classification												
101	A0A3B5XTY5	Cupin type-1 domain-containing protein OS=*Triticum aestivum*	12.77	21.51	7	1.35	0.17	4.73E-02	None	Nutrient reservoir activity	None	11-S seed storage protein, plant
250	A0A3B6MQA1	RRM domain-containing protein OS=*Triticum aestivum*	6.96	22.54	4	1.20	0.05	4.00E-02	None	RNA binding	Ribonucleoprotein complex	Eukaryotic RNA-binding
309	A0A3B6EP73	Uncharacterized protein OS=*Triticum aestivum*	5.62	15.13	3	1.40	0.20	2.29E-02	None	None	None	None predicted
323	A0A3B6FKP0	PH domain-containing protein OS=*Triticum aestivum*	5.21	10.76	3	1.71	0.34	7.96E-03	None	None	None	Ricin B-like lectin EULS3-like
618	A0A3B6TCF4	Uncharacterized protein OS=*Triticum aestivum*	2.06	3.303	1	1.23	0.09	2.76E-02	SNARE complex assembly	SNARE binding	Endosome	None predicted
647	A0A3B5XZW3	Remorin C-terminal domain-containing protein OS=*Triticum aestivum*	2.02	6.78	1	-1.65	0.02	1.98E-02	None	None	None	None predicted

---

[a] Protein number assigned in the ProteinPilot software.

[b] Protein accession number from the UniProt database (http://www.uniprot.org) searches against sequences of *Triticum aestivum* only, accessed on 6 June 2024.

[c] Protein score generated by ProteinPilot software relating to the confidence of protein identification.

[d] Percentage coverage is determined by the number of amino acids of sequenced peptides against the total length of the protein, with a threshold of at least 95% confidence.

[e] Sequenced peptide refers to the number of peptides sequenced. All positively identified proteins were identified based on a single peptide.

[f] Ratio represents the average fold change. A positive value indicates upregulation, while a negative value indicates downregulation.

[g] Standard deviation obtained from comparing control and treatment values.

[h] Probability-value of the quantified difference between the control and drought-stressed leaf proteins.

[i] Gene ontology analysis as predicted from the UniProt database (http://www.ebi.ac.uk/QuickGO/). P=Biological Process, F=Molecular Function, and C= Cellular Component.

j Protein amily names as predicted by the InterPro database (http://www.ebi.ac.uk/interpro/) accessed on 6 June 2024.

Table 4.3: List of drought-responsive leaf proteins of the drought-tolerant wheat variety BW35695 identified using iTRAQ and LC-MS/MS.

No.[a]	Accession[b]	Protein name	Scor[c]	% Cov[d]	Seq. Pep[e]	Ratio[f]	SD[g]	p-value[h]	Gene ontology analysis[i]			Family name[j]
									P	F	C	
Primary metabolism												
17	A0A2X0S1W6	Glutamate synthase (ferrodoxin) OS=*Triticum aestivum* GN=CAMPLR22A2D_LOCUS1173	28.93	11.77	18	-1.12	0.07	2.30E-02	Glutamate biosynthetic process	Glutamate synthase (NADH) activity	None	Electron transfer and nitrogen metabolism enzyme
24	A0A3B6PIU3	Enoyl reductase (ER) domain-containing protein OS=*Triticum aestivum*	26.37	46.74	15	1.34	0.12	6.13E-03	None	Oxidoreductase activity	None	NADPH-dependent oxidoreductase AOR-like
36	A0A3B6MJZ2	5-methyltetrahydropteroyltriglutamate--homocysteine S-methyltransferase OS=*Triticum aestivum*	22.4	18.05	12	1.37	0.18	7.84E-03	Methionine biosynthetic process	Methyltransferase activity	None	Cobalamin-independent methionine synthase
44	A0A3B6GU52	Glycine cleavage system P protein OS=*Triticum aestivum*	20.23	15.62	15	-1.17	0.06	1.35E-02	Glycine catabolic process	Glycine dehydrogenase (decarboxylating) activity	Mitochondrion	Glycine dehydrogenase (decarboxylating)
99	A0A3B6UC94	Acid phosphatase OS=*Triticum aestivum*	12.22	30.36	7	2.05	0.28	5.05E-04	None	Acid phosphatase activity	None	Acid phosphatase, plant
177	A0A3B6FKL0	Nucleoside phosphorylase domain-containing protein OS=*Triticum aestivum*	7.75	21.61	5	1.66	0.27	3.78E-03	Nucleoside metabolic process	Catalytic activity	None	Phosphorylase superfamily
191	A0A3B6H1E6	Glucan endo-1,3-beta-D-glucosidase OS=*Triticum aestivum*	7.2	22.26	4	1.21	0.17	4.73E-02	Carbohydrate metabolic process	Hydrolase activity, acting on glycosyl bonds	Plasma membrane	Glycoside hydrolase family 17, plant
304	A0A3B6MZI6	UDP-glucose 6-dehydrogenase OS=*Triticum aestivum*	4.76	11.46	4	1.25	0.18	3.78E-02	Glycosaminoglycan biosynthetic process	UDP-glucose 6-dehydrogenase activity	Nucleus	UDP-glucose 6-dehydrogenase, eukaryotic type
508	A0A1D5URN5	Fibronectin type III-LIKE domain-containing protein OS=*Triticum aestivum* GN=CAMPLR22A2D_LOCUS3716	2.36	3.76	2	-1.15	0.05	3.59E-02	Xylan catabolic process	Xylan 1,4-beta-xylosidase activity	Extracellular region	Beta-D-xylosidase
513	A0A3B6B442	Aspartate/glutamate/uridylate kinase domain-containing protein OS=*Triticum aestivum*	2.07	3.86	1	-1.92	0.34	4.08E-02	Glutamine family amino acid biosynthetic process	Acetylglutamate kinase activity	Cytoplasm	Glutamate/ acetylglutamate kinase
519	A0A3B6TUD9	Thiamine thiazole synthase, chloroplastic	2.05	5.98	2	-1.74	0.13	3.42E-02	Thiamine biosynthetic process	Pentosyltransferase activity	Chloroplast	Thiamine thiazole synthase

		OS=*Triticum aestivum* GN=THI1										
541	A0A3B6KK25	3-dehydroquinate synthase OS=*Triticum aestivum*	2,03	7,00	1	-1.42	0.07	1,38E-02	Amino acid family biosynthetic process	3-dehydroquinate synthase activity	Cytoplasm	Dehydroquinate synthase
675	A0A3B6NHD8	O-methyltransferase ZRP4 OS=*Triticum aestivum*	1.96	10.99	2	1.56	0.41	3.89E-02	Aromatic compound biosynthetic process	S-adenosylmethionine-dependent methyltransferase activity	None	O-methyltransferase COMT-type
837	A0A3B5ZXG4	Glycosyltransferase OS=*Triticum aestivum* OX=4565 PE=3 SV=1	1.14	3.16	1	-1.50	0.12	2.23E-02	None	UDP-glycosyltransferase activity	None	UDP-glucuronosyl/ UDP-glucosyltransferase
868	A0A3B6MS26	Glucose-6-phosphate 1-epimerase OS=*Triticum aestivum*	0.77	5.35	1	-2.37	0.15	1.86E-03	Carbohydrate metabolic process	Glucose-6-phosphate 1-epimerase activity	Cytoplasm	Glucose-6-phosphate 1-epimerase
1037	A0A3B6KPK9	Beta-glucosidase OS=*Triticum aestivum*	13.38	13.30	8	2.27	0.88	4.53E-02	Carbohydrate metabolic process	Beta-glucosidase activity	Extracellular region	Cellulase degradation glycosyl hydrolase 3
Energy												
1	P11383	Ribulose bisphosphate carboxylase large chain OS=*Triticum aestivum* GN=rbcL	72.15	71.91	189	-1.24	0.10	3.23E-02	photosynthesis	Ribulose-bisphosphate carboxylase activity	Chloroplast	RuBisCO large subunit type I
2	P20858	ATP synthase subunit beta, chloroplastic OS=*Triticum aestivum* GN=atpB	55.08	67.87	82	-1.34	0.11	3.09E-02	ATP biosynthesis process	Proton-transporting ATP synthase activity, rotational mechanism	Chloroplast	ATPase alpha/beta chains
3	P12112	ATP synthase subunit alpha, chloroplastic OS=*Triticum aestivum* GN=atpA	54.35	49.01	62	-1.46	0.15	1.40E-02	ATP biosynthesis process	Proton-transporting ATP synthase activity, rotational mechanism	Chloroplast	ATPase alpha/beta chains
10	A0A3B6TID0	Transketolase OS=*Triticum aestivum*	35.39	39.19	30	-1.21	0.06	7.17E-03	Pentose-phosphate shunt	Transketolase activity	Cytosol	Transketolase, bacterial-like
15	P24065	Photosystem II CP47 reaction center protein OS=*Triticum aestivum* GN=psbB	31.02	30.71	39	-2.02	0.12	1.01E-02	Photosynthesis	Chlorophyll binding	Photosystem II	Photosystem II CP47 reaction centre protein
16	A0A3B6AYY2	23 kDa subunit of oxygen evolving system of photosystem II OS=*Triticum aestivum*	30.74	57.14	57	1.56	0.35	4.27E-02	Photosynthesis	Calcium ion binding	Photosystem II	PsbP

22	A0A3B5Z5T0	Malate dehydrogenase OS=*Triticum aestivum*	27.38	45.75	19	1.20	0.14	3.94E-02	Malate metabolic process	L-malate dehydrogenase activity	Cytoplasm	Malate dehydrogenase, type 1
41	A0A3B6N1I7	Photosystem I reaction center subunit II, chloroplastic OS=*Triticum aestivum*	21.89	57.35	18	-1.57	0.19	1.60E-02	Photosynthesis	None	Photosystem I	Photosystem I PsaD
45	A0A3B6LQN1	Chlorophyll a-b binding protein, chloroplastic OS=*Triticum aestivum*	19.89	50.94	27	-1.63	0.11	2.36E-02	Photosynthesis	Chlorophyll binding	Chloroplast	Chlorophyll A-B binding protein
46	A0A3B6JMT4	Glyceraldehyde-3-phosphate dehydrogenase OS=*Triticum aestivum*	27.81	35.36	27	-2.20	0.42	4.92E-02	Glucose metabolic process	Glyceraldehyde-3-phosphate dehydrogenase activity	None	Glyceraldehyde-3-phosphate dehydrogenase, type 1
49	A0A3B6MII9	Phosphopyruvate hydratase OS=*Triticum aestivum*	18.38	30.94	9	1.19	0.07	4.48E-03	Glycolytic process	Phosphopyruvate hydratase activity	Phosphopyruvate hydratase complex	Enolase
50	W5GFA4	Chlorophyll a-b binding protein, chloroplastic OS=*Triticum aestivum*	18.15	48.33	49	-1.36	0.17	2.82E-02	Photosynthesis	Chlorophyll binding	Chloroplast	Chlorophyll A-B binding protein
79	W5C4P1	Uncharacterized protein OS=*Triticum aestivum* GN=CAMPLR22A2D_LOCUS2058	14.58	33.18	14	-1.92	0.08	1.06E-02	Photosynthesis	Electron transporter, transferring electron within the cyclic electron transport pathway of photosynthesis activity	Chloroplast	Oxygen-evolving enhancer protein 3, plants
81	W5AY52	Chlorophyll a-b binding protein, chloroplastic OS=*Triticum aestivum* GN=CAMPLR22A2D_LOCUS3228	14.2	40.78	10	-1.67	0.08	1.53E-03	Photosynthesis	Chlorophyll binding	Chloroplast	Chlorophyll A-B binding protein
90	W5D4R0	Photosystem II 22 kDa protein, chloroplastic OS=*Triticum aestivum*	13.37	28.31	7	-1.63	0.13	5.52E-03	None	None	Chloroplast thylakoid membrane	Chlorophyll A-B binding protein
113	A0A3B6MXE7	Photosystem I reaction center subunit III OS=*Triticum aestivum*	11.64	27.71	9	-1.36	0.09	5.36E-03	Photosynthesis	None	Photosystem I	Photosystem I PsaF, reaction centre subunit III
124	A0A3B6QKY1	Aconitate hydratase OS=*Triticum aestivum*	11.24	6.67	5	2.05	0.47	5.72E-03	Citrate metabolic process	Aconitate hydratase activity	Cytosol	Aconitase/Iron-responsive element-binding protein 2
134	P58386	Photosystem I P700 chlorophyll a apoprotein A2	10.27	11.85	11	-2.39	0.09	2.93E-03	Photosynthesis	Chlorophyll binding	Photosystem I	Photosystem I PsaB

		OS=*Triticum aestivum* GN=psaB										
136	A0A3B6QDB2	Photosystem II protein D1 OS=*Triticum aestivum*	10	20.70	7	-1.57	0.14	2.89E-02	Photosynthesis	Chlorophyll binding	Photosystem II	Photosynthetic reaction centre, L/M
139	P58311	Photosystem I P700 chlorophyll a apoprotein A1 OS=*Triticum aestivum* GN=psaA	10.09	6.53	7	-2.39	0.04	9.95E-03	Photosynthesis	Chlorophyll binding	Photosystem I	Photosystem I PsaA
148	A0A3B6HUR4	Chlorophyll a-b binding protein, chloroplastic OS=*Triticum aestivum*	9.39	20.14	7	-1.91	0.09	4.14E-03	Photosynthesis	Chlorophyll binding	Chloroplast	Chlorophyll A-B binding protein
165	A0A3B6AWZ1	Chlorophyll a-b binding protein, chloroplastic OS=*Triticum aestivum*	8.48	27.99	13	-1.58	0.05	3.46E-03	Photosynthesis	Chlorophyll binding	Chloroplast	Chlorophyll A-B binding protein
172	W5F8Z5	Chlorophyll a-b binding protein, chloroplastic OS=*Triticum aestivum*	8.93	34.22	10	-1.69	0.07	1.88E-04	Photosynthesis	Chlorophyll binding	Chloroplast	Chlorophyll A-B binding protein
184	A0A1D5V1G5	Chlorophyll a-b binding protein, chloroplastic OS=*Triticum aestivum* GN=CAMPLR22A2D_LOCUS1931	7.56	21.68	7	-1.39	0.14	3.31E-02	Photosynthesis	Chlorophyll binding	Chloroplast	Chlorophyll A-B binding protein
275	A0A3B5Z4J5	ATP synthase subunit b, chloroplastic OS=*Triticum aestivum*	5.52	16.57	3	-1.55	0.09	2.09E-02	Proton motive force-driven ATP synthesis	Proton transmembrane transporter activity	Membrane	ATPase, FO complex, subunit b/b’
297	P69415	Photosystem I iron-sulfur center OS=*Triticum aestivum* GN=psaC	5.01	27.16	4	-1.65	0.06	3.97E-02	Photosynthesis	4 iron, 4 sulfur cluster binding	Photosystem I	Photosystem I protein PsaC
301	A0A3B6PUD8	Photosystem II 10 kDa polypeptide, chloroplastic OS=*Triticum aestivum*	4.99	27.14	4	-1.64	0.08	5.55E-03	Photosynthesis	None	photosystem II	Photosystem II PsbR
311	A0A3B6RH69	Chlorophyll a-b binding protein, chloroplastic OS=*Triticum aestivum*	4.47	17.41	6	-1.44	0.08	2.20E-02	Photosynthesis	Chlorophyll binding	Chloroplast	Chlorophyll A-B binding protein
374	A0A3B5ZZE4	Chlorophyll a-b binding protein, chloroplastic OS=*Triticum aestivum*	13.34	52.09	24	-1.44	0.12	2.91E-02	Photosynthesis	Chlorophyll binding	Chloroplast	Chlorophyll A-B binding protein
551	F6K744	Chlorophyll a-b binding protein, chloroplastic OS=*Triticum aestivum*	17.15	52.26	29	-2.27	0.06	1.71E-03	Photosynthesis	Chlorophyll binding	Chloroplast	Chlorophyll A-B binding protein
824	A0A3B6U9Q7	Cytochrome b/b6 C-terminal region profile domain-containing protein OS=*Triticum aestivum*	1.11	5.75	1	-3.44	0.21	1.90E-02	Photosynthesis	Ubiquinol-cytochrome-c reductase activity	Thylakoid	Cytochrome b6/f complex, subunit IV

Protein synthesis/folding/degradation

26	A0A3B6TR29	ATP-dependent zinc metalloprotease OS=*Triticum aestivum* GN=FtsH2	25.44	24.52	14	-1.38	0.09	1.98E-02	Proteolysis	ATP-dependent peptidase activity	Membrane	ATP-dependent zinc metalloprotease, FtsH
59	W5ECL2	Large ribosomal subunit uL2 C-terminal domain-containing protein OS=*Triticum aestivum*	16.68	26.05	11	1.27	0.18	3.15E-02	Translation	Structural constituent of ribosome	Ribosome	Large ribosomal subunit protein uL2
85	A0A3B6QDU5	50S ribosomal protein L3, chloroplastic OS=*Triticum aestivum*	13.1	41.67	15	1.30	0.07	1.33E-02	Translation	Structural constituent of ribosome	Ribosome	Large ribosomal subunit protein uL3
120	A0A3B6JLK1	Large ribosomal subunit protein L15/eL18 domain-containing protein OS=*Triticum aestivum*	10.99	16.60	7	1.33	0.21	3.20E-02	Translation	Structural constituent of ribosome	Ribosome	Large ribosomal subunit protein uL15
154	W5D067	Small ribosomal subunit protein uS7c OS=*Triticum aestivum*	9.14	16.00	7	-1.41	0.06	3.16E-02	Translation	Structural constituent of ribosome	Ribosome	Ribosomal protein uS7
167	W5ASA4	Uncharacterized protein OS=*Triticum aestivum* GN=CAMPLR22A2D_LOCUS2419	8	37.66	6	1.61	0.41	4.51E-02	Translation	Structural constituent of ribosome	Ribosome	Small ribosomal subunit protein uS19
173	A0A3B6JPZ3	Chaperonin CPN60-2, mitochondrial OS=*Triticum aestivum*	8.04	7.45	4	-1.30	0.14	2.46E-02	Protein refolding	ATP-dependent protein folding chaperone	Mitochondrion	Chaperonin Cpn60/GroEL
215	W5GTW2	Large ribosomal subunit protein eL1 domain-containing protein OS=*Triticum aestivum*	6.4	21.64	3	1.38	0.23	2.92E-02	Translation	Structural constituent of ribosome	Ribosome	Large ribosomal subunit protein eL14
226	P11534	Large ribosomal subunit protein uL2cz/uL2cy OS=*Triticum aestivum* GN=rpl2-B	6.33	16.12	3	1.25	0.10	4.02E-02	Translation	Structural constituent of ribosome	Ribosome	Large ribosomal subunit protein uL2
246	A0A3B6JIR3	Heat shock cognate 70kDa protein OS=*Triticum aestivum*	16.71	19.82	12	1.55	0.34	4.59E-02	Chaperone cofactor-dependent protein refolding	Protein folding chaperone	Cytoplasm	Heat shock protein 70 family
248	A0A3B6TJK6	Small ribosomal subunit protein uS10 domain-containing protein OS=*Triticum aestivum*	5.94	19.35	4	1.44	0.20	2.99E-02	Translation	Structural constituent of ribosome	Ribosome	Small ribosomal subunit protein uS10
259	A0A1D6DK86	40S ribosomal protein S24 OS=*Triticum aestivum*	5.77	24.82	3	1.34	0.20	3.03E-02	Translation	Structural constituent of ribosome	Ribosome	Small ribosomal subunit protein eS24
271	A0A3B6B204	Large ribosomal subunit protein uL23 N-terminal domain-containing protein OS=*Triticum aestivum*	5.46	15.91	4	1.59	0.16	5.55E-04	Translation	Structural constituent of ribosome	Ribosome	Large ribosomal subunit protein uL23

282	W5D739	KOW domain-containing protein OS=*Triticum aestivum* GN=TRAES_3BF073700020CFD_c1	5.29	17.20	4	1.64	0.24	4.49E-03	Translation	Structural constituent of ribosome	Ribosome	Large ribosomal subunit protein uL24
376	Q93XQ6	Peptidyl-prolyl cis-trans isomerase OS=*Triticum aestivum* GN=CyP2	5.37	26.32	9	1.41	0.11	1.21E-02	Protein folding	Peptidyl-prolyl cis-trans isomerase activity	Cytoplasm	Cyclophilin-type peptidyl-prolyl cis-trans isomerase
382	A0A3B6MTE3	Peptidylprolyl isomerase OS=*Triticum aestivum*	3.87	14.41	2	1.64	0.38	3.20E-02	None	Peptidyl-prolyl cis-trans isomerase activity	None	Peptidyl-prolyl cis-trans isomerase FKBP18-like
393	W5D7B8	60S ribosomal protein L18a OS=*Triticum aestivum*	3.75	12.92	2	1.40	0,20	3,92E-02	Translation	Structural constituent of ribosome	Ribosome	Large ribosomal subunit protein eL20
395	A0A3B6HYY4	Dipeptiylpeptidase IV N-terminal domain-containing protein OS=*Triticum aestivum*	3.75	5.16	3	1.37	0.14	3.39E-03	None	Serine-type peptidase activity	None	None predicted
432	A0A3B6N0K3	50S ribosomal protein L17, chloroplastic OS=*Triticum aestivum*	3.17	9.42	2	1.51	0,21	3,22E-03	Translation	Structural constituent of ribosome	Ribosome	Large ribosomal subunit protein bL17
660	A0A3B6A2B9	60S ribosomal protein L37a, OS=*Triticum aestivum*	2	16.84	2	2.54	0.42	9.27E-03	Translation	Structural constituent of ribosome	Ribosome	Large ribosomal subunit protein eL43
714	A0A3B6KFH9	Uncharacterized protein OS=*Triticum aestivum*	6.42	17.06	4	1.26	0.06	4.33E-02	Translation	Structural constituent of ribosome	Ribosome	Large ribosomal subunit protein uL22
740	A0A3B6N3E4	Sigma 54 modulation/S30EA ribosomal protein C-terminal domain-containing protein OS=*Triticum aestivum*	1.91	6.64	2	1.33	0.14	1.06E-02	Negative regulation of translation elongation	Ribosomal small subunit binding	Cytosolic small ribosomal subunit	Ribosome hibernation promoting factor, long/plastid
799	W5FV77	40S ribosomal protein S23 OS=*Triticum aestivum*	1.41	7.75	1	1.21	0.15	4.87E-02	Translation	Structural constituent of ribosome	Ribosome	Small ribosomal subunit protein uS12
817	A0A341U9I2	Small ribosomal subunit protein uS2c OS=*Triticum aestivum*	1.28	5.34	1	-1.40	0.10	2.10E-02	Translation	Structural constituent of ribosome	Ribosome	Small ribosomal subunit protein uS2
859	A0A3B6QGX5	60S ribosomal protein L6 OS=*Triticum aestivum*	2.22	10.08	2	1.65	0.29	4.00E-02	Translation	Structural constituent of ribosome	Ribosome	Large ribosomal subunit protein eL6

877	A0A3B6UD00	50S ribosomal protein L20 OS=*Triticum aestivum*	0.77	5.88	1	1.83	0.45	1.28E-02	Translation	Structural constituent of ribosome	Ribosome	Large ribosomal subunit protein bL20
985	W5D1D3	30S ribosomal protein S20, chloroplastic OS=*Triticum aestivum*	1.1	3.19	1	1.36	0.22	4.40E-02	Translation	Structural constituent of ribosome	Ribosome	Small ribosomal subunit protein bS20
Transporters												
171	A0A3B6LLS3	Uncharacterized protein OS=*Triticum aestivum*	7.96	19.64	5	1.29	0.18	4.38E-02	Monoatomic anion transmembrane transport	Voltage-gated monoatomic anion channel activity	Mitochondrion	Porin, eukaryotic type
333	A0A3B6GKQ2	Non-specific lipid-transfer protein OS=*Triticum aestivum*	4.17	10.67	2	1.71	0.40	1.31E-02	Lipid transport	Lipid binding	None	Plant non-specific lipid-transfer protein/Par allergen
400	A0A3B5YX09	Chloroplast inner envelope protein OS=*Triticum aestivum*	5.86	12.11	4	-1.50	0.10	2.53E-02	Protein import into chloroplast stroma	None	TOC-TIC super complex I	Protein TIC110, chloroplastic
458	A0A3B6I0D3	STI1/HOP DP domain-containing protein OS=*Triticum aestivum*	2.66	3.11	1	1.74	0.39	1.84E-02	Protein targeting to chloroplast	Chloroplast targeting sequence binding	None	None predicted
Transcription												
306	A0A3B6NX48	Histone H2A OS=*Triticum aestivum*	6.62	35.00	6	1.45	0.13	1.51E-02	Heterochromatin formation	Nucleosomal DNA binding	Nucleus	Histone H2A
309	A0A3B6NJ44	STI1 domain-containing protein OS=*Triticum aestivum*	4.49	5.59	2	1.47	0.34	4.15E-02	Chaperone cofactor-dependent protein refolding	Hsp70 protein binding	Histone deacetylase complex	None predicted
401	A0A3B6LSN3	MBD domain-containing protein OS=*Triticum aestivum*	3.5	5.68	2	1.52	0.18	7.18E-03	Transcription regulation	DNA binding	Nucleus	Methyl-CpG-binding domain-containing protein 10/11
444	Q8LRU5	HMG-I/Y protein HMGa OS=*Triticum aestivum* GN=HMGa	2.94	5.29	1	1.60	0.40	3.88E-02	Negative regulation of DNA recombination	Nucleosomal DNA binding	Nucleus	High mobility group protein HMGA
515	Q43312	Protein H2A.7 OS=*Triticum aestivum* GN=H2A-10	4.27	12.69	2	-1.37	0.13	2.44E-02	Heterochromatic formation	Nucleosomal DNA binding	Nucleus	Histone H2A
645	A0A3B6MXZ6	H15 domain-containing protein OS=*Triticum aestivum*	2	7.45	1	1.84	0.44	4.79E-02	Negative regulation of DNA recombination	Nucleosomal DNA binding	Nucleus	Linker histone H1/H5
734	A0A3B6GNG0	Histone H2B OS=*Triticum aestivum*	29.6	69.12	54	1.53	0.24	5.14E-03	None	DNA binding	Nucleus	Histone H2B
958	A0A3B6QBC0	Histone H2B OS=*Triticum aestivum*	31.04	69.66	51	1.34	0.19	2.53E-02	None	DNA binding	Nucleus	Histone H2B

Defence/ROS detoxification												
70	A0A3B6C505	(S)-2-hydroxy-acid oxidase OS=*Triticum aestivum*	21.9	38.30	14	-1.49	0.09	1.15E-02	Response to other organism	(S)-2-hydroxy-acid oxidase activity	Peroxisome	Alpha-hydroxy acid dehydrogenase, FMN-dependent
72	F1DKC1	Catalase OS=*Triticum aestivum* GN=CAT3	15.61	18.42	7	1.48	0.20	1.39E-02	Response to oxidative stress	Catalase activity	Cytoplasm	Catalase
209	A0A3B6PS76	Thioredoxin domain-containing protein OS=*Triticum aestivum*	6.72	10.26	5	1.22	0.08	1.69E-02	None	Oxidoreductase activity	None	Thioredoxin-like protein CDSP32
212	A0A3B6EFA0	Uncharacterized protein OS=*Triticum aestivum*	6.58	17.31	3	2.66	0.73	4.24E-03	Regulation of abscisic acid biosynthetic process	None	None	Nodulin-related protein ½ family
252	A0A3B6HWK9	Germin-like protein OS=*Triticum aestivum*	5.9	10.05	3	1.44	0.29	4.12E-02	None	Manganese ion binding	Apoplast	Germin
330	Q8W428	Chitinase OS=*Triticum aestivum* GN=Chi 2	4.16	18.27	3	-1.56	0.17	9.40E-03	Chitin catabolic process	Chitinase activity	None	Glycoside hydrolase, family 19
497	A0A3B6C7J3	Ultraviolet-B receptor UVR8 OS=*Triticum aestivum*	2.13	3.17	1	1.22	0.09	1.59E-02	None	None	None	Ubiquitin ligases and GTPase regulators
526	A0A3B6C860	Peroxidase OS=*Triticum aestivum*	2.04	2.48	1	1.39	0.14	5.84E-03	Response to oxidative stress	Peroxidase activity	Extracellular region	Plant peroxidase
561	A0A172WCB1	Cold-responsive LEA/RAB-related COR protein OS=*Triticum aestivum* GN=Wrab17.1	6.95	29.52	6	3.23	1.19	1.01E-02	None	None	None	None predicted
676	A0A3B6TZ07	GH18 domain-containing protein OS=*Triticum aestivum*	1.96	2.95	1	1.84	0.28	1.98E-03	Carbohydrate metabolic process	Chitinase activity	Extracellular region	Glycoside hydrolase 18 family chitinases
792	A0A3B6MJX1	Pathogen-related protein OS=*Triticum aestivum*	1.36	6.38	1	-2.00	0.13	1.68E-02	None	None	None	Pathogen-related defense protein
Secondary metabolism												
158	A0A3B6TV37	Amine oxidase domain-containing protein OS=*Triticum aestivum*	8.61	10.54	5	1.67	0.33	2.10E-02	Spermine catabolic process	Oxidoreductase activity	None	Flavin monoamine oxidase and related enzymes
482	A0A3B6QDX1	Delta-aminolevulinic acid dehydratase OS=*Triticum aestivum*	2.29	6.61	1	-1.59	0.17	8.35E-03	Chlorophyll biosynthetic process	Porphobilinogen synthase activity	Cytosol	Delta-aminolevulinic acid dehydratase family
1125	A0A3B5Y2F9	Dienelactone hydrolase domain-containing protein	4.37	11.25	2	1.60	0.22	2.30E-03	None	Hydrolase activity	None	Dienelactone hydrolase family

		OS=*Triticum aestivum*										
Cell structure												
107	W5FAY5	Actin OS=*Triticum aestivum*	11.81	22.55	8	-1.50	0.15	3.53E-02	None	ATP binding	Cytoskeleton	Actin family
Unclear classification												
57	A0A3B6LG11	NAD-dependent epimerase/dehydratase domain-containing protein OS=*Triticum aestivum*	16.89	23.08	10	-1.23	0.08	4.60E-03	rRNA processing	RNA binding	Cytosol	None predicted
122	A0A3B6MQA1	RRM domain-containing protein OS=*Triticum aestivum*	10.67	23.36	8	-1.24	0.12	4.05E-02	None	RNA binding	Ribonucleoprotein complex	Eukaryotic RNA-binding
260	A0A3B6LS14	Cupin type-1 domain-containing protein OS=*Triticum aestivum*	5.89	12.57	4	1.38	0.18	3.28E-02	None	None	None	Seed storage and functional proteins
383	A0A3B6GTL4	DJ-1/PfpI domain-containing protein OS=*Triticum aestivum*	3.84	7.98	2	-1.79	0.11	5.38E-04	Glyoxal metabolic process	None	Cytoplasm	Protein/nucleic acid deglycase DJ-1
415	A0A3B6TRL4	Thylakoid membrane protein slr0575 OS=*Triticum aestivum*	3.34	8.40	2	-1.78	0.19	1.58E-02	None	None	Membrane	Protein of unknown function DUF2854
658	A0A3B6AVR1	Uncharacterized protein OS=*Triticum aestivum*	2	7,34	1	-1.63	0,06	4,05E-02	None	Deaminase activity	Cytosol	RidA family
801	A0A3B6N353	Pentacotripeptide-repeat region of PRORP domain-containing protein OS=*Triticum aestivum*	1.32	1.47	1	2.10	0.41	3.42E-03	None	None	None	Tetratricopeptide-like helical domain superfamily
839	W5CRR3	DUF538 domain-containing protein OS=*Triticum aestivum* GN=TRAES_3BF076300030CFD_c1	1.03	12.43	2	-2.38	0.13	1.91E-03	None	None	None	Protein of unknown function DUF538
862	A0A3B5ZXF0	Protein kinase domain-containing protein OS=*Triticum aestivum*	0.83	1.84	1	1.92	0.44	9.42E-03	None	Protein kinase activity	None	None predicted

[a] Protein number assigned in the ProteinPilot software.

[b] Protein accession number from the UniProt database (http://www.uniprot.org) searches against sequences of *Triticum aestivum* only, accessed on 6 June 2024.

[c] Protein score generated by ProteinPilot software relating to the confidence of protein identification.

[d] Percentage coverage is determined by the number of amino acids of sequenced peptides against the total length of the protein, with a threshold of at least 95% confidence.

[e] Sequenced peptide refers to the number of peptides sequenced. All positively identified proteins were identified based on a single peptide.

[f] Ratio represents the average fold change. A positive value indicates upregulation, while a negative value indicates downregulation.

[g] Standard deviation obtained from comparing control and treatment values.

[h] Probability-value of the quantified difference between the control and drought-stressed leaf proteins.

[i] Gene ontology analysis as predicted from the UniProt database (http://www.ebi.ac.uk/QuickGO/). P=Biological Process, F=Molecular Function, and C= Cellular Component.

j Protein amily names as predicted by the InterPro database (http://www.ebi.ac.uk/interpro/) accessed on 6 June 2024.

4.3.3 Gene ontology analysis

The differentially expressed proteins were submitted for GO annotation to establish their cellular components, molecular functions, and biological processes (Tables 4.2 and 4.3). Cellular component terms describe where a protein is located within a cell to perform a specific function (Thomas, 2017). The molecular function GO terms describe the molecular activities of proteins, while biological processes describe a set of molecular activities performed by proteins (Thomas, 2017).

4.3.3.1 Cellular components of differentially expressed leaf proteins

Figure 4.3 illustrates the cellular component predictions of drought-responsive leaf proteins of both wheat varieties. The results revealed that 28% and 22% of the differentially expressed proteins had no predicted cellular components for BW4074 and BW35695, respectively. The BW4074 and BW35695 wheat leaf proteomes have common cellular locations which include cytoplasm/cytosol (26% and 12%), ribosome (13% and 19%) and chloroplast (7% and 15%), respectively. Cellular components with the least number of proteins in BW4074 included the endoplasmic reticulum lumen, endosome, GET complex, peroxisome and pyruvate dehydrogenase complex, while in BW35695, the proteins were located in the cytoskeleton, histone deacetylase complex, phosphopyruvate hydratase complex and the TOC-TIC super complex I. The cell component results show a diverse localization pattern of the drought-responsive proteins in both varieties, with some of the cell locations being common to both varieties (Figure 4.3).

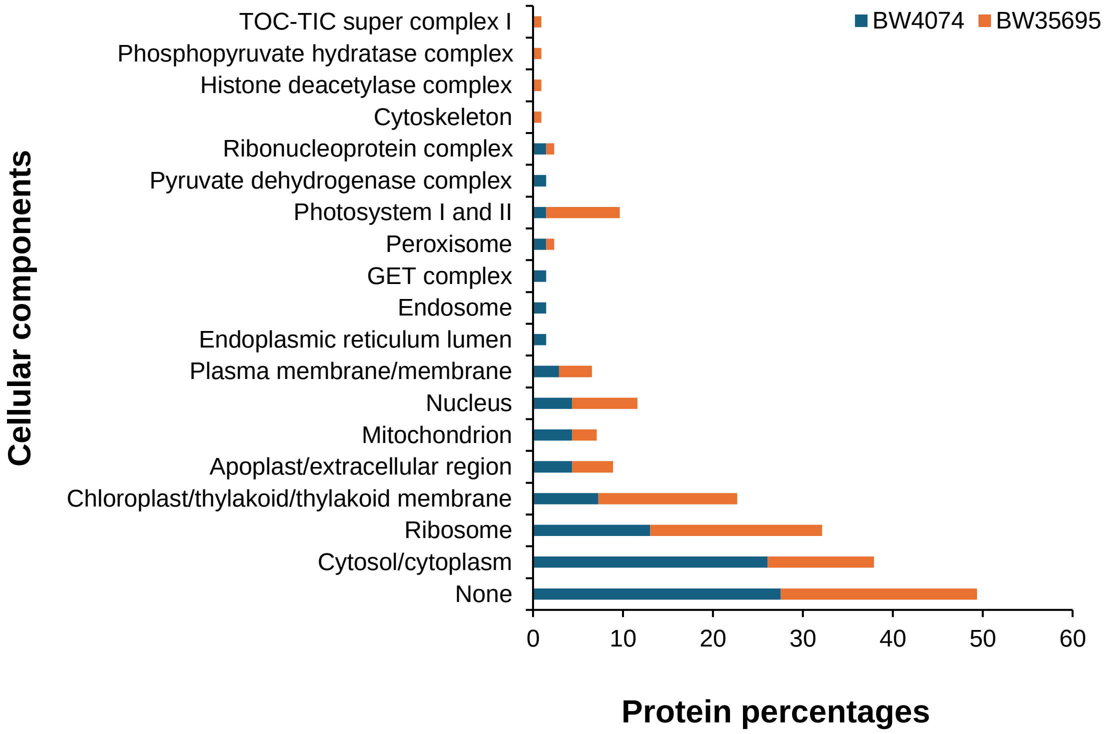

Figure 4.3: Cellular component predictions of the drought-responsive wheat leaf proteins.

4.3.3.2 Biological processes of differentially expressed leaf proteins

Figure 4.4 illustrates a wide variety of biological processes that are associated with the leaf proteomes of both wheat varieties. Amongst the 69 and 110 differentially expressed leaf proteins in BW4074 and BW35695, 22 (31%) and 20 (18%) had no predicted biological processes. Twelve (17%) proteins predicted to be involved in translation in BW4074 comprised the largest proportion compared to other biological processes. However, in BW35695, translation and photosynthesis were the most highly represented biological processes with 18 (16%) proteins each. Photosynthesis, glucose metabolic process, glycolytic process, pentose-phosphate shunt and protein folding were equally represented in BW4074 with 3 (4%) proteins each. The remaining proteins were distributed across several other biological processes (Figure 4.4). Overall, most drought-responsive proteins of both wheat varieties appeared to be involved in translation-related processes, while BW35695 also had more proteins related to photosynthesis.

Figure 4.4: Biological processes of the drought-responsive wheat leaf proteins.

4.3.3.3 Molecular functions of differentially expressed leaf proteins

The drought-responsive leaf proteins identified in BW4074 and BW35695 were also annotated across a broad range of molecular functions (Figure 4.5). Proteins with no known molecular functions were 7 (10%) and 14 (13%) in BW404 and BW35695, respectively. The predicted molecular functions for BW4074 and BW35695 included structural constituent of ribosome (12% and 18%), oxidoreductase activity (7% and 3%), DNA binding (1% and 3%) and peptidyl-prolyl cis-trans isomerase activity (4% and 2%), respectively. However, it was observed that the two wheat varieties also exhibited different molecular functions for the drought-responsive leaf proteins. For instance, BW35695, the drought-tolerant variety had proteins involved in chlorophyll binding (13%), chitinase activity (2%) and Hsp70 protein binding (1%). Conversely, the drought-susceptible variety, BW4074 had proteins involved in superoxide dismutase activity (3%), transaldolase activity (1%), and omega-amidase activity (1%) (Figure 4.5).

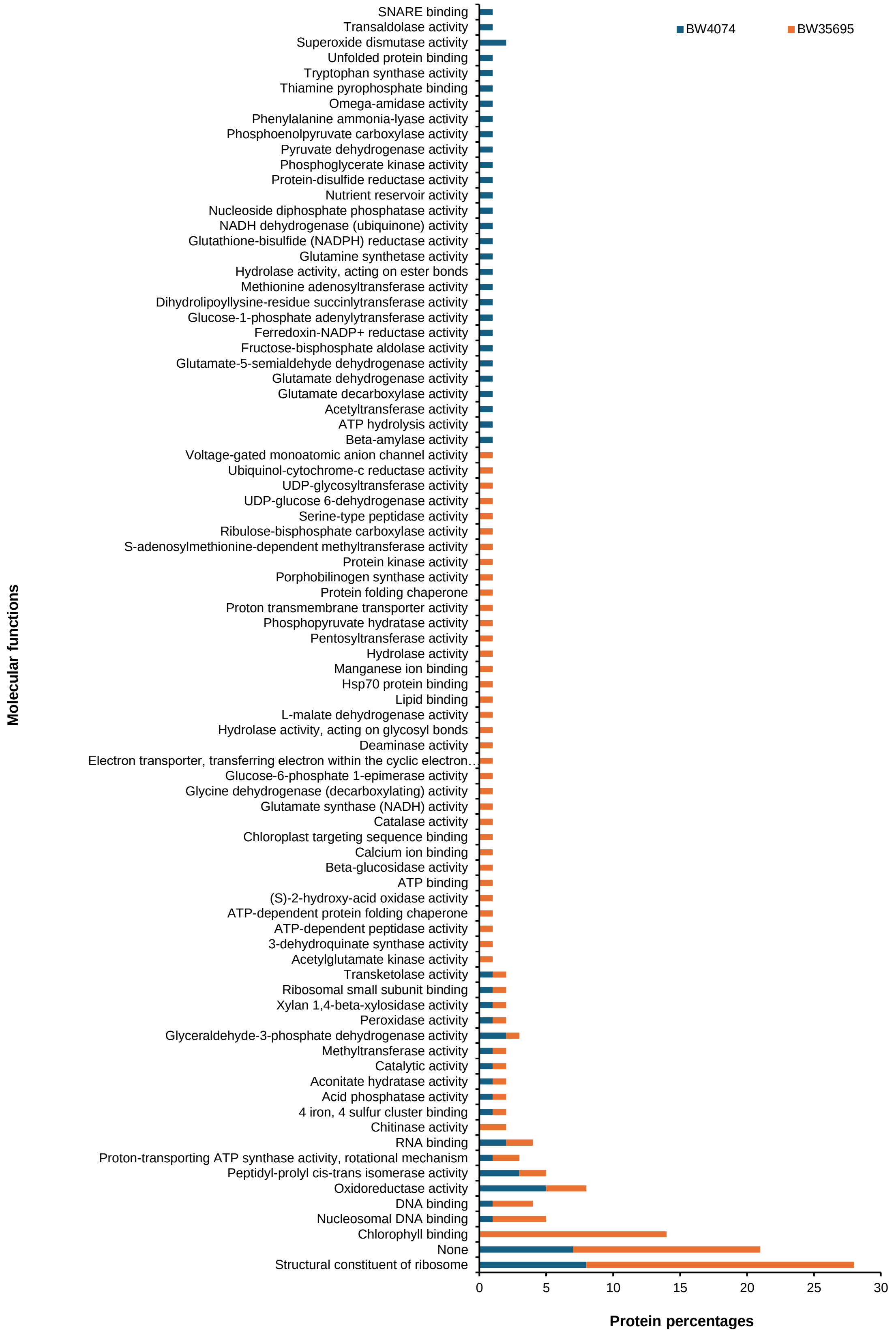

Figure 4.5: Molecular functions of the drought-responsive wheat leaf proteins.

4.3.4 Functional categories of the drought-responsive wheat leaf proteins

The drought-responsive leaf proteins were categorised into putative functional groups according to Bevan *et al*. (1998) and other relevant literature sources (Tables 4.2 and 4.3). The drought-responsive leaf proteins in BW4074 were classified into eight functional groups, while BW35695 had nine functional categories (Figure 4.6). Eight of the functional groups were common to both BW4074 and BW35695, and included primary metabolism (23% and 14%), energy (23% and 28%), protein synthesis/folding/degradation (20% and 25%), defence/ROS detoxification (13% and 10%), transcription (4% and 7%), secondary metabolism (6% and 3%) and cell structure (2% and 1%), respectively. The BW35695 proteome data included a unique transporters functional category which constituted 4% of the stress responsive proteins. However, some of the drought-responsive proteins in both BW4074 and BW35695 were unclassified (9% and 8%) due to limited GO annotations.

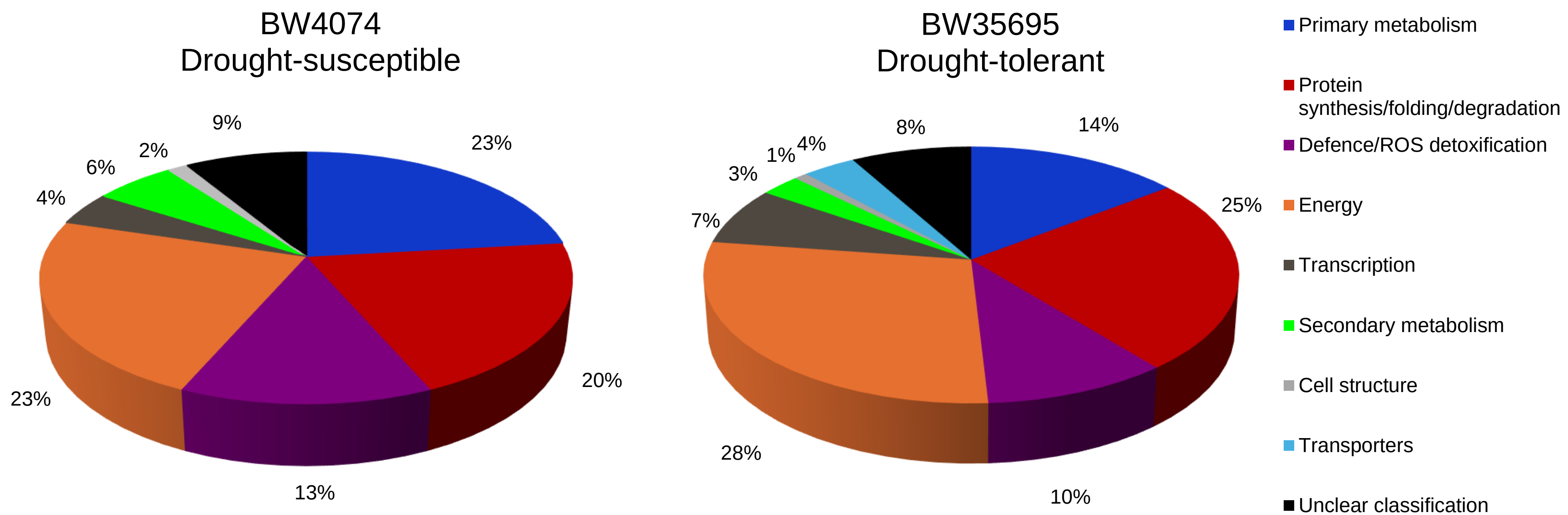

Figure 4.6: Functional categories of the drought-responsive leaf proteins of wheat plants.

Figure 4.7 illustrates the distribution patterns of up and downregulated proteins in each functional group per wheat variety. Both varieties exhibited a higher number of upregulated proteins in the defence/ROS detoxification, protein synthesis/folding/degradation, and transcription functional groups. The drought-tolerant wheat variety, BW35695 had a relatively large number of downregulated proteins in the energy functional category but an upregulation of transporters-related proteins. A brief description of some of the proteins within each functional category is provided below.

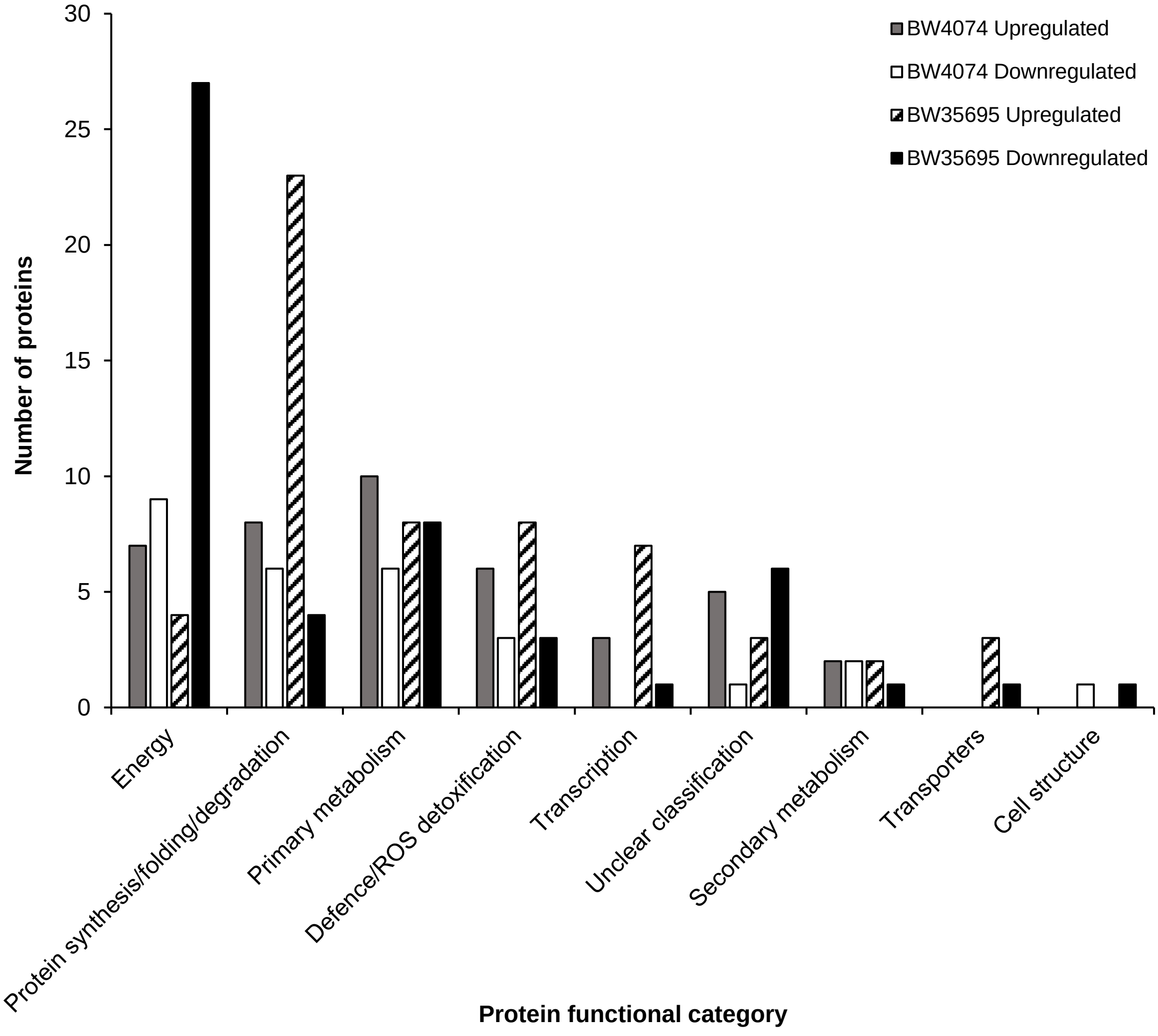

Figure 4.7: Number of up and downregulated drought-responsive leaf proteins in each functional group for both wheat varieties.

4.3.4.1 Energy

Out of the 69 drought-responsive leaf proteins in BW4074, 16 (23%) were involved in energy metabolism (Table 4.2; Figure 4.6). Of these proteins, 7 (44%) were upregulated while 9 (56%) were downregulated. Examples of the top three upregulated include fructose-bisphosphate aldolase with accession A0A3B6FUA0, pyruvate dehydrogenase E1 component subunit beta (accession A0A3B6TJ01) and phosphoenolpyruvate carboxylase (accession A0A3B6MR18). Conversely, the top three downregulated energy-related proteins include ferredoxin--NADP reductase, chloroplastic (A0A3B6TBB9), transketolase (A0A3B6BZB5) and glyceraldehyde-3-phosphate dehydrogenase (A0A3B6KSW8).

For BW35695, the energy-related functional group had the largest number of drought-responsive leaf proteins with 31 (28%) entries (Table 4.3; Figure 4.6). Of these proteins, 4 (13%) were upregulated, while 27 (87%) were downregulated. Most of the downregulated proteins were involved in photosynthesis including 10 chlorophyll a/b binding proteins and 10 photosystem I and II related proteins.

4.3.4.2 Protein synthesis/folding/degradation

The protein synthesis/folding/degradation functional category consisted of 14 (20%) drought-responsive proteins in BW4074 and 27 (25%) in BW35695 (Figure 4.6). Among these proteins, 8 (57%) in BW4074 and 23 (85%) for BW35695 were upregulated, while 6 (43%) in BW4074 and 4 (15%) in BW35695 were downregulated. Most ribosomal proteins involved in translation were upregulated in both wheat varieties (Tables 4.2 and 4.3). The downregulated proteins included those involved in protein folding/refolding such as peptidyl-prolyl cis-trans isomerase (accession W5H9B7) and a trigger factor ribosome-binding bacterial domain-containing protein (accession W5D1B3) in BW4074, and a chaperonin CPN60-2, mitochondrial (accession A0A3B6JPZ3) in BW35695. The drought-tolerant variety also had two proteolysis-related proteins (Table 4.3), which were an upregulated dipeptiylpeptidase IV N-terminal domain-containing protein (accession A0A3B6HYY4) and a downregulated ATP-dependent zinc metalloprotease (accession A0A3B6TR29).

4.3.4.3 Primary metabolism

The primary metabolism functional group consisted of 16 (23%) drought-responsive proteins in BW4074 (Table 4.2; Figure 4.6), of which 10 (63%) were upregulated. The three most upregulated proteins included an enoyl reductase (ER) domain-containing protein (accession A0A3B6FGE7), an aminocyclopropanecarboxylate oxidase (accession A0A3B6MSL2) and a delta-1-pyrroline-5-carboxylate synthase (accession W5ACM8). Conversely, three most downregulated proteins included a GDSL esterase/lipase (accession A0A3B6QKI8), glutamine synthetase (accession Q45NB2) and glutamate dehydrogenase (accession A0A3B6DHI0).

For BW35695, 16 (14%) of the drought-responsive proteins were assigned to the primary metabolism group (Table 4.3; Figure 4.6) with an equal number of up and downregulated proteins. The upregulated proteins included a beta-glucosidase (accession A0A3B6KPK9), acid phosphatase (accession A0A3B6UC94) and a nucleoside phosphorylase domain-containing protein (accession A0A3B6FKL0), while downregulated proteins included an aspartate/glutamate/uridylate kinase domain-containing protein (accession A0A3B6B442), a thiamine thiazole synthase, chloroplastic (accession A0A3B6TUD9) and a glucose-6-phosphate 1-epimerase (accession A0A3B6MS26).

4.3.4.4 Defence/ROS detoxification

Nine (13%) of the 69 drought-responsive leaf proteins in BW4074 were categorised under the defence/ROS detoxification functional group (Table 4.2; Figure 4.6). Of these proteins, six were upregulated including a superoxide dismutase [Cu-ZN] (accession H9NAV6), glutathione reductase (accession A0A3B6HMK6), and a cold induced 16 (accession S6AWC2). The three downregulated proteins included a pathogenesis related protein-1.2 (accession O82715), a peroxidase (accession A0A3B6CH98) and a putative PDI-like protein (accession D8L9B5).

The drought-tolerant variety, BW35695, had 11 (10%) differentially expressed proteins categorised in the defence/ROS detoxification functional group (Table 4.3; Figure 4.6). Of these proteins, 8 (73%) were upregulated while 3 (27%) were downregulated. The most upregulated proteins included an uncharacterized nodulin-related protein (A0A3B6EFA0), a cold-responsive LEA/RAB-related COR protein (A0A172WCB1) and a GH18 domain-containing protein (accession A0A3B6TZ07). The downregulated proteins included (S)-2-hydroxy-acid oxidase (accession A0A3B6C505), chitinase (accession Q8W428) and a pathogen-related protein (accession A0A3B6MJX1).

4.3.4.5 Transcription

Only three (4%) out of the 69 differentially expressed drought-responsive proteins in BW4074 were involved in transcription-related processes (Table 4.2; Figure 4.6). All three proteins were upregulated with fold changes ranging from 1.36 to 1.99. These included an MBD domain-containing protein (accession A0A3B6LSN3), H15 domain-containing protein (accession A0A3B6LV22) and HABP4_PAI-RBP1 domain-containing protein (accession A0A3B6A3G3) (Table 4.2). For, BW35695, 8 (7%) drought-responsive leaf proteins were categorized in this functional group (Table 4.3; Figure 4.6). Most of the proteins were upregulated including an

H15 domain-containing protein (accession A0A3B6MXZ6), an MBD domain-containing protein (accession A0A3B6LSN3) and a STI1 domain-containing protein (accession A0A3B6NJ44). The only downregulated protein in this functional group was a protein H2A.7 (accession Q43312) with a fold change of -1.37.

4.3.4.6 Other functional groups

Other drought-responsive proteins were categorised into the secondary metabolism and cell structure functional groups in both varieties (Tables 4.2 and 4.3) and in the transporters category in BW35695 (Table 4.3). The proteins related to secondary metabolism in BW4074 included an upregulated phenylalanine ammonia-lyase (accession A0A3B6QF91) and CN hydrolase domain-containing protein (accession A0A3B6IV90). Downregulated proteins were a zeta-carotene desaturase (accession A0A3B6C785) and an AB hydrolase-1 domain-containing protein (accession A0A3B6DPV0).

For BW35695, two upregulated proteins, an amine_oxidase domain-containing protein (accession A0A3B6TV37) and a dienelactone hydrolase domain-containing protein (accession A0A3B5Y2F9), and one downregulated delta-aminolevulinic acid dehydratase (accession A0A3B6QDX1) were classified under the secondary metabolism group (Table 4.3). The cell structure functional group consisted of one downregulated drought-responsive protein in each of the two wheat varieties. In BW4074, this protein was identified as a cyanobacterial aminoacyl-tRNA synthetase CAAD domain-containing protein (accession A0A3B6SEK0) with a fold change of -1.87. For BW35695, the downregulated protein was an actin protein (accession W5FAY5) with a fold change of -1.50. The drought-tolerant variety, BW35695 also had upregulated transporter-related proteins, including a non-specific lipid-transfer protein (accession A0A3B6GKQ2), an STI1/HOP DP domain-containing protein (accession

A0A3B6I0D3) and an uncharacterized protein (accession A0A3B6I0D3). Additionally, a chloroplast inner envelope protein (accession A0A3B5YX09) was downregulated with a fold change of -1.50.

4.3.4.7 Unclear classification

A total of 6 (9%) and 9 (8%) of the drought-responsive leaf proteins in BW4074 and BW35695 had unclear classification (Figure 4.6). Collectively, the protein family or superfamily names of the unclear classification proteins included ricin B-like lectin EULS3-like, eukaryotic RNA-binding, seed storage functional proteins, ridA family, tetratricopeptide-like helical domain superfamily and protein of unknown function DUF538 (Table 4.2 and Table 4.3). For BW4074, 5 of the 6 proteins were upregulated, while the downregulated protein was a remorin C-terminal domain-containing protein (accession A0A3B5XZW3) with a fold change of -1.65. In BW35695, 6 of the 9 proteins were downregulated, while the other three were upregulated. Among the upregulated proteins were a cupin type-1 domain-containing protein (accession A0A3B6LS14), pentacotripeptide-repeat region of PRORP domain-containing protein (accession A0A3B6N353) and a protein kinase domain-containing protein (accession A0A3B5ZXF0).

4.3.5 Common drought-responsive proteins between the wheat varieties

Nine drought-responsive proteins were common between the two wheat varieties (Figure 4.2). The wheat varieties had comparable upward or downward fold changes for six of these common drought-responsive proteins. Four of these common proteins, a 5-methyltetrahydropteroyltriglutamate-homocysteine S-methyltransferase (accession A0A3B6MJZ2), a small ribosomal subunit protein uS10 domain-containing protein (accession A0A3B6TJK6), a peptidylprolyl isomerase (accession A0A3B6MTE3) and an MBD domain-containing protein (accession A0A3B6LSN3) were upregulated. Conversely, the downregulated proteins included a fibronectin type III-like domain-containing protein (accession A0A1D5URN5) which was more downregulated in BW4074 and a Photosystem I iron-sulfur center protein (accession P69415) which was more downregulated in BW35695. Differential expression patterns were also observed between the varieties, a 30S ribosomal protein S20 (accession W5D1D3) was downregulated in BW4074 but upregulated in BW35695, while an unclassified RRM domain-containing protein (accession A0A3B6MQA1) was upregulated in BW4074 but downregulated in BW35695.

4.3.6. KEGG pathway enrichment analysis

A KEGG pathway enrichment analysis was conducted to understand the functions of the drought-responsive leaf proteins in both wheat varieties. The KEGG analysis connects a group of genes to a network of interacting molecules within the cell, such as a pathway or complex, reflecting a higher-level biological function (Kanehisa and Goto, 2000). The analysis revealed 18 enriched pathways in BW4074 and 12 in BW35695 (Figure 4.8). Nine pathways were common to both wheat varieties, including the citrate cycle (TCA cycle), carbon fixation in photosynthetic organisms, photosynthesis, carbon metabolism, biosynthesis of amino acid, ribosomes, glyoxylate and dicarboxylate metabolism, RNA degradation and metabolic pathways. However, pathways such as photosynthesis, and ribosome pathways were significantly enriched in BW35695 compared to BW4074 (Figure 4.8).

The KEGG analysis also revealed pathways that were unique to each of the two wheat varieties. In the drought susceptible variety, BW4074, unique pathways included alanine aspartate and glutamate metabolism, peroxisome, glycolysis-gluconeogenesis and biosynthesis of secondary metabolites (Figure 4.8). Conversely, in BW35695, unique pathways included photosynthesis-antenna proteins, 2-Oxocarboxylic acid metabolism, and amino sugar and nucleotide sugar metabolism (Figure 4.8).

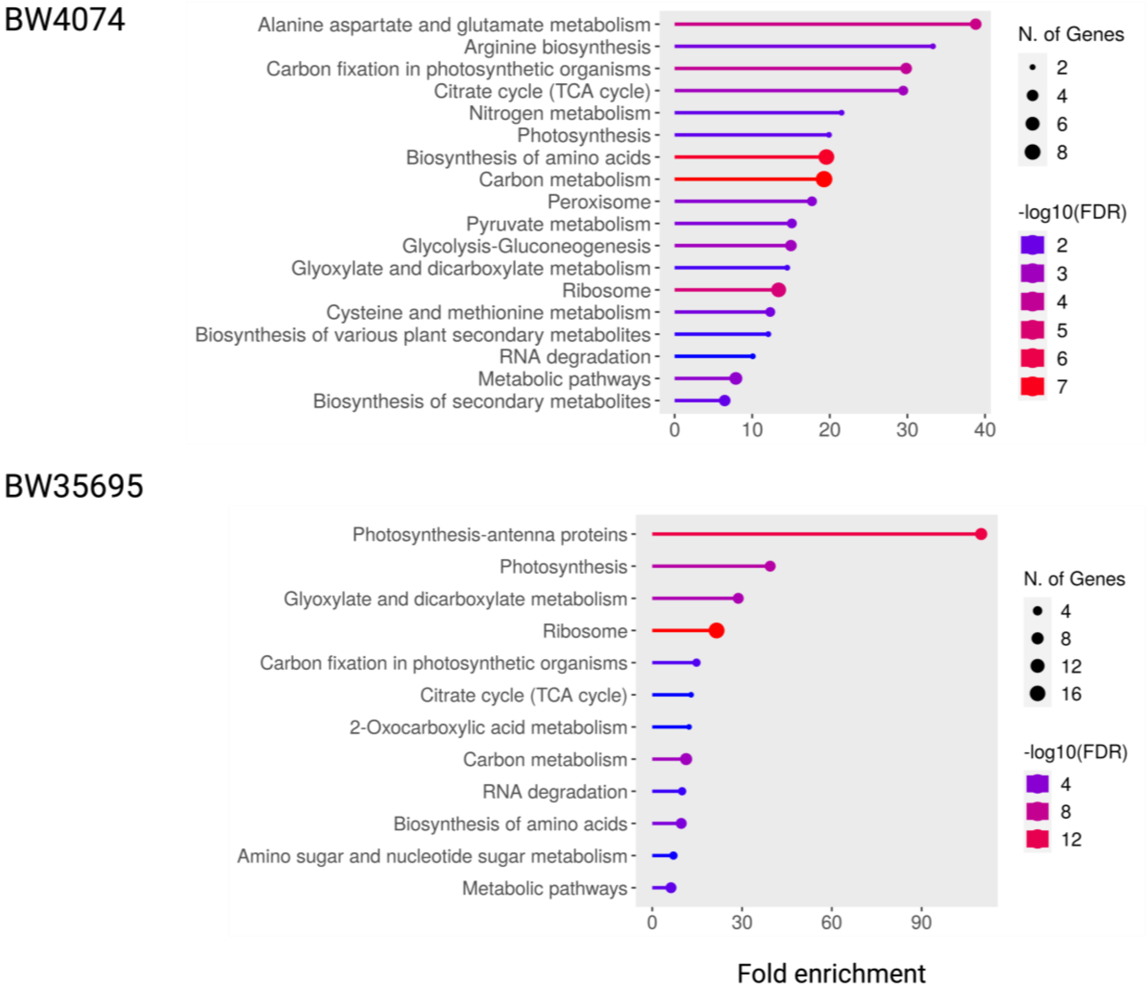

Figure 4.8: KEGG pathway enrichment analysis of drought-responsive leaf proteins of wheat. BW4074 is drought-susceptible, while BW35695 is drought-tolerant. The significance of the KEGG pathway is based on the Student's *t*-test ($p \leq 0.05$). The size of the dot in the figure corresponds to the number of genes associated with each pathway, as indicated by the legend. To correct for multiple testing, the False Discovery Rate (FDR) was calculated using the Benjamini-Hochberg method. The FDR values are represented by colours on a logarithmic scale as shown in the legend of the graph.

4.3.6 Protein-protein interaction analysis

To identify the interactions of the drought-responsive leaf proteins of BW4074 and BW35695 wheat varieties, a protein interaction analysis was conducted using the STRING database version 12.0. Some of the drought-responsive leaf proteins in both wheat varieties were predicted to interact with each other, while others showed no direct connection (Figure 4.9). Two main interacting protein functional groups were identified in each wheat variety. In BW4074, these two groups were primary metabolism and protein synthesis and the associated leaf proteins were either up or downregulated following drought stress treatment in both functional groups (Figure 4.9).

For BW35695, the two main interacting groups were photosynthesis and protein synthesis (Figure 4.9). The photosynthesis-related proteins were mainly downregulated following drought stress treatment as indicated by blue nodes in Figure 4.9. In the protein synthesis category, the majority of the proteins were upregulated in response to drought stress as represented by red nodes (Figure 4.9), while two ribosomal proteins with accessions A0A341U912 and W5D067 were downregulated. Overall, the protein-protein interaction networks indicate that the drought-responsive proteins interact with one another to varying extents, possibly to coordinate the necessary response mechanisms under drought conditions. Additionally, these interactions may vary among wheat plants with contrasting drought phenotypes.

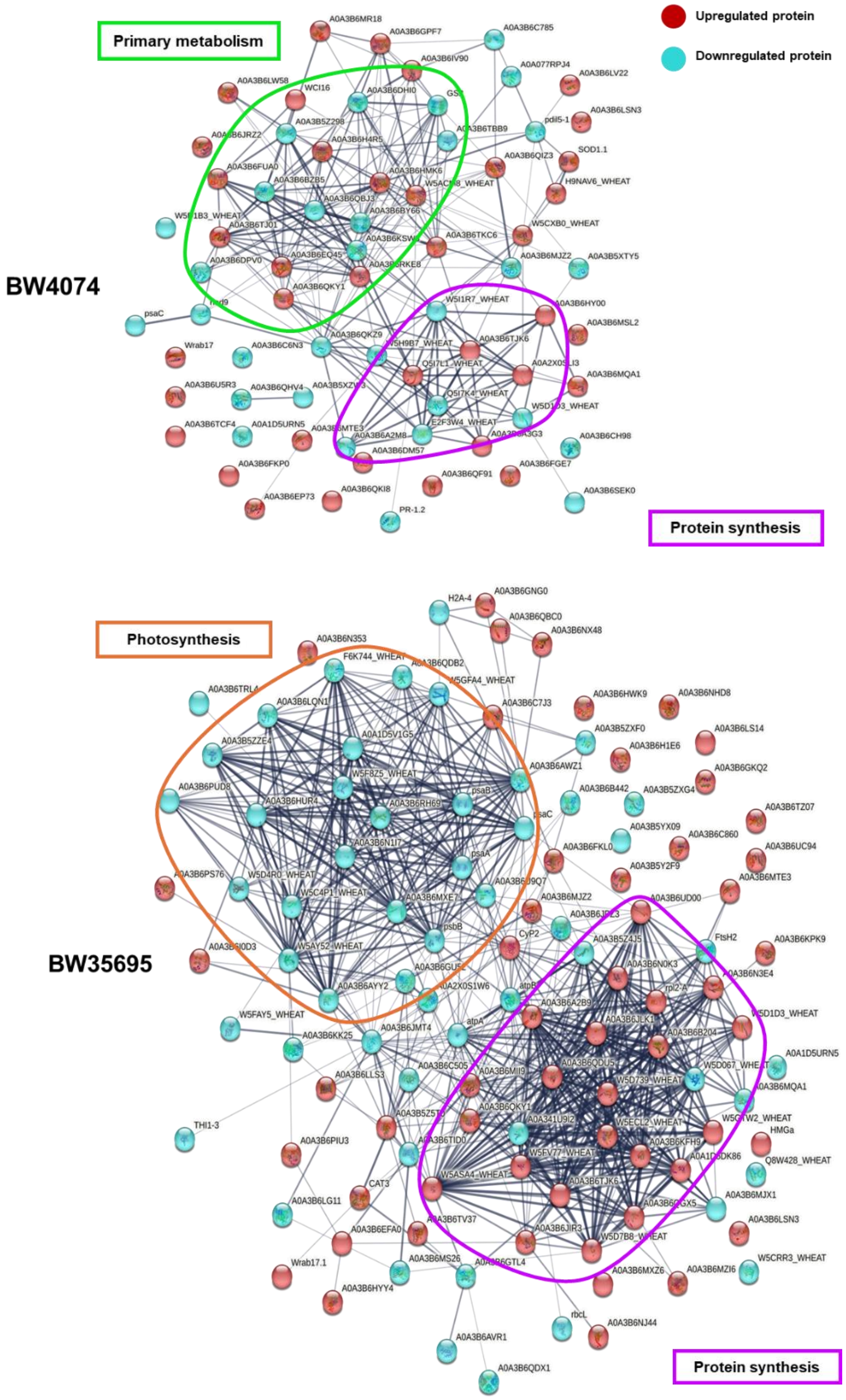

Figure 4.9: Protein-protein interaction of drought-responsive leaf proteins using the STRING database. BW4074 is drought-susceptible, while BW35695 is drought-tolerant. In this network, nodes are proteins; lines represent functional associations between the proteins. Nodes in red are upregulated proteins while nodes in blue are downregulated proteins. Thicker lines represent stronger associations between the interacting proteins.

4.4 Discussion

When plants are exposed to abiotic stress factors such as drought, they modulate their gene expression profiles, resulting in expression changes of proteins and metabolites (Shinozaki and Yamaguchi-Shinozaki, 2007). These molecular changes may result in a range of physiological and metabolic responses towards the imposed stress (Zargar *et al*., 2022). As such, this study analysed the differential expression patterns of leaf proteins of BW4074 (drought-susceptible) and BW35695 (drought-tolerant) wheat varieties in response to 28 days of drought stress treatment using the iTRAQ method. The aim was to comparatively evaluate differences and similarities in proteome changes of these two contrasting wheat varieties to drought. A total of 1062 and 882 leaf proteins were positively identified in BW4074 and BW35695 wheat varieties, respectively. Out of these positively identified leaf proteins, 69 in BW4074 (Table 4.2) and 110 in BW35695 (Table 4.3) were drought-responsive. The drought-responsive leaf proteins were categorised into 8 and 9 functional groups in BW4074 and BW35695, respectively, according to (Bevan *et al*., 1998) and bioinformatic tools (Figure 4.6). Gene Ontology analysis was conducted to identify cellular components, biological processes and molecular functions of the drought-responsive proteins.

Photosynthesis is a complex physiological process important for energy production in plants. However, like other plant physiological processes, it is affected by drought stress (Chaves *et al*., 2009). In this study, photosynthesis-related proteins were more highly represented in the drought-tolerant variety than in the drought-susceptible variety (Tables 4.2 and 4.3). In BW35695, the drought-responsive proteins associated with photosynthesis included chlorophyll a-b binding proteins and photosystem I and II-related proteins which were mostly downregulated possibly as a response to suppress ROS-induced cell damage (Foyer, 2018). Ford *et al*. (2011) also reported the downregulation of photosynthesis-related proteins in the leaves of one drought-sensitive (Kukri) and two drought-tolerant (Excalibur and RAC875) wheat cultivars in response to cyclic drought stress. The expression levels of light-harvesting complex proteins decreased significantly in Kukri compared to Excalibur and RAC875, while oxygen-evolving complex proteins increased significantly across the wheat varieties (Ford *et al*., 2011). The authors suggested that the observed downregulation of proteins involved in photosynthesis might be a response mechanism to avoid increased ROS accumulation (Ford *et al*., 2011).

The KEGG enrichment analysis revealed that the photosynthesis antenna and photosynthesis pathways were significantly enriched in BW35695 (Figure 4.8), which supports the observed massive downregulation of photosynthesis-related proteins in this wheat variety (Table 4.3 and Figure 4.7). Analysis of protein-protein interactions in BW35695 also revealed the downregulation of photosynthesis-related proteins, which may play a critical role in BW35695 drought stress response. A comparative proteomic study of maize varieties subjected to drought stress also reported the photosynthesis antenna proteins pathway as the most significantly enriched pathway in the drought-tolerant maize variety (Zenda *et al*., 2018).

Drought stress affects various aspects of cellular metabolism in plants (Anjum *et al*., 2011), including wheat, as illustrated by the large number of primary and secondary metabolism-related drought-responsive proteins identified in the current study (Tables 4.2 and 4.3). In this study, the KEGG analysis also revealed primary metabolism as the most enriched pathway in the drought-susceptible variety (Figure 4.8). Primary and secondary metabolic processes play essential roles in plant growth and development and in response to various stresses (Salam *et al*., 2023). The primary metabolism functional group included biological processes such as methionine biosynthetic process, tryptophan biosynthetic process, glucose metabolic process, fatty acid biosynthetic process, xylan catabolic process, carbohydrate metabolic process, glyoxal metabolic process, nucleoside metabolic process and pentose-phosphate shunt (Table 4.2 and 4.3). Many of the proteins in this functional group were upregulated in the BW4074 wheat variety after 28 days of drought stress treatment, while in BW35695, the proteins were equally up and downregulated (Figure 4.7). This potentially indicates the differential abilities of contrasting wheat varieties to modulate cellular metabolic functions under drought stress conditions.

Plants use various strategies to maintain growth and development during stressful conditions, such as stabilizing proteins and cellular structures (Krasensky and Jonak, 2015). Protein synthesis plays a major role in abiotic stress adaptation and the ribosome serves as the site for protein synthesis in cells. The protein-protein interaction analysis also highlighted protein synthesis-related proteins as the most interacting functional group in both varieties (Figure 4.9). The drought-responsive proteins involved in protein synthesis mainly consisted of ribosomal proteins involved in translation (Tables 4.2 and 4.3) and were upregulated in both wheat varieties, however, the increase was more evident in BW35695 (Figure 4.7). The increase in translation-related proteins possibly acts as a mechanism to enhance stress tolerance by synthesising other stress-responsive proteins. Increased and decreased abundances of ribosomal proteins was also observed in the leaves and roots of plant species such as wheat (Faghani *et al*., 2015), foxtail millet (*Setaria italica*) (Pan *et al*., 2018) and sorghum (*Sorghum bicolor*) (Goche *et al*., 2020) under drought stress conditions.

Under harsh environmental conditions, maintaining the structural integrity of proteins is essential for optimal growth and development of plants. This can be achieved via a variety of processes, including the removal of damaged and/or misfolded proteins (Goldberg, 2003; Sun *et al*., 2021). Protein misfolding or the accumulation of unfolded proteins widely occurs under abiotic stresses (Bao and Howell, 2017). In this study, peptidyl-prolyl cis-trans isomerase proteins were upregulated in both wheat varieties (Table 4.2 and 4.3), possibly indicating that the wheat varieties were trying to maintain normal protein folding during drought stress. Peptidyl-prolyl cis-trans isomerases are a superfamily of molecular chaperones with major roles in protein folding (Dunyak and Gestwicki, 2016). In a comparative leaf proteome study on chickpea genotypes, the abundance of peptidyl-prolyl cis-trans isomerase CYP38, increased in the drought-tolerant genotype after 5 days of water limitation (Vessal *et al*., 2020). The authors highlighted that the increased expression of the peptidyl-prolyl cis-trans isomerase CYP38 could possibly indicate that the drought-tolerant genotype is able to maintain correct protein folding and stability more effectively than the drought-susceptible genotype (Vessal *et al*., 2020).

With regards to proteins responsible for protein degradation, a downregulated ATP-dependent zinc metalloprotease was only observed in the drought-tolerant variety (Table 4.3). ATP-dependent zinc metalloproteases function in maintaining protein quality, degrading damaged proteins in plants during normal conditions and in response to abiotic stresses (Kidric *et al*., 2014; Moloi and Ngara, 2023). Contrary to the current study, a comparative proteomic study conducted on the leaves of chickpea genotypes reported a significant increase of the ATP-dependent zinc metalloprotease FTSH in the drought-tolerant genotype while being reduced in the drought-sensitive genotype (Vessal *et al*., 2020). The authors suggested that this endopeptidase together with other upregulated proteins may play a role in drought tolerance in chickpeas (Vessal *et al*., 2020). The above-mentioned studies suggest the importance of protein degradation in plants under drought stress.

Drought stress significantly increases the production and accumulation of ROS, leading to the oxidative damage of macromolecules (Foyer and Noctor, 2005; Hasanuzzaman *et al*., 2013). In the current study, proteins related to defence/ROS detoxification were differentially expressed in both BW4074 and BW35695 following the 28 days of drought stress treatment (Table 4.2 and 4.3). In BW4074, such proteins included superoxide dismutase [Cu-ZN], glutathione reductase, group3 late embryogenesis abundant (LEA) protein, cold induced 16 and monodehydroascorbate and were all upregulated (Table 4.2). The upregulated defence/ROS detoxification proteins in BW35695 included catalase, thioredoxin domain-containing protein, germin-like protein, ultraviolet-B receptor UVR8, peroxidase, cold-responsive LEA/RAB-related COR protein and the GH18 domain-containing protein (Table 4.3). Both wheat varieties possibly maintained cellular redox homeostasis by accumulating a wide range of ROS antioxidant scavengers following the 28 days of drought stress treatment. Ford *et al*. (2011) also identified a chloroplastic and cytosolic Cu/Zn-SOD in the leaves of a drought-sensitive and two drought-tolerant wheat cultivars in response to a cyclic drought-stress treatment and all three cultivars exhibited increased ROS scavenging capacity under drought stress conditions. Nemati *et al*. (2019) also reported the upregulation of ROS detoxification proteins in drought-tolerant and sensitive wheat varieties under drought stress. The authors suggested that the upregulation of such protein was a mechanism of drought stress tolerance (Nemati *et al*., 2019).

The drought-susceptible wheat variety BW4074 upregulated a group3 LEA protein under drought stress (Table 4.2). Late embryogenesis abundant proteins play important roles in the protection of plants against abiotic stresses (Kosová *et al*., 2021). The drought-tolerant wheat variety BW35695 accumulated a cold-responsive LEA/RAB-related protein, which prevents cellular dehydration under stress conditions (Kosová *et al*., 2021). Another protein that accumulated in BW35695 was a germin-like protein, which is a ubiquitous plant protein that functions in plant defence against various stress factors (Govindan *et al*., 2024). Collectively, the upregulation of these defence/ROS detoxification proteins suggests that both wheat varieties triggered a range of defence mechanisms in response to the imposed drought stress.

Transcription-related proteins such as H15 domain-containing protein, MBD domain-containing protein in both wheat varieties (Tables 4.2 and 4.3), and HABP4_PAI-RBP1 domain-containing protein, HMG-I/Y protein HMGa and STI1 domain-containing protein in BW35695 were upregulated in response to drought stress (Tables 4.2 and 4.3). Most of these transcription-related proteins in BW35695 were histones (Table 4.3). Histone proteins function in DNA packaging and gene regulation under abiotic stresses (Yuan *et al*., 2013). Upregulation of histone proteins has also been reported in the proteomes of maize (Schulze *et al*., 2021) and wheat (Li *et al*., 2018) under drought stress. The upregulation of transcription-related proteins observed in the current study may suggest that the wheat varieties facilitated the expression of other drought-responsive proteins in response to drought stress conditions. As illustrated in the leaf proteome data of this study (Tables 4.2 and 4.3) and the putative functional groupings of these proteins (Figure 4.6), the 28 days of drought stress triggered expression changes of a wide range of stress-responsive proteins. Collectively, such differentially expressed proteins may ultimately contribute to the drought phenotypes of each wheat genotype.

4.5 Conclusion

The two wheat varieties BW4074 and BW35695 accumulated differentially expressed proteins in response to drought stress, which were assigned to a range of putative functional groups. The drought-responsive proteins involved in energy metabolism, protein synthesis/folding/degradation and defence/ROS detoxification were highly represented in both wheat varieties. Analysis of the protein-protein interaction network revealed that the most interacting proteins in BW35695 were involved in photosynthesis and protein synthesis, while in BW4074, primary metabolism and protein synthesis were the main interacting functional groups. The results highlight that wheat adjusts its leaf protein expression patterns in response to drought stress, thereby modulating various biological processes.

CHAPTER 5

GENE EXPRESSION ANALYSIS OF WHEAT LEAVES IN RESPONSE TO DROUGHT STRESS

5.1 Introduction

Following the leaf proteome analyses of BW4074 and BW35695 wheat varieties using the isobaric tag for relative and absolute quantitation (iTRAQ) proteomic method (Chapter 4), a few proteins from the iTRAQ data (Tables 4.2 and 4.3) were selected for gene expression analysis. Omics techniques, such as the iTRAQ proteomic method are used to investigate plant responses to drought and provide snapshots of molecular changes in plants under drought stress conditions (Cui *et al*., 2019; Wang *et al*., 2019; Li *et al*., 2021). However, it is important to validate quantitative proteomic data to ascertain the biological functions of the identified stress-responsive proteins. The validation processes may involve the use of various techniques, including western blotting to determine protein expression levels in cells, quantitative real-time polymerase chain reaction (qRT-PCR) for assessing the gene expression levels of the gene coding for the protein of interest. Other functional validation techniques include enzyme activity assays to evaluate the activity of well-known soluble proteins and the use of transgenic plants that either overexpress or repress specific genes under stress conditions (Rhee and Mutwil, 2014). The advantages and disadvantages of these validation techniques will not be discussed here but have been extensively reviewed elsewhere (Rabilloud and Lescuyer, 2014; Niu *et al*., 2018; Mehta *et al*., 2022).

The current study used qRT-PCR for gene expression analysis between control and drought-stressed wheat plants of both varieties following 28 days of drought stress. Quantitative real-time PCR has been widely used to analyse gene expression changes between plant varieties under drought stress conditions after proteomic analyses (Zeng *et al*., 2019; Goche *et al*., 2020) and after physiological and biochemical analyses (Nasirzadeh *et al*., 2021; Dashtaki *et al*., 2023). Zeng *et al*. (2019) used qRT-PCR for gene expression analysis of differentially expressed root proteins of two maize (*Zea mays*) varieties subjected to 20% polyethylene glycol (PEG)-6000 osmotic stress treatment. Six proteins that were upregulated in the drought-tolerant variety but downregulated in the drought-susceptible variety and two, upregulated in both maize varieties were selected for gene expression analysis. The qRT-PCR results revealed that the tolerant maize variety exhibited increased expression levels of all eight genes, aligning with the proteomic data. In contrast, the susceptible variety exhibited a decrease in transcript levels of two genes and an increase in another two genes, which also corresponded with the proteomic data. However, the other three genes remained unchanged, while one increased following drought stress treatment in the drought-susceptible variety. The authors suggested that the variations observed in the gene expression levels between the maize varieties could be due to various post-transcriptional and translational modifications as a result of drought stress (Zeng *et al*., 2019).

In a study conducted by Dashtaki *et al*. (2023), qRT-PCR was also used for gene expression analysis in the leaves of two wheat varieties following drought stress treatment. The qRT-PCR data showed that the gene expression levels of *catalase (CAT), ascorbate peroxidase (APX), guaiacol peroxidase (GPX), pyrroline-5-carboxylate synthase (P5CS), and pyrroline-5-carboxylate reductase (P5CR)* increased significantly under drought stress conditions in the drought-tolerant wheat genotype compared to the semi-tolerant and sensitive genotypes. Additionally, there was a strong correlation between the proline levels in the leaves and the expression of *P5CS* and *P5CR* in the same tissue. The authors suggested that the up-regulation of genes of defensive systems such as CAT, APX, GPX and proline in the tolerant wheat genotype indicates that these genes play significant roles under drought stress conditions and can be reasonable targets for developing drought-tolerant wheat varieties (Dashtaki *et al*., 2023). Taken together, the above-mentioned studies highlight the different gene expression patterns in contrasting genotypes of a species under drought stress and the importance of validating proteomic data.

This chapter aimed to comparatively evaluate gene expression changes of a few targets in the leaves of BW4074 (drought-susceptible) and BW35695 (drought-tolerant) wheat varieties exposed to drought stress using qRT-PCR.

5.2 Materials and methods

5.2.1 Total leaf RNA extractions

Total RNA was extracted from BW4074 and BW35695 wheat leaves harvested on days 14 and 28 of drought stress treatment. Three biological replicates were prepared for both the control and drought stress treatment groups. The total RNA extractions were carried out using the Spectrum™ Plant Total RNA Kit (Catalog No: STRN50; Sigma-Aldrich, St. Louis, USA) according to the manufacturer's instructions. Briefly, leaf and root samples were ground to a fine powder in liquid nitrogen. Thereafter, 500 µl of Lysis solution containing 2-mercaptoethanol was added to 100 mg of the powdered material. The mixture was immediately vortexed vigorously for 30 seconds and incubated on a heat block at 56 °C for 5 minutes. Following incubation, the samples were centrifuged at 21 300 × *g* for 3 minutes and the lysate supernatant was transferred into collection tubes containing filtration columns. All centrifugation steps in this study were done at room temperature unless stated otherwise. The samples were centrifuged at 21 300 × *g* for 1 minute to collect the clarified flow-through lysate. For the RNA binding step, Protocol A from the Spectrum™ Plant Total RNA Kit (Sigma-Aldrich) was followed. Briefly, 500 µl of the Binding Solution was added to the lysate supernatant and mixed by pipetting five times. From this mixture, 700 µl was collected and pipetted into a binding column placed in a collection tube and centrifuged at 21 300 × *g* for 1 minute to bind the RNA. The flow-through liquid was discarded and 500 µl of Wash Solution 1 was added to the binding column and centrifuged at 21 300 × *g* for 1 minute.

After RNA binding, an On-Column DNase Digestion step was performed to remove trace amounts of DNA during RNA purification using the On-Column DNase Digestion kit (Catalog No: DNASE70; Sigma-Aldrich). The DNase digestion working solution was prepared as a master mix for all samples by mixing 10 µl DNase 1 with 70 µl DNase digestion buffer for each digestion. The 80 µl digestion mixture was then added to the binding column and incubated for 15 minutes at room temperature. Thereafter, the binding column was washed with 500 µl Wash Solution 1 while centrifuging at 21 300 × *g* for 1 minute, and the flow-through liquid was discarded. The binding column was washed twice with 500 µl Wash Solution 2, while centrifuging at 21 300 × g for 30 seconds each time. Thereafter, the binding column was dried by centrifuging at 21 300 × *g* for 1 minute. After drying, the binding column was transferred into a new clean collection tube, and 50 µl of Elution Solution was added onto the centre of the binding column, left to sit at room temperature for a minute before centrifuging at 21 300 × *g* for 1 minute. The resulting eluate was then collected and quantified using a SMART Drop™ L (ACCURIS Instruments, New Jersey, USA).

5.2.2 Agarose gel electrophoresis of total RNA samples

Leaf total RNA (300 ng) was visually analysed on a 1.2% (w/v) agarose gel. The agarose gel was prepared with 1X MOPS (3-(N-Morpholino)-propanesulfonic acid) buffer [20 mM MOPS pH 7.0, 2 mM sodium acetate pH 7.0, 1 mM EDTA (Ethylenediaminetetraacetic acid) pH 8.0], and 5% SafeView™ Classic (Applied Biological Materials Inc., Richmond, Canada). The gel was left to polymerise while the RNA samples were being prepared. The leaf total RNA samples were prepared at a ratio of 1:1 with the RNA loading dye (2X) (New England Biolabs Inc., Massachusetts, USA) and incubated on a heat block at 65 °C for 10 minutes. The samples were pulse centrifuged, loaded onto the agarose gel, and electrophoresed at 90 V for 45 minutes in 1X MOPS containing 5% SafeView™ Classic reagent (Applied Biological Materials Inc.). The agarose gel was then scanned using a Molecular Imager Gel Doc™ XR+ with Image Lab™ software version 5.2.1 (BIO-RAD, Hercules, USA).

5.2.3 Complementary cDNA synthesis

A GoScript™ Reverse Transcriptase System (Catalog No: A5003; Promega, Southampton, UK) was used for cDNA synthesis according to the manufacturer’s instructions with minor modifications. Only the day 28 of drought stress treatment leaf RNA samples were used for cDNA synthesis in this study. For the first-strand cDNA synthesis, a reaction mixture containing 0.5 µg of Oligo(dT) and 1 µg of total leaf RNA was prepared to a total volume of 11.8 µl using nuclease-free water in low-profile PCR tubes. The reaction mixture was incubated in a T100™ Thermal cycler (BIO-RAD) at 70 °C for 5 minutes, followed by a 5 minute incubation on ice. A reverse transcriptase reaction mixture was then prepared in a 0.5 ml Eppendorf tube for the second-strand cDNA synthesis as illustrated in Table 5.1.

Table 5.1: Reverse transcription reaction mixture.

Component	**Volume (µl)**
GoScript 5X reaction buffer	4
1.5-5.0 mM magnesium chloride	1.8
0.5 mM dNTPs	1
Recombinant RNasin® Ribonuclease inhibitor	0.4
GoScript reverse transcriptase	1
Total	**8.2**

The reverse transcription reaction mixture was added to the first-strand cDNA synthesis mixture, mixed by pipetting and incubated in the T100™ Thermal cycler (BIO-RAD). cDNA synthesis was performed using the thermal cycling conditions illustrated in Table 5.2. Thereafter, the cDNA was diluted at a ratio of 1:50 with nuclease-free water and stored at -20 °C before qRT-PCR analysis.

Table 5.2: Thermal cycling conditions for cDNA synthesis.

Step	**Temperature (°C)**	**Time**
Annealing	25	5 minutes
Elongation	42	1 hour
Denaturation	70	15 minutes
Hold	12	∞

5.2.4 Primer design for drought stress-responsive target genes

Six drought-responsive leaf proteins were randomly selected from the iTRAQ results (Table 4.2 and 4.3) for use in gene expression analysis. The *wheat α-tubulin* (Ma *et al.*, 2017) and an *elongation factor-1 alpha* (Kumar *et al.*, 2018) were used as reference control genes to normalize the expression data. Primer sequences of the target wheat leaf genes were designed on the National Centre for Biotechnology Information (NCBI) database using the Primer-BLAST software (Ye *et al.*, 2012). The forward and reverse primer sequences were designed using the following specifications: *Triticum aestivum* (taxid: 4565), GC clamp 1, 50 bp minimum and 150 bp maximum primer sizes. The primer sequences were sent to Inqaba Biotechnical Industries (Menlo Park, South Africa) for synthesis and supply. The primers were diluted with nuclease-free water for a 100 µM working stock solution before testing their specificity. The wheat target genes and their respective primer sequences are shown in Table 5.3.

Table 5.3: List of primer sequences of wheat leaf target and reference genes.

Accession no.*	**Gene name**	**Forward Primer (5'>3')**	**Reverse Primer (5'>3')**
A0A3B6U9Q7	*CYTB_CTER domain-containing protein*	AGTTGTAGGTGCAACTTCGG	GGCTCGAGCAAGAGTGAAAG
A0A3B6N353	*Pentacotripeptide-repeat region of PRORP domain-containing protein*	CGGCATGAGGCTGTTTTCTG	CCACAGAGGTGTAGTGCTCC
A0A3B6EFA0	*Uncharacterized protein*	AGCTGGTGATATCTGGTTCTG	ACAACCGAAATCCTGCAATCG
P58311	*Photosystem I P700 chlorophyll a apoprotein A1*	GAGTGCTTTAGGCCGTCCAC	TCGCAAGGAAAGCGAAAACC
W5ACM8	*Delta-1-pyrroline-5-carboxylate synthase*	CTCGGCCAGGAGATAAACTCG	AGCACGTCCTACAGGTTTGG
A0A3B6TZ07	*GH18 domain-containing protein*	CAGATTGGTCGCACAGTTATGG	TCTTGCATTTGCTGCTGTGC
Reference gene	*Wheat α-tubulin*	ATCTGTGCCTTGACCGTATCAGG	GACATCAACATTCAGGACACCATC
Reference gene	*Elongation factor-1 alpha*	GCTGTCAAGTTTGCTGAGATCC	GTACTGAGCGAAGGTCTCCAC

*Accession numbers of target genes obtained from isobaric tag for relative and absolute quantitation (iTRAQ) proteomic data in Tables (4.2 and 4.3). The reference genes and their primer sequences were obtained from literature sources (Ma *et al*., 2017; Kumar *et al*., 2018).

5.2.5 Polymerase chain reaction for primer testing

Conventional PCR analysis was used to test for primer specificity before gene expression analysis. All six primer pairs and those of the two reference control genes *wheat α-tubulin* and *elongation factor-1 alpha* (Table 5.3) were used for primer testing. Both control and drought-stressed samples were used for primer testing using a OneTag Quick-Load 2X Master Mix with Standard Buffer (Cataloq No: M04865; New England Biolabs Inc.). The reaction mixtures (Table 5.4) were prepared in low-profile PCR tubes and incubated in the T100™ Thermal cycler (BIO-RAD) under the thermal cycling conditions described in Table 5.5.

Table 5.4: Reaction mixture preparation for primer testing.

Component	**Reaction mixture (µl)**	**Final concentration (µM)**
100 µM Forward Primer	0.2	4
100 µM Reverse Primer	0.2	4
One-Taq Quick-Load 2X master mix	5	1X
Nuclease-free water	3.6	–
cDNA (diluted 1:20)	1	–
Total	10	

Table 5.5: Thermal cycling conditions for conventional PCR.

Step	**Temperature (°C)**	**Time**	**Cycles**
Initial denaturation	94	30 seconds	1
Denaturation	94	30 seconds	40
Annealing	60	60 seconds	
Extension	68	60 seconds	
Final extension	68	5 minutes	
Hold	12	∞	

After the PCR run, the amplicons were electrophoresed on a 3.5% (w/v) agarose gel in tris acetate-(ethylenedinitrilo)-tetraacetic acid (TAE) buffer [40 mM Tris-acetate and 0.5 M EDTA (pH 8)] containing 5% SafeView™ Classic (Applied Biological Materials Inc.). A 50 bp DNA Ladder (New England Biolabs Inc.) and PCR products were electrophoresed at 120 V for 120 minutes in 1X TAE running buffer. The gels were scanned using the Molecular Imager Gel Doc™ XR+ with Image Lab™ software version 5.2.1 (BIO-RAD).

5.2.6 qRT-PCR analysis

The SsoAdvanced Universal SYBR Green Supermix Kit (Catalog No: 1725270, BIO-RAD) was used to perform qRT-PCR following the manufacturer's instructions. Due to the high cost of the kit, only six target genes from total RNA samples of day 28 control and drought-stressed leaves were analysed. The qRT-PCR analysis was performed using six randomly selected target genes, the *Photosystem I P700 chlorophyll a apoprotein* A1 (*P58311), pentacotripeptide-repeat region of PRORP domain-containing protein* (*A0A3B6N353*), *delta-1-pyrroline-5-carboxylate synthase* (*W5ACM8*), *GH18 domain-containing protein* (*A0A3B6TZ07*), *uncharacterized protein* (*A0A3B6EFA0*), *Cytochrome b/b6 C-terminal region profile domain-containing protein* (*A0A3B6U9Q7*) and two reference control genes *wheat α-tubulin* and *elongation factor-1 alpha*. The expression levels of the corresponding proteins from the iTRAQ data are summarised in Table 5.6.

Table 5.6: Drought stress-responsive wheat leaf proteins selected for qRT-PCR analysis.

Protein name	Wheat Variety	Accession no.*	Fold change
Photosystem I P700 chlorophyll a apoprotein A1	BW35695	P58311	-2.39
Pentacotripeptide-repeat region of PRORP domain-containing protein	BW35695	A0A3B6N353	2.10
Delta-1-pyrroline-5-carboxylate synthase	BW4074	W5ACM8	1.52
GH18 domain-containing protein	BW35695	A0A3B6TZ07	1.84
Uncharacterized protein	BW35695	A0A3B6EFA0	2.66
CYTB_CTER domain-containing protein	BW35695	A0A3B6U9Q7	-3.44

*Accession number obtained from the UniProt database (http://ww.uniprot.org). BW4074 (drought-susceptible) and BW35695 (drought-tolerant).

To perform the qRT-PCR analysis, a reaction mixture was prepared as shown in Table 5.7. A volume of 15 µl of the reaction mixture containing all reagents except for cDNA was initially prepared as a master mix for each gene in 0.5 ml Eppendorf tube. This mixture was then added to a 5 µl cDNA solution diluted 1:50 in a 96-well plate, making a total reaction volume of 20 µl. Three biological replicates of both control and drought-stressed samples were prepared for the qRT-PCR analysis.

Table 5.7: Reaction mixture preparation.

Component	Volume (µl)	Final concentration (µM)
SsoAdvanced Universal SYBR Green Supermix (2X)	10	-
100 µM Forward Primer	0.8	4
100 µM Reverse Primer	0.8	4
cDNA (diluted 1:50)	5	-
Nuclease-free water	3.4	-
Total	**20**	

The qRT-PCR was performed on a CFX Connect Real-Time System (BIO-RAD) following the thermal cycling conditions shown in Table 5.8.

Table 5.8: Thermal cycling conditions for qRT-PCR.

Step	**Temperature (°C)**	**Time (seconds)**	**Cycles**
Initial denaturation	95	30	1
Denaturation	95	10	40
Annealing/Extension	60	30	
Melt-Curve	65-95, 0.5 increment	0.05	1

The data was analysed using default settings in the CFX Manager software version 4.1.2433.1219 (BIO-RAD) to determine the relative normalized gene expression changes. The formula for the normalized expression on the CFX Manager software compares the relative quantity of a gene of interest to a reference gene across different samples.

$$\text{Relative expression}_{\text{sample (GOI)}} = \text{RQ}_{\text{sample (GOI)}}/\ \text{RQ}_{\text{sample (Ref 1)}} \times \text{RQ}_{\text{sample (Ref 2)}} \times \text{RQ}_{\text{sample (Ref n)}}{}^{1/n}$$

Where RQ = relative quantity of a sample, Ref = reference target in a run that includes one or more reference targets in each sample, n = number of reference targets and GOI = gene of interest (one target)

A Student’s *t*-test was used to compare the relative normalized expression changes between the control and drought-stressed samples at a 5% level of significance.

5.3 Results

5.3.1 Leaf total RNA extraction from wheat plants

The total RNA extracted from leaves of both wheat varieties at days 14 and 28 was quantified and electrophoresed on a 1.2% (w/v) agarose gel for quality checks. Figures 5.1A and B show that the quality of the leaf total RNA extraction for the control and drought-stressed samples for all biological replicates was good. After quality checks, only the 28-day leaf RNA samples from both wheat varieties were used for cDNA synthesis in preparation for gene expression analysis, due to time constraints and the availability of reagents.

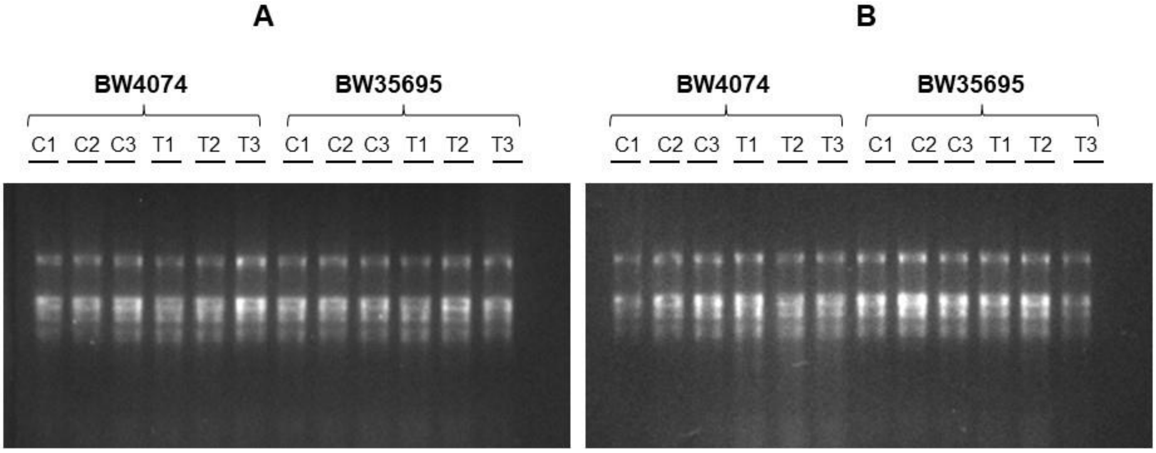

Figure 5.1: Leaf total RNA extracts of wheat plants on a 1.2% (w/v) agarose gel. BW4074, drought-susceptible and BW35695 drought-tolerant (A) shows leaf RNA at day 14 and (B) leaf RNA at day 28 of drought stress treatment. A 300 ng total RNA was loaded in each lane. Three biological replicates were prepared for the control (C1-C3) and drought stress treatment (T1-T3) groups.

5.2.2 Gene expression analysis using qRT-PCR

Convectional PCR was used to assess the specificity of the six wheat primer sets and two reference genes. PCR amplicon yields and size specificities varied with genes across the two wheat varieties (results not shown). Following the primer testing, primer sets were subsequently used for qRT-PCR analysis. The gene expression data was obtained from the CFX manager software (BIO-RAD) and the results indicated that the qRT-PCR data validated the protein data for one of the targets. For instance, the *delta-1-pyrroline-5-carboxylate synthase* (*W5ACM8*) gene was upregulated in BW4074 following drought stress treatment (Figure 5.2), which aligned with the iTRAQ results which showed an increase in the corresponding protein (Tables 4.2 and 5.6). The gene expression results also demonstrated that *Photosystem I P700 chlorophyll a apoprotein A1* and *CYTB_CTER domain-containing protein* genes were downregulated in both varieties, with statistical significance difference between control and drought-stressed plants only observed in BW4074 (Figure 5.2). However, the iTRAQ data showed that Photosystem I P700 chlorophyll a apoprotein A1 (P58311) and CYTB_CTER domain-containing protein (A0A3B6U9Q7) were significantly downregulated in BW35695 (Table 4.3 and 5.6) and were not identified as drought-responsive in BW4074 (Table 4.2). Additionally, the *GH18 domain-containing protein (A0A3B6TZ07)* and the *Uncharacterized protein (A0A3B6EFA0*) exhibited no significant changes in expression following drought stress treatment in both varieties (Figure 5.2), despite their respective proteins being significantly upregulated in BW35695 (Table 4.3 and 5.6). These results highlight different gene expression patterns between the wheat varieties following the 28 days of drought stress treatment.

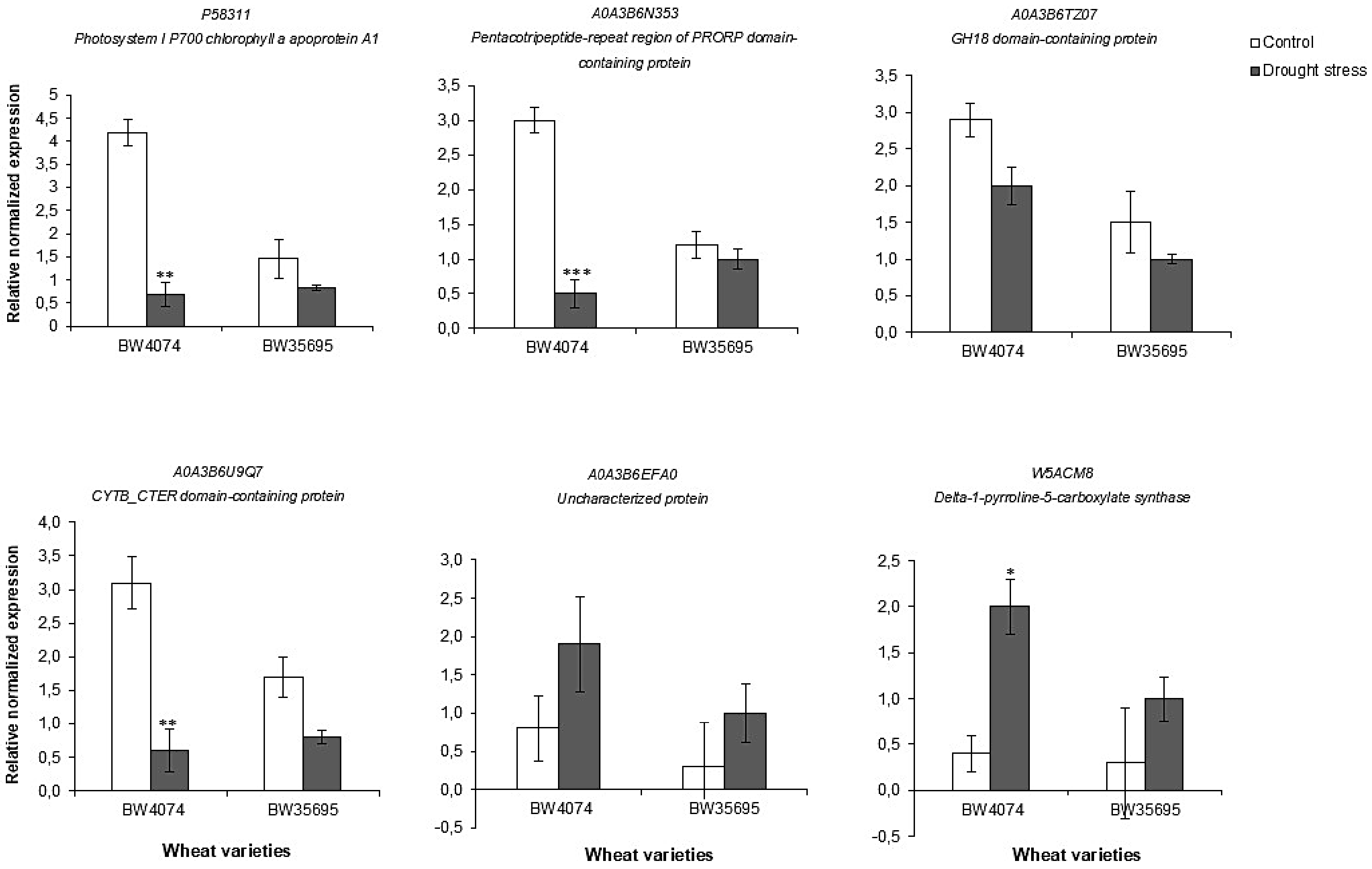

Figure 5.2: Gene expression analysis in wheat leaf tissue following drought stress treatment. Drought-susceptible BW4074 and drought-tolerant BW35695 wheat varieties were exposed to drought stress by withholding water for 28 days. Gene expression analysis was performed using qRT-PCR and the CFX Manager software version 4.1.2433.1219. Data is presented as mean ± SE (*n* = 3). *, ** and **** = significance at $p \leq 0.05$, 0.01 and 0,001, respectively, using a Student’s *t*-test.

5.4 Discussion

Plants alter their gene expression to enhance their adaptability and survival under drought stress conditions. In this study, gene expression analysis was conducted to validate the leaf proteome data presented in Chapter 4. Total RNA was extracted from leaf tissue of both wheat varieties at 14 and 28 days of drought stress treatment to study the differences in gene expression between control and drought-stressed samples. To visually analyse the quality of the extracted total RNA, an agarose gel electrophoresis was performed. The results showed that leaf extracts were of good quality, however, the RNA extract did not separate well possibly due to high or low voltage, high or low temperature or poor buffer conductivity (Figure 5.1).

Gene expression analysis was conducted using randomly selected six wheat leaf target genes of the two varieties subjected to drought stress (Figure 5.2). The drought-tolerant variety BW35695 exhibited no statistically significant differences in gene expression between the control and drought-stressed plants for all six target genes. In contrast, the drought-susceptible variety BW4074 showed up and down regulations in gene expression in four of the six wheat target genes (Figure 5.2). The gene expression analysis results possibly indicate that the abundances of the proteins and transcripts accumulate at different time points (Zhao *et al*., 2018). Nevertheless, the expression level of a *delta-1-pyrroline-5-carboxylate synthase (P5CS)* was significantly increased in BW4074 following drought stress treatment which correlated with the drought-responsive proteome data (Table 5.6). The *delta-1-pyrroline-5-carboxylate synthase gene* is involved in proline biosynthesis and the gene and its metabolite are known to accumulate in various plant species in response to drought (Szabados and Savouré, 2010). However, in the current study, the drought-susceptible variety, BW4074 exhibited no statistically significant change in proline accumulation in the leaves following the 28 days of drought stress treatment (Figure 3.11A) and only increased significantly in the roots (Figure 3.11B).

In contrast the *P5CS* gene was also differentially expressed in response to drought stress in other wheat varieties but much higher in the leaves of a drought-tolerant variety compared to the sensitive one (Dashtaki *et al*., 2023). The authors highlighted that the increased expression of the *P5CS* gene in the wheat varieties correlated with higher proline levels in the wheat leaves and also that the *P5CS* gene had the potential to enhance wheat's drought tolerance (Dashtaki *et al*., 2023).

Both wheat varieties also showed the downregulation of *Photosystem I P700 chlorophyll a apoprotein A1* and *CYTB_CTER domain-containing protein* following drought stress treatment, even though the significant difference was only observed in BW4074 (Figure 5.2). The corresponding proteins of these genes were downregulated in BW35695, but not identified in BW4074. The results also suggest that the abundance of the transcripts and proteins varied following the 28 days of stress treatment.

5.5 Conclusion

Overall, gene expression analysis showed that some of the six wheat target genes were differentially regulated between the two wheat varieties in response to drought stress. Additionally, the accumulation of transcripts and proteins may occur at different time points of the stress treatment, resulting in changes in cellular stress responses. Therefore, in future studies, it is important to conduct gene expression analysis at different time points during stress treatment.

CHAPTER 6

GENERAL DISCUSSION, CONCLUSIONS, AND RECOMMENDATIONS

Drought stress negatively impacts plant growth and productivity and contributes to global food insecurity (Seleiman *et al*., 2021). Therefore, it is important to develop crops that can withstand drought stress and help sustain agricultural productivity. Wheat (*Triticum aestivum*) is ranked globally as the second most cultivated cereal crop after maize (*Zea mays*) (FAOSTAT, 2023) and serves as an important source of protein and calories in the human diet. Therefore, it is imperative to enhance its tolerance to drought to help ensure food security. Investigating the responses of cereal crops to drought may provide insights into the mechanisms underlying drought stress tolerance to develop drought-resilient crops.

This study investigated the morpho-physiological, biochemical and leaf proteome responses of the drought-susceptible BW4074 and drought-tolerant BW35695 wheat plants under drought stress conditions. Two-week-old potted wheat plants were exposed to drought stress by withholding water for 28 days. The gravimetric soil moisture content measurements showed that the withholding water resulted in a significant decrease in moisture in progressively drying soils in both wheat varieties, however, no significant differences were observed in water utilisation between the varieties (Figure 3.4). The imposed stress was equivalent to mild and moderate drought stress conditions (Samarah, 2005; Bai *et al*., 2006) on days 14 and 28 of the stress treatment, respectively. Although both BW4074 and BW35695 wheat plants were exposed to similar levels of water deficit stress (Figure 3.4), significant differences were observed in some physiological and biochemical responses of the two varieties to drought. This possibly highlights some of the key adaptive responses that contribute to the contrasting drought phenotypes of the two wheat varieties (Table 3.1).

Drought stress negatively affects diverse plant processes including growth, yield, membrane integrity, pigment content, water relations and photosynthesis (Anjum *et al.*, 2011). In response to drought stress, plants employ diverse stress-adaptive responses, such as maintaining a higher leaf relative water content (RWC), increasing the accumulation of osmolytes such as proline and glycine betaine, enhancing enzymatic and non-enzymatic antioxidant activities, and accumulating stress-responsive genes, proteins and other metabolites (Bandurska, 2022). Maintaining a high leaf RWC under drought-stress conditions ensures that cells remain hydrated for optimal metabolic activities (Qiao *et al.*, 2024). Several comparative studies of different plant species such as soybean (*Glycine max* L.) (Xu *et al.*, 2023), sorghum (*Sorghum bicolor*) (Goche *et al.*, 2020), and wheat (Akter *et al.*, 2023), have also reported that drought-tolerant varieties maintained higher RWC under water limiting conditions than the drought-susceptible counterparts. Similarly, in this study, the drought-tolerant wheat variety, BW35695, maintained a higher RWC than its drought-susceptible counterpart, BW4074 (Figure 3.5). This aspect also correlated well with increased contents of osmolytes such as proline and glycine betaine observed under drought stress (Figure 3.11). These osmolytes are known to play a role in maintaining water uptake and osmotic adjustment, and also as osmoprotectants that protect cell membrane integrity, stabilize enzymes and other proteins, and mitigate oxidative damage under drought stress (Ashraf and Foolad, 2007; Ghosh *et al.*, 2022).

Under water deficit stress, ROS generation increases in the chloroplast, mitochondria and peroxisomes, leading to oxidative stress, and subsequently the oxidative stress damage of various cellular components (Mittler *et al.*, 2022). In this study, superoxide anion and hydrogen peroxide contents significantly increased in the leaves and roots of both wheat varieties following the 28-day drought stress treatment (Figure 3.8). However, BW35695 exhibited lower levels of these ROS molecules when compared to BW4074, in both tissue types.

Furthermore, the drought-susceptible BW4074 exhibited greater membrane lipid damage than the drought-tolerant BW35695 in both leaves and roots (Figure 3.9). The lower membrane lipid damage observed in BW35695 could be due to the variety's enhanced ROS scavenging capacity, which is facilitated by increased enzymatic antioxidant activities such as superoxide dismutase, guaiacol peroxidase and ascorbate peroxidase (Figure 3.10), as well as higher proline, glycine betaine content (Figure 3.11) and carotenoid content (Figure 3.7). Similar results have been reported in other comparative studies of wheat (Dashtaki *et al*., 2023) and soybean (Xu *et al*., 2023) where lipid peroxidation was reduced in drought-tolerant genotypes due to their higher antioxidant activities compared to the drought-susceptible genotypes.

Although antioxidant enzyme activity was suppressed in BW4074 (Figure 3.10), the leaf proteome results obtained using the iTRAQ method revealed an up-regulation of proteins such as superoxide dismutase [Cu-Zn], glutathione reductase and monodehydroascorbate reductase (Table 4.2). The upregulation of these ROS-detoxifying proteins suggests that BW4074 may be using other antioxidant enzymes to protect its cells from oxidative stress, and these enzymes could be different from those assayed for in the biochemical analyses of the current study (Figure 3.10). The drought-tolerant variety also upregulated other ROS detoxification proteins such as catalase, a thioredoxin domain-containing protein, and a peroxidase (Table 4.3). Collectively, the leaf proteome results revealed a variety of antioxidant enzymes in the wheat plants under drought stress. This suggests the need for additional biochemical assays to account for this diversity in the drought-responsive proteome of wheat in future studies.

The drought-tolerant BW35695 also exhibited a remarkable downregulation of photosynthesis-related proteins (Tables 4.3) , possibly as a protective strategy to reduce ROS-induced oxidative damage. A similar downregulation of photosynthesis-related proteins was observed in the leaves of a drought-sensitive (Kukri) and two drought-tolerant (Excalibur and RAC875) wheat cultivars in response to cyclic drought stress (Ford *et al*., 2011). The authors suggested that a decrease in photosynthesis could be a response mechanism to avoid increased ROS accumulation (Ford *et al*., 2011).

Apart from the ROS detoxification and photosynthesis-related proteins, the iTRAQ analysis also identified transcription and translation-related proteins in both varieties (Tables 4.2 and 4.3). The transcription-related proteins were upregulated in both wheat varieties, and these included histone proteins which facilitate the transcription regulation of stress-responsive proteins (Yuan *et al.*, 2013). Translational-related proteins were upregulated in both wheat varieties following drought stress which possibly enhanced the synthesis of stress-responsive proteins in both wheat varieties under the stress conditions of the study (Table 4.2 and 4.3). Figure 6.1 below highlights some of the key drought response mechanisms observed in the wheat varieties.

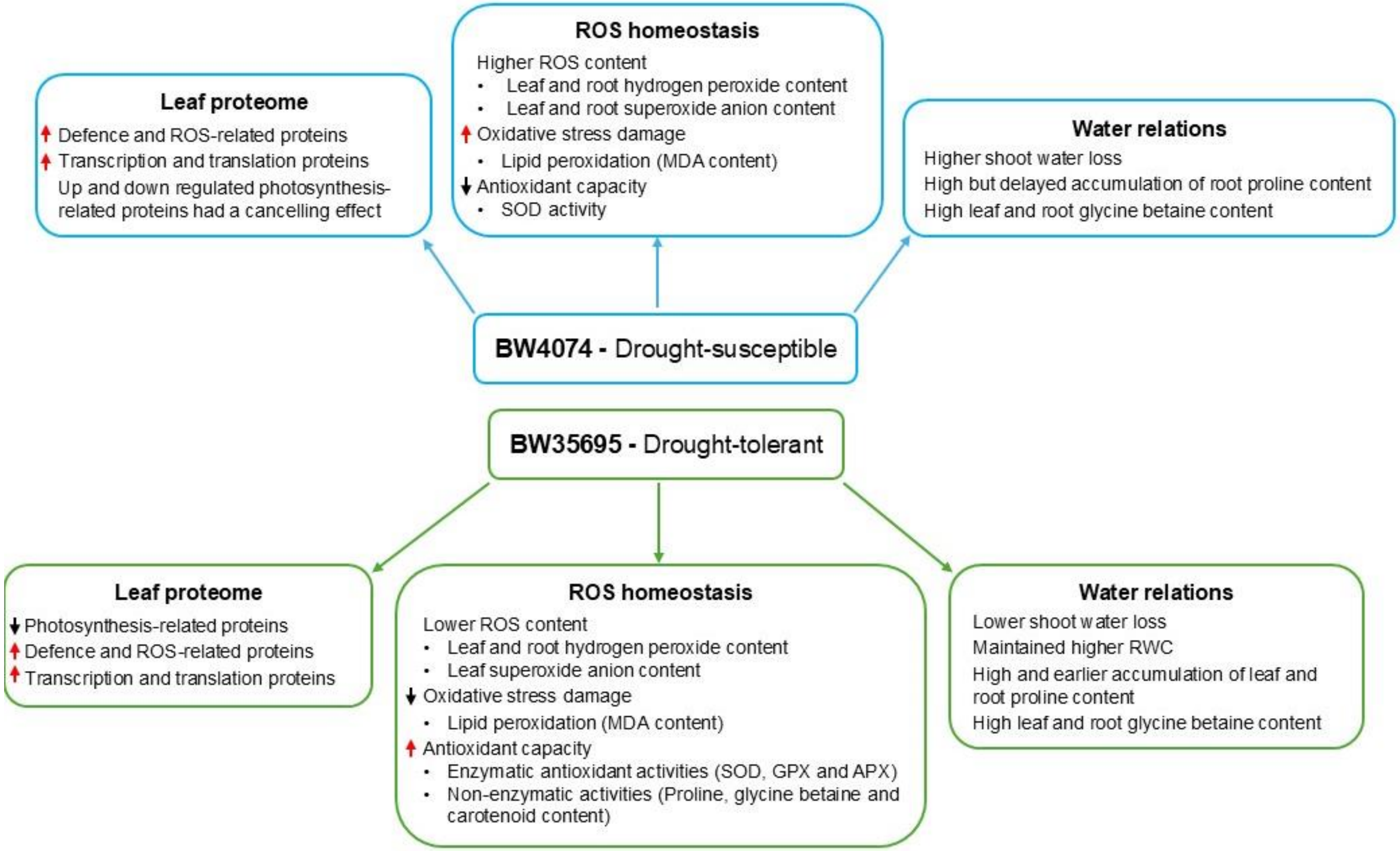

Figure 6.1: An overview of the morpho-physiological, biochemical, and leaf proteome results of wheat plants generated in the current study. BW35695 is the drought-tolerant, while BW4074 is the drought-susceptible wheat varieties. MDA, malondialdehyde; ROS, reactive oxygen species; RWC, relative water content, SOD, superoxide dismutase, GPX, guaiacol peroxidase, APX, ascorbate peroxidase. Red arrows indicate an up-regulation or increase in response to drought, while black arrows indicate a down-regulation or decrease. ROS, reactive oxygen species.

Following the proteomic analysis, six proteins were randomly selected from the lists of differentially expressed proteins in the two wheat varieties for gene expression analysis using quantitative real-time polymerase chain reaction (qRT-PCR). The qRT-PCR results validated the expression of one of the target genes in BW4074, a *delta-1-pyrroline-5-carboxylate synthase* (*W5ACM8*) which is involved in proline biosynthesis (Figure 5.2). All six target genes in BW35695 were not differentially expressed under drought stress, which possibly indicates that the abundances of the proteins and transcripts accumulate at different time points. Therefore, future studies should conduct gene expression analysis using leaf and root tissue samples harvested at different time points during the drought stress treatment. Such an experimental workflow will assist in evaluating both the temporal and spatial aspects of gene expression under drought stress (Wang *et al*., 2011).

Overall, the comparative physiological, biochemical and proteomic analyses showed that the two wheat varieties responded differently to drought stress, possibly highlighting their divergent drought phenotypes (Table 3.1). The drought-tolerant variety, BW35695, was better able to tolerate the imposed drought stress than the drought-susceptible variety, BW4074. Future research could also focus on analysing the root proteome under drought stress conditions, as the roots are the first organs to detect the onset of water deficit stress. The root proteome analysis could also enable researchers to better understand the differences and similarities in drought stress signalling pathways between the two wheat varieties.

The functional validation studies of the proteome data could also be conducted using different methods. Various system biology approaches such as western blotting (Handler *et al*., 2018), enzyme activity assays (Niu *et al*., 2018), or transgenic plant biology (Abdeeva *et al*., 2012) could also be employed for functional validation of the proteomic data. The two wheat varieties

BW4074 and BW35695 could also be exposed to different levels of drought stress (that is mild, moderate and severe) followed by re-watering to get better insights into their drought response and recovery mechanisms. Other studies have exposed plants to different stress levels and done recovery assessments to better understand drought response mechanisms (Mejri *et al*., 2016; Dien *et al*., 2019).

Measurements of various photosynthesis-related parameters such as the chlorophyll index and photosynthesis rate could also be conducted to understand why the assayed photosynthetic pigments significantly increased in the drought-tolerant variety, BW35695, following the 28-day drought stress treatment (Figure 3.7), yet the proteome data showed down-regulation of photosynthesis-related proteins (Table 4.3, Figure 4.7). Furthermore, field studies measuring yield components of the varieties could also be conducted as drought stress is known to affect the yield of wheat plants (Xu *et al*., 2023). Based on the integrated comparative physiological, biochemical and proteomic analyses conducted in the current study, the drought-tolerant wheat variety, BW35695 was better adapted to drought stress when compared to the drought-susceptible wheat variety, BW4074. The information obtained could offer valuable insight for plant breeding initiatives aimed at improving the drought tolerance of agriculturally important food crops.

REFERENCES

Abdallah, C., Dumas-gaudot, E., Renaut, J., & Sergeant, K. (2012). Gel-based and gel-free quantitative proteomics approaches at a glance. *International Journal of Plant Genomics., 2012,* 1–17.

Abdeeva, I., Abdeev, R., Bruskin, S., & Piruzian, E. (2012). Transgenic plants as a tool for plant functional genomics. In Y. Ö. Çiftçi (Ed.), *Transgenic Plants-Advances and Limitations* (pp. 259–284). IntechOpen.

Abid, M., Ali, S., Kang Qi, L., Zahoor, R., Tian, Z., Jiang, D., Snider, J. L., & Dai, T. (2018). Physiological and biochemical changes during drought and recovery periods at tillering and jointing stages in wheat (*Triticum aestivum* L.). *Scientific Reports*, *8,* 4615.

Abreu, I. A., Farinha, A. P., Negrão, S., Gonçalves, N., Fonseca, C., Mafalda, R., Batista, R., Saibo, N. J. M., & Oliveira, M. M. (2013). Coping with abiotic stress: Proteome changes for crop improvement. *Journal of Proteomics*, *93*, 145–168.

Agarwal, P. K., & Jha, B. (2010). Transcription factors in plants and ABA dependent and independent abiotic stress signalling. *Biologia Plantarum*, *54*, 201–212.

Aggarwal, S., & Yadav, A. K. (2016). Dissecting the iTRAQ Data Analysis. In K. Jung (Ed.), *Statistical Analysis in Proteomics* (pp. 277–291). Springer Science and Business Media.

Ahmad, P., Jaleel, C. A., Salem, M. A., Nabi, G., & Sharma, S. (2010). Roles of enzymatic and nonenzymatic antioxidants in plants during abiotic stress. *Critical Reviews in Biotechnology*, *30*, 161–175.

Ahmad, Z., Waraich, E. A., Akhtar, S., Anjum, S., Ahmad, T., Mahboob, W., Hafeez, O. B. A., Tapera, T., Labuschagne, M., & Rizwan, M. (2018). Physiological responses of wheat to drought stress and its mitigation approaches. *Acta Physiologiae Plantarum*, *40,* 80.

Ahmed, N., Zhang, Y., Li, K., Zhou, Y., Zhang, M., & Li, Z. (2019). Exogenous application of glycine betaine improved water use efficiency in winter wheat (*Triticum aestivum* L.) via modulating photosynthetic efficiency and antioxidative capacity under conventional and limited irrigation conditions. *The Crop Journal*, *7*, 635–650.

Akter, N., Brishty, T. A., Karim, M. A., Ahmed, M. J. U., & Islam, M. R. (2023). Leaf water status and biochemical adjustments as a mechanism of drought tolerance in two contrasting wheat (*Triticum aestivum* L.) varieties. *Acta Physiologiae Plantarum, 45*, 50.

Alam, I., Sharmin, S. A., Kim, K., Yang, J. K., Choi, M. S., & Lee, B. (2010). Proteome analysis of soybean roots subjected to short-term drought stress. *Plant Soil, 333*, 491–505.

Ali, A. E. E., Husselmann, L. H., Tabb, D. L., & Ludidi, N. (2023). Comparative proteomics analysis between maize and sorghum uncovers important proteins and metabolic pathways mediating drought tolerance. *Life*, *13*, 170.

Ali, G. M., & Komatsu, S. (2006). Proteomic analysis of rice leaf sheath during drought stress. *Journal of Proteome Research*, *5,* 396–403.

Amoah, J. N., & Seo, Y. W. (2021). Effect of progressive drought stress on physio-biochemical responses and gene expression patterns in wheat. *3 Biotech*, *11*, 440.

Anjum, S. A., Tanveer, M., Ashraf, U., Hussain, S., Shahzad, B., Khan, I., & Wang, L. (2016). Effect of progressive drought stress on growth, leaf gas exchange, and antioxidant production in two maize cultivars. *Environmental Science and Pollution Research*, *23*, 17132–17141.

Anjum, S. A., Xie, X.-Y., Wang, L.-C., Saleem, M. F., Man, C., & Lei, W. (2011). Morphological, physiological and biochemical responses of plants to drought stress. *African Journal of Agricultural Research*, *6*, 2026–2032.

Apel, K., & Hirt, H. (2004). Reactive oxygen species: metabolism, oxidative stress, and signal transduction. *Annual Review of Plant Biology*, *55*, 373–399.

Ashoub, A., Beckhaus, T., Berberich, T., Karas, M., & Bruggemann, W. (2013). Comparative analysis of barley leaf proteome as affected by drought stress. *Planta*, *237*, 771–781.

Ashraf, M. (2009). Biotechnological approach of improving plant salt tolerance using antioxidants as markers. *Biotechnology Advances*, *27*, 84–93.

Ashraf, M., & Foolad, M. R. (2007). Roles of glycine betaine and proline in improving plant abiotic stress resistance. *Environmental and Experimental Botany*, *59*, 206–216.

Ashraf, M., & Harris, P. J. C. (2004). Potential biochemical indicators of salinity tolerance in plants. *Plant Science*, *166*, 3–16.

Ashraf, M., & Harris, P. J. C. (2013). Photosynthesis under stressful environments: An overview. *Photosynthetica*, *51*, 163–190.

Aslam, B., Basit, M., Nisar, M. A., Khurshid, M., & Rasool, M. H. (2017). Proteomics: Technologies and their applications. *Journal of Chromatographic Science*, *55*, 182–196.

Athar, H. R., Ashraf, M., Lieth, H., & Kratochwil, A. (2009). Strategies for crop improvement against salinity and drought stress: An overview. In H. Ashraf, M., Ozturk, M., Athar (Ed.), *Salinity and Water Stress: Improving Crop Efficiency* (pp. 1–16). Springer Science and Business Media B.V.

Atkinson, N. J., & Urwin, P. E. (2012). The interaction of plant biotic and abiotic stresses: from genes to the field. *Journal of Experimental Botany*, *63*, 3523–3543.

Ayala, A., Muñoz, M. F., & Argüelles, S. (2014). Lipid peroxidation: Production, metabolism, and signaling mechanisms of malondialdehyde and 4-hydroxy-2-nonenal. *Oxidative Medicine and Cellular Longevity*, *2014*, 360438.

Bai, L. P., Sui, F. G., Ge, T. Da, Sun, Z. H., Lu, Y. Y., & Zhou, G. S. (2006). Effect of soil drought stress on leaf water status, membrane permeability and enzymatic antioxidant system of maize. *Pedosphere*, *16*, 326–332.

Bandurska, H. (2022). Drought stress responses: Coping strategy and resistance. *Plants*, *11*, 922.

Bandurska, H., & Stroiński, A. (2003). ABA and proline accumulation in leaves and roots of wild (*Hordeum spontaneum*) and cultivated (*Hordeum vulgare* 'Maresi') barley genotypes under water deficit conditions. *Acta Physiologiae Plantarum*, *25*, 55–61.

Bao, Y., & Howell, S. H. (2017). The unfolded protein response supports plant development and defense as well as responses to abiotic stress. *Frontiers in Plant Science*, *8*, 344.

Bapela, T., Shimelis, H., Tsilo, T. J., & Mathew, I. (2022). Genetic improvement of wheat for drought tolerance: Progress, challenges and opportunities. *Plants*, *11*, 1331.

Barkla, B. J. (2016). Identification of abiotic stress protein biomarkers by proteomic screening of crop cultivar diversity. *Proteomes*, *4*, 26.

Barrs, H. D., & Weatherley, P. E. (1962). A re-examination of the relative turgidity technique for estimating water deficits in leaves. *Australian Journal of Biological Sciences*, *15*, 413–428.

Bartels, D., & Sunkar, R. (2005). Drought and salt tolerance in plants. *Critical Reviews in Plant Sciences*, *24*, 23–58.

Basu, S., Ramegowda, V., Kumar, A., & Pereira, A. (2016). Plant adapatation to drought stress. *F1000Research*, *5*, 1554.

Begg, J. E., & Turner, N. C. (1976). Crop water deficits. *Advances in Agronomy*, 161–217.

Bevan, M., Bancroft, I., Bent, E., Love, K., Goodman, H., Dean, C., Bergkamp, R., Dirkse, W., Van Staveren, M., Stiekema, W., Drost, L., Schueller, S., & Chalwatzis, N. (1998). Analysis of 1.9 Mb of contiguous sequence from chromosome 4 of Arabidopsis thaliana. *Nature, 391*, 485–488.

Bhatnagar-Mathur, P., Vadez, V., & Sharma, K. K. (2008). Transgenic approaches for abiotic stress tolerance in plants: Retrospect and prospects. *Plant Cell Reports*, *27*, 411–424.

Blum, A. (2017). Osmotic adjustment is a prime drought stress adaptive engine in support of plant production. *Plant Cell and Environment*, *40*, 4–10.

Bohnert, H. J., Donald, E. N., & Jensen, R. G. (1995). Adaptations to environmental stresses. *The Plant Cell*, *7*, 1099–1111.

Bowser, B. L., & Robinson, R. A. (2023). Enhanced multiplexing technology for proteomics. *Annual Review of Analytical Chemistry,* 16, 379-400.

Bradford, M. M. (1976). A rapid and sensitive method for the quantitation of microgram quantities of protein utilizing the principle of protein-dye binding. *Analytical Biochemistry*, *72*, 248–254.

Bray, E. A. (1997). Plant responses to water deficit. *Trends in Plant Science*, *2*, 48–54.

Chandramouli, K., & Qian, P. (2009). Proteomics: challenges, techniques and possibilities to overcome biological sample complexity. *Human Genomics and Proteomics*, *2009*, 239204.

Chaves, M. M., Flexas, J., & Pinheiro, C. (2009). Photosynthesis under drought and salt stress: regulation mechanisms from whole plant to cell. *Annals of Botany*, *103*, 551–560.

Chen, D., Wang, S., Cao, B., Cao, D., Leng, G., Li, H., Yin, L., Shan, L., & Deng, X. (2016). Genotypic variation in growth and physiological response to drought stress and re-watering reveals the critical role of recovery in drought adaptation in maize seedlings. *Frontiers in Plant Science*, *6*, 1241.

Chen, H., & Jiang, J.-G. (2010). Osmotic adjustment and plant adaptation to environmental changes related to drought and salinity. *Environmental Reviews, 18*, 309–319.

Chen, S., & Harmon, A. C. (2006). Advances in plant proteomics. *Proteomics*, *6*, 5504–5516.

Chen, X., Sun, Y., Zhang, T., Shu, L., Roepstorff, P., & Yang, F. (2021). Quantitative proteomics using isobaric labeling: A practical guide. *Genomics, Proteomics &*

Bioinformatics, *19*, 689–706.

Chinnusamy, V., Schumaker, K., & Zhu, J. (2004). Molecular genetic perspectives on cross-talk and specificity in abiotic stress signalling in plants. *Journal of Experimental Botany*, *55*, 225–236.

Chmielewska, K., Rodziewicz, P., & Swarcewicz, B. (2016). Analysis of drought-induced proteomic and metabolomic changes in barley (*Hordeum vulgare* L.) leaves and roots unravels some aspects of biochemical mechanisms involved in drought tolerance. *Frontiers in Plant Science*, *7*, 1108.

Choudhury, F. K., Rivero, R. M., Blumwald, E., & Mittler, R. (2017). Reactive oxygen species, abiotic stress and stress combination. *The Plant Journal*, *90*, 856–867.

Cramer, G. R., Urano, K., Delrot, S., Pezzotti, M., & Shinozaki, K. (2011). Effects of abiotic stress on plants: a systems biology perspective. *BioMed Central Plant Biology*, *11*, 163.

Cui, G., Zhao, Y., Zhang, J., Chao, M., Xie, K., Zhang, C., Sun, F., Liu, S., & Xi, Y. (2019). Proteomic analysis of the similarities and differences of soil drought and polyethylene glycol stress responses in wheat (*Triticum aestivum* L.). *Plant Molecular Biology*, *100*, 391–410.

da Silva, E. C., de Albuquerque, M. B., Azevedo Neto, A. D. de, & Silva Junior, C. D. da. (2013). Drought and its consequences to plants – From idividual to ecosystem. In S. Akıncı (Ed.), *Responses of organisms to water stress* (pp. 17–47). Intech Open.

Danquah, A., de Zelicourt, A., Colcombet, J., & Hirt, H. (2014). The role of ABA and MAPK signaling pathways in plant abiotic stress responses. *Biotechnology Advances*, *32*, 40–52.

Dashtaki, M., Bihamta, M. R., Majidi, E., & Azizi nejad, R. (2023). Differential responses of wheat genotypes to irrigation regimes through antioxidant defense system, grain yield, gene expression, and grain fatty acid profile. *Cereal Research Communications*, *51*, 879–890.

de Sousa, T., Ribeiro, M., Sabença, C., & Igrejas, G. (2021). The 10,000-year success story of wheat. *Foods*, *10*, 2124.

Delauney, A. J., & Verma, D. P. S. (1993). Proline biosynthesis and osmoregulation in plants. *The Plant Journal*, *2*, 2154–2223.

Dien, D. C., Mochizuki, T., & Yamakawa, T. (2019). Effect of various drought stresses and subsequent recovery on proline, total soluble sugar and starch metabolisms in rice (*Oryza sativa* L.) varieties. *Plant Production Science*, *22*, 530–545.

Dien, D. C., Thu, T. T. P., Moe, K., & Yamakawa, T. (2019). Proline and carbohydrate metabolism in rice varieties (*Oryza sativa* L.) under various drought and recovery conditions. *Plant Physiology Reports*, *24*, 376–387.

Dumanović, J., Nepovimova, E., Natić, M., Kuča, K., & Jaćević, V. (2021). The significance of reactive oxygen species and antioxidant defense system in plants: A concise overview. *Frontiers in Plant Science*, *11*, 552969.

Dunyak, B. M., & Gestwicki, J. E. (2016). Peptidyl-proline isomerases (PPIases): Targets for natural products and natural product-inspired compounds. *Journal of Medicinal Chemistry*, *59*, 9622–9644.

Duque, A. S., Martinho De Almeida, A., Bernardes, A., Silva, D., Marques, J., Farinha, A. P., Santos, D., Fevereiro, P., De, S., & Araújo, S. (2013). Abiotic stress responses in plants: Unraveling the complexity of genes and networks to survive. In K. Vahdati & C. Leslie (Eds.), *Abiotic Stress - Plant Responses and Applications in Agriculture* (pp. 50–101). IntechOpen.

Fadoul, H. E., El Siddig, M. A., Abdalla, A. W. H., & El Hussein, A. A. (2018). Physiological and proteomic analysis of two contrasting *Sorghum bicolor* genotypes in response to drought stress. *Australian Journal of Crop Science*, *12*, 1543–1551.

Faghani, E., Gharechahi, J., Komatsu, S., Mirzaei, M., Khavarinejad, R. A., Najafi, F., Farsad, L. K., & Salekdeh, G. H. (2015). Comparative physiology and proteomic analysis of two wheat genotypes contrasting in drought tolerance. *Journal of Proteomics*, *114*, 1–15.

Fahad, S., Bajwa, A. A., Nazir, U., Anjum, S. A., Farooq, A., Zohaib, A., Sadia, S., Nasim, W., Adkins, S., Saud, S., Ihsan, M. Z., Alharby, H., Wu, C., Wang, D., & Huang, J. (2017). Crop production under drought and heat stress: Plant responses and management options. *Frontiers in Plant Science*, *8*, 1147.

Fang, Y., & Xiong, L. (2015). General mechanisms of drought response and their application in drought resistance improvement in plants. *Cellular and Molecular Life Sciences*, *72*, 673–689.

FAOSTAT. (2023). *Food and Agricultural Organisation of the United Nations*. https://www.fao.org/faostat/en/#compare (Accessed 2023-12-29)

Farooq, M., Hussain, M., & Siddique, K. H. M. (2014). Drought stress in wheat during flowering and grain-filling periods. *Critical Reviews in Plant Sciences*, *33*, 331–349.

Farooq, M., Wahid, A., Kobayashi, N., Fujita, D., & Basra, S. M. A. (2009). Plant drought stress: effects, mechanisms and management. *Agronomy for Sustainable Development*, *29*, 185–212.

Ford, K. L., Cassin, A., & Bacic, A. (2011). Quantitative proteomic analysis of wheat cultivars with differing drought stress tolerance. *Frontiers in Plant Science*, *2*, 44.

Foyer, C. H. (2018). Reactive oxygen species, oxidative signaling and the regulation of photosynthesis. *Environmental and Experimental Botany*, *154*, 134.

Foyer, C. H., & Noctor, G. (2005). Redox homeostasis and antioxidant signaling: A metabolic interface between stress perception and physiological responses. *The Plant Cell*, *17*, 1866–1875.

Franks, S. J. (2011). Plasticity and evolution in drought avoidance and escape in the annual plant Brassica rapa. *New Phytologist*, *190*, 249–257.

García-Descalzo, L., García-López, E., Alcázar, A., Baquero, F., & Cid, C. (2012). Gel electrophoresis of proteins. In S. Magdeldin (Ed.), *Gel electrophoresis-Principles and basics* (pp. 57–68). IntechOpen.

Ghatak, A., Chaturvedi, P., & Weckwerth, W. (2017). Cereal crop proteomics: Systemic analysis of crop drought stress responses towards marker-assisted selection breeding. *Frontiers in Plant Science*, *8*, 757.

Ghobadi, M., Taherabadi, S., Ghobadi, M. E., Mohammadi, G. R., & Jalali-Honarmand, S. (2013). Antioxidant capacity, photosynthetic characteristics and water relations of sunflower (*Helianthus annuus* L.) cultivars in response to drought stress. *Industrial Crops and Products, 50*, 29–38.

Ghosh, U. K., Islam, M. N., Siddiqui, M. N., Cao, X., & Khan, M. A. R. (2022). Proline, a multifaceted signalling molecule in plant responses to abiotic stress: understanding the physiological mechanisms. *Plant Biology, 24*, 227–239.

Gill, S. S., & Tuteja, N. (2010). Reactive oxygen species and antioxidant machinery in abiotic stress tolerance in crop plants. *Plant Physiology and Biochemistry, 48*, 909–930.

Goche, T., Shargie, N. G., Cummins, I., Brown, A. P., Chivasa, S., & Ngara, R. (2020). Comparative physiological and root proteome analyses of two sorghum varieties responding to water limitation. *Scientific Reports, 10*, 11835.

Gokul, A., Fahiem Carelse, M., Niekerk, L. A., Klein, A., Ludidi, N., Mendoza-Cozatl, D., & Keyster, M. (2021). Exogenous 3,3′-diindolylmethane improves vanadium stress tolerance in *Brassica napus* seedling shoots by modulating antioxidant enzyme activities. *Biomolecules, 11*, 436.

Goldberg, A. L. (2003). Protein degradation and protection against misfolded or damaged proteins. *Nature, 426,* 895–899.

Govindan, G., K R, S., Alphonse, V., & Somasundram, S. (2024). Role of germin-Like proteins (GLPs) in biotic and abiotic stress responses in major crops: A review on plant defense mechanisms and stress tolerance. *Plant Molecular Biology Reporter, 42,* 450–468.

Graves, P. R., & Haystead, T. A. J. (2002). Molecular biologist's guide to proteomics. *Microbiology and Molecular Biology Reviews, 66*, 39–63.

Grote, U., Fasse, A., Nguyen, T. T., & Erenstein, O. (2021). Food security and the dynamics of wheat and maize value chains in Africa and Asia. *Frontiers in Sustainable Food Systems, 4*, 617009.

Guo, P., Baum, M., Grando, S., Ceccarelli, S., Bai, G., Li, R., Von Korff, M., Varshney, R. K., Graner, A., & Valkoun, J. (2009). Differentially expressed genes between drought-tolerant and drought-sensitive barley genotypes in response to drought stress during the reproductive stage. *Journal of Experimental Botany, 60,* 3531–3544.

Handler, D. C., Pascovici, D., Mirzaei, M., Gupta, V., Salekdeh, G. H., & Haynes, P. A. (2018). The art of validating quantitative proteomics data. *Proteomics, 18*, 1800222.

Harb, A., Simpson, C., Guo, W., Govindan, G., Kakani, V. G., & Sunkar, R. (2020). The effect of drought on transcriptome and hormonal profiles in barley genotypes with contrasting drought tolerance. *Frontiers in Plant Science, 11*, 618491.

Hare, P. D., & Cress, W. A. (1997). Metabolic implications of stress-induced proline accumulation in plants. *Plant Growth Regulation, 21*, 79–102.

Hasanuzzaman, M., Nahar, K., Gill, S. S., & Fujita, M. (2013). Drought stress responses in plants, oxidative stress, and antioxidant defense. In N. Tuteja & S. S. Gill. (Eds.), *Climate Change and Plant Abiotic Stress Tolerance* (pp. 209–250). Wiley-VCH Verlag.

Hiscox A N, J. D., & Israelstam, D. G. F. (1979). A method for the extraction of chlorophyll from leaf tissue without maceration. *Canadian Journal of Botany, 57*, 1332–1334.

Hlahla, J. M., Mafa, M. S., van der Merwe, R., Alexander, O., Duvenhage, M. M., Kemp, G.,

& Moloi, M. J. (2022). The photosynthetic efficiency and carbohydrates responses of six edamame (*Glycine max.* L. Merrill) cultivars under drought Stress. *Plants*, *11*, 394.

Huang, J., Chen, Q., Rong, Y., Tang, B., Zhu, L., Ren, R., Shi, T., & Chen, Q. (2021). Transcriptome analysis revealed gene regulatory network involved in PEG-induced drought stress in Tartary buckwheat (*Fagopyrum tararicum*). *PeerJ*, *9*, e11136.

Hurkman, W. J., & Tanaka, C. K. (2007). High-resolution two-dimensional gel electrophoresis: A cornerstone of plant proteomics. In J. Šamaj & J. Thelen (Eds.), *Plant Proteomics* (pp. 14–28). Springer Berlin.

Huseynova, I. M. (2012). Photosynthetic characteristics and enzymatic antioxidant capacity of leaves from wheat cultivars exposed to drought. *Biochimica et Biophysica Acta - Bioenergetics*, *1817*, 1516–1523.

Huseynova, I. M., Aliyeva, D. R., Mammadov, A. C., & Aliyev, J. A. (2015). Hydrogen peroxide generation and antioxidant enzyme activities in the leaves and roots of wheat cultivars subjected to long-term soil drought stress. *Photosynthesis Research*, *125*, 279–289.

Hussain, H. A., Men, S., Saddam, H., Chen, Y., Ali, S., Zhang, S., Zhang, K., Li, Y., Xu, Q., Liao, C., & Wang, L. (2019). Interactive effects of drought and heat stresses on morpho-physiological attributes, yield, nutrient uptake and oxidative status in maize hybrids. *Scientific Reports*, *9*, 1–12.

IPCC. (2023). *Climate Change 2023: Synthesis Report. Contribution of Working Groups I, II and III to the Sixth Assessment Report of the Intergovernmental Panel on Climate Change*.

Iqbal, M. J., Shams, N., & Fatima, K. (2022). Nutritional quality of wheat. In M.-R. Ansari (Ed.), *Wheat* (pp. 1–38). IntechOpen.

Jaleel, C. A., Manivannan, P., Wahid, A., Frooq, M., Somasundaram, R., & Panneerselvam, R. (2009). Drought stress in plants: a review on morphological characteristics and pigments composition. *International Journal of Agriculture and Biology*, *11*, 100–105.

Jan, N., Rather, A. M. U. D., John, R., Chaturvedi, P., Ghatak, A., Weckwerth, W., Zargar, S. M., Mir, R. A., Khan, M. A., & Mir, R. R. (2023). Proteomics for abiotic stresses in legumes: present status and future directions. *Critical Reviews in Biotechnology*, *43*, 171–190.

Jedmowski, C., Ashoub, A., Beckhaus, T., Berberich, T., Karas, M., & Brüggemann, W. (2014). Comparative analysis of *Sorghum bicolor* proteome in response to drought stress and following recovery. *International Journal of Proteomics*, *2014*, 395905.

Ji, W., Cong, R., Li, S., Li, R., Qin, Z., Li, Y., & Li, J. (2016). Comparative proteomic analysis of soybean leaves and roots by iTRAQ provides insights into response mechanisms to short-term salt stress. *Frontiers in Plant Science*, *7*, 1–15.

Jiang, Z., Jin, F., Shan, X., & Li, Y. (2019). iTRAQ-based proteomic analysis reveals several strategies to cope with drought stress in maize seedlings. *International Journal of Molecular Sciences*, *20*, 1–17.

Jogaiah, S., Govind, S. R., Tran, L. P., Jogaiah, S., Govind, S. R., & Tran, L. P. (2013). Systems biology-based approaches toward understanding drought tolerance in food crops. *Critical Reviews in Biotechnology*, *33*, 23–29.

Kanehisa, M., & Goto, S. (2000). KEGG: Kyoto Encyclopedia of Genes and Genome. *Nucleic Acids Research*, *28*, 27–30.

Kausar, R., Arshad, M., Shahzad, A., & Komatsu, S. (2013). Proteomics analysis of sensitive and tolerant barley genotypes under drought stress. *Amino Acids*, *44*, 345–359.

Kellner, R. (2000). Proteomics . Concepts and perspectives. *Journal of Analytical Chemistry*, *366*, 517–524.

Khadka, K., Earl, H. J., Raizada, M. N., & Navabi, A. (2020). A physio-morphological trait-based approach for breeding drought tolerant wheat. *Frontiers in Plant Science*, *11*, 715.

Khanna-Chopra, R., & Selote, D. S. (2007). Acclimation to drought stress generates oxidative stress tolerance in drought-resistant than -susceptible wheat cultivar under field conditions. *Environmental and Experimental Botany*, *60*, 276–283.

Kidric, M., Kos, J., & Sabotic, J. (2014). Proteases and their endogenous inhibitors in the plant response to abiotic stress. *Botanica Serbica, 38*, 139–158.

Kim, S. G., Lee, J., Kim, J., Kwon, Y. S., Bae, D., Bae, H. H., Son, B., Baek, S., Kwon, Y., Woo, M., & Shin, S. (2015). Physiological and proteomic analysis of the response to drought stress in an inbred Korean maize line. *Plant Omics Journal*, *8*, 159–168.

Knight, H., & Knight, M. R. (2001). Abiotic stress signalling pathways: Specificity and cross-talk. *Trends in Plant Science*, *6*, 262–267.

Kopecká, R., Kameniarová, M., Černý, M., Brzobohatý, B., & Novák, J. (2023). Abiotic stress in crop production. *International Journal of Molecular Sciences*, *24*, 6603.

Kosová, K., Klíma, M., Prášil, I. T., & Pavel Vítámvás. (2021). COR/LEA Proteins as Indicators of frost tolerance in Triticeae : A comparison of controlled versus field conditions. *Plants*, *10*, 789.

Kosová, K., Vítámvás, P., Urban, M. O., Prášil, I. T., & Renaut, J. (2018). Plant abiotic stress proteomics: The major factors determining alterations in cellular proteome. *Frontiers in Plant Science*, *9*, 122.

Krasensky, J., & Jonak, C. (2015). Drought, salt, and temperature stress-induced metabolic rearrangements and regulatory networks. *Journal of Experimental Botany*, *63*, 1593–1608.

Kumar, J., Gunapati, S., Kianian, S. F., & Singh, S. P. (2018). Comparative analysis of transcriptome in two wheat genotypes with contrasting levels of drought tolerance. *Protoplasma*, *255*, 1487–1504.

Kumar, S., Sachdeva, S., Bhat, K. V., & Vats, S. (2018). Plant responses to drought stress: Physiological, biochemical and molecular basis. In S. Vats (Ed.), *Biotic and Abiotic Stress Tolerance in Plants* (pp. 1–25). Springer, Singapore.

Kusvuran, S., & Dasgan, H. Y. (2017). Effects of drought stress on physiological and biochemical changes in *Phaseolus vulgaris* L. *Legume Research*, *40*, 55–62.

Laemmli, U. K. (1970). Cleavage of structural proteins during the assembly of the head of bacteriophage T4. *Nature*, *227*, 680–685.

Lamaoui, M., Jemo, M., Datla, R., & Bekkaoui, F. (2018). Heat and drought stresses in crops and approaches for their mitigation. *Frontiers in Chemistry*, *6*, 26.

Lau, S. E., Hamdan, M. F., Pua, T. L., Saidi, N. B., & Tan, B. C. (2021). Plant nitric oxide signaling under drought stress. *Plants*, *10*, 360.

Laxa, M., Liebthal, M., Telman, W., Chibani, K., & Dietz, K. J. (2019). The role of the plant antioxidant system in drought tolerance. *Antioxidants*, *8*, 94.

Li, H., Li, Y., Ke, Q., Kwak, S., Zhang, S., & Deng, X. (2020). Physiological and differential proteomic analyses of imitation drought stress response in *Sorghum bicolor* root at the seedling stage. *International Journal of Molecular Sciences, 21*, 1–26.

Li, H., Yang, M., Zhao, C., Wang, Y., & Zhang, R. (2021). Physiological and proteomic analyses revealed the response mechanisms of two different drought-resistant maize varieties. *BMC Plant Biology, 21*, 513.

Li, N., Zhang, S., Liang, Y., Qi, Y., Chen, J., Zhu, W., & Zhang, L. (2018). Label-free quantitative proteomic analysis of drought stress-responsive late embryogenesis abundant proteins in the seedling leaves of two wheat (*Triticum aestivum* L.) genotypes. *Journal of Proteomics*, *172*, 122–142.

Li, Y. H., Cui, J. Y., Zhao, Q., Yang, Y. Z., Wei, L., Yang, M. D., Liang, F., & Ding, S. T. (2019). Physiology and proteomics of two maize genotypes with different drought resistance. *Biologia Plantarum*, *63,* 519–528.

Lilley, K. S., & Dupree, P. (2018). Methods of quantitative proteomics and their application to plant organelle characterization. *Journal of Experimental Botany*, *57*, 1493–1499.

Lim, C. W., Baek, W., Jung, J., Kim, J., & Lee, S. C. (2015). Function of ABA in stomatal defense against biotic and drought stresses. *International Journal of Molecular Sciences*, *16*, 15251–15270.

Liwani, U., Magwaza, L. S., Sithole, N. J., Odindo, A. O., & Tsilo, T. J. (2018). Physiological responses of irrigated wheat (*Triticum aestivum* L.) genotypes to water stress. *Acta Agriculturae Scandinavica, Section B-Soil & Plant Science*, *68*, 524–533.

Ma, J., Li, R., Wang, H., Li, D., Wang, X., & Zhang, Y. (2017). Transcriptomics analyses reveal wheat responses to drought stress during reproductive stages under field conditions. *Fontiers in Plant Science*, *8*, 592.

Machado, S., & Paulsen, G. M. (2001). Combined effects of drought and high temperature on water relations of wheat and sorghum. *Plant and Soil*, *233*, 179–187.

Mafakheri, A., Siosemardeh, A., Bahramnejad, B., Struik, P. C., & Sohrabi, Y. (2010). Effect of drought stress on yield, proline and chlorophyll contents in three chickpea cultivars. *Australian Journal of Crop Science*, *4*, 580–585.

Magdeldin, S., Enany, S., Yoshida, Y., Xu, B., Zhang, Y., Zureena, Z., Lokamani, I., Yaoita, E., & Yamamoto, T. (2014). Basics and recent advances of two dimensional-polyacrylamide gel electrophoresis. *Clinical Proteomics*, *11*, 16.

Mahajan, S., & Tuteja, N. (2005). Cold, salinity and drought stresses: an overview. *Archives of Biochemistry and Biophysics*, *444*, 139–158.

Marcek, T., Hamow, K. A., Vegh, B., Janda, T., & Darko, E. (2019). Metabolic response to drought in six winter wheat genotypes. *PLOS ONE, 14*, 1–23.

Marcińska, I., Czyczyło-Mysza, I., Skrzypek, E., Filek, M., Grzesiak, S., Grzesiak, M. T., Janowiak, F., Hura, T., Dziurka, M., Dziurka, K., Nowakowska, A., & Quarrie, S. A. (2013). Impact of osmotic stress on physiological and biochemical characteristics in drought-susceptible and drought-resistant wheat genotypes. *Acta Physiologiae Plantarum, 35,* 451–461.

Mbow, C., Rosenzweig, C., Barioni, L. G., Benton, T. G., Herrero, M., Krishnapillai, M., Liwenga, E., Pradhan, P., Rivera-Ferre, M. G., Sapkota, T., Tubiello, F. N., & Xu, Y. (2019). Food security. In N. Benkeblia, A. Challino, A. Khan, & J. R. Porter (Eds.), *Climate Change and Land: an IPCC special report on climate change, desertification, land degradation, sustainable land management, food security, and greenhouse gas fluxes in terrestrial ecosystems* (pp. 437–550). Cambridge University Press.

Mehta, D., Ahkami, A. H., Walley, J., Xu, S. L., & Uhrig, R. G. (2022). The incongruity of validating quantitative proteomics using western blots. *Nature Plants, 12,* 1320–1321.

Mejri, M., Siddique, K. H. M., Saif, T., Abdelly, C., & Hessini, K. (2016). Comparative effect of drought duration on growth, photosynthesis, water relations, and solute accumulation in wild and cultivated barley species. *Journal of Plant Nutrition and Soil Science, 179,* 327–335.

Melkozernov, A. N., & Blankenship, R. E. (2006). Photosynthetic Functions of Chlorophylls. In B. Grimm, R. J. Porra, W. Rüdiger, & H. Scheer (Eds.), *Chlorophylls and Bacteriochlorophylls: Bio-chemistry, Biophysics, Functions and Applications* (pp. 397–412). Springer.

Michaletti, A., Naghavi, M. R., Toorchi, M., Zolla, L., & Rinalducci, S. (2018). Metabolomics and proteomics reveal drought-stress responses of leaf tissues from spring-wheat. *Scientific Reports, 8,* 1–18.

Mirzabaev, A., Bezner Kerr, R., Hasegawa, T., Pradhan, P., Wreford, A., Cristina Tirado von der Pahlen, M., & Gurney-Smith, H. (2023). Severe climate change risks to food security and nutrition. *Climate Risk Management, 39,* 100473.

Mittler, R. (2006). Abiotic stress, the field environment and stress combination. *Trends in Plant Science, 11,* 15–19.

Mittler, R., Zandalinas, S. I., Fichman, Y., & Van Breusegem, F. (2022). Reactive oxygen species signalling in plant stress responses. *Nature Reviews Molecular Cell Biology, 23,* 663–679.

Moloi, M. J., & van der Merwe, R. (2021). Drought tolerance responses in vegetable-type soybean involve a network of biochemical mechanisms at flowering and pod-filling stages. *Plants, 10,* 1502.

Moloi, S. J., & Ngara, R. (2023). The roles of plant proteases and protease inhibitors in drought response : a review. *Frontiers in Plant Science, 14,* 1165845.

Monteoliva, L., & Albar, J. P. (2004). Differential proteomics: An overview of gel and non-gel based approaches. *Briefings in Functional Genomics and Proteomics, 3,* 220–239.

Moosavi, S. S., Abdi, F., Reza, M., Tahmasebi-enferadi, S., & Maleki, M. (2020). Phenological, morpho-physiological and proteomic responses of *Triticum boeoticum* to drought stress. *Plant Physiology and Biochemistry, 156,* 95–104.

Mwadzingeni, L., Shimelis, H., Dube, E., Laing, M. D., & Tsilo, T. J. (2016). Breeding wheat for drought tolerance: Progress and technologies. *Journal of Integrative Agriculture, 15,* 935–943.

Naderi, S., Fakheri, B., Maali-amiri, R., & Mahdinezhad, N. (2020). Tolerance responses in wheat landrace Bolani are related to enhanced metabolic adjustments under drought stress. *Plant Biochemistry & Physiology*, *150*, 244–253.

Nasirzadeh, L., Sorkhilaleloo, B., Majidi Hervan, E., & Fatehi, F. (2021). Changes in antioxidant enzyme activities and gene expression profiles under drought stress in tolerant, intermediate, and susceptible wheat genotypes. *Cereal Research Communications*, *49*, 83–89.

Nelson, G. C., Rosegrant, M. W., Koo, J., Robertson, R., Sulser, T., Zhu, T., Ringler, C., Msangi, S., Palazzo, A., Batka, M., Magalhaes, M., Ewing, R. V.-S. M., & Lee, D. (2009). *Climate change impact on agriculture and costs of adaptation*. International Food Policy Research Institute.

Nemati, M., Piro, A., Norouzi, M., Moghaddam Vahed, M., Nisticò, D. M., & Mazzuca, S. (2019). Comparative physiological and leaf proteomic analyses revealed the tolerant and sensitive traits to drought stress in two wheat parental lines and their F6 progenies. *Environmental and Experimental Botany*, *158*, 223–237.

Ngara, R. (2009). *A Proteomic analysis of drought and salt stress responsive proteins of different sorghum varieties. [PhD thesis]*. University of the Western Cape, South Africa.

Ngara, R., & Chivasa, S. (2023). Applications of "omics" technologies in plant responses to combined drought and heat stress: Trends and future perspectives. In N. K. Gupta, Y. Shavrukov, R. K. Singhal, & N. Borisjuk (Eds.), *Multiple Abiotic Stress Tolerances in Higher Plant* (pp. 267–276). Taylor & Francis.

Ngara, R., Goche, T., Swanevelder, D. Z. H., & Chivasa, S. (2021). Sorghum's whole-plant transcriptome and proteome responses to drought stress: A review. *Life*, *11*, 1–25.

Niu, L., Xu, X., Liu, H., Wu, X., & Wang, W. (2018). On the promising role of enzyme activity assay in interpreting comparative proteomic data in plants. *Proteomics*, *18*, 1800234.

Nxele, X., Klein, A., & Ndimba, B. K. (2017). Drought and salinity stress alters ROS accumulation, water retention, and osmolyte content in sorghum plants. *South African Journal of Botany*, *108*, 261–266.

OECD-FAO. (2022). Cereals. In *Agricultural Outlook 2022-2031*.

Oeljeklaus, S., Meyer, H. E., & Warscheid, B. (2009). Advancements in plant proteomics using quantitative mass spectrometry. *Journal of Proteomics*, *72*, 545–554.

Ogbaga, C. C., Stepien, P., & Johnson, G. N. (2014). Sorghum (*Sorghum bicolor*) varieties adopt strongly contrasting strategies in response to drought. *Physiologia Plantarum*, *152*, 389–401.

Osmolovskaya, N., Shumilina, J., Kim, A., Didio, A., Grishina, T., Bilova, T., Keltsieva, O. A., Zhukov, V., Tikhonovich, I., Tarakhovskaya, E., Frolov, A., & Wessjohann, L. A. (2018). Methodology of drought stress research: Experimental setup and physiological characterization. *International Journal of Molecular Sciences*, *19*, 4089.

Owen, C. B., Hughes, D. J., Baquero-Perez, B., Berndt, A., Sophie, S., Jackson, B. R., & Whitehouse, A. (2014). Utilising proteomic approaches to understand oncogenic human herpesviruses (Review). *Molecular and Clinical Oncology*, *2*, 891–903.

Pan, J., Li, Z., Wang, Q., Garrell, A. K., Liu, M., Guan, Y., Zhou, W., & Liu, W. (2018). Comparative proteomic investigation of drought responses in foxtail millet. *BMC Plant Biology*, *18*, 1–19.

Passioura, J. B. (2012). Phenotyping for drought tolerance in grain crops: When is it useful to breeders? *Functional Plant Biology*, *39*, 851–859.

Pavli, O. I., Vlachos, C. E., Kalloniati, C., Flemetakis, E., & Skaracis, G. N. (2013). Metabolite profiling reveals the effect of drought on sorghum (*Sorghum bicolor* L. Moench) metabolism. *Plant Omics*, *6*, 371–376.

Paysan-Lafosse, T., Blum, M., Chuguransky, S., Grego, T., Pinto, B. L., Salazar, G. A., Bileschi, M. L., Bork, P., Bridge, A., Colwell, L., Gough, J., Haft, D. H., Letunić, I., Marchler-Bauer, A., Mi, H., Natale, D. A., Orengo, C. A., Pandurangan, A. P., Rivoire, C., Bateman, A. (2023). InterPro in 2022. *Nucleic Acids Research*, *51*, D418–D427.

Pei, L., Li, H., Zhou, Y., Li, W., Jiang, Y., & Li, H. (2022). Exogenous glycinebetaine application contributes to abiotic stress tolerance in maize. *Journal of Plant Biology*, *65*, 517–529.

Pirzad, A., Shakiba, M. R., Zehtab-salmasi, S., & Mohammadi, S. A. (2011). Effect of water stress on leaf relative water content , chlorophyll , proline and soluble carbohydrates in *Matricaria chamomilla* L . *Journal of Medicinal Plants Research*, *5*, 2483–2488.

Prajapat, P., Singh, D., Tripathi, S., Patel, K., Abbas, H., & Patel, A. (2018). Effect of water stress on antioxidative enzymes and glycine betaine content in drought tolerant and drought susceptible cotton (*Gossypium hirsutum* L .) genotypes. *Indian Journal of Biochemistry & Biophysics*, *55*, 198–204.

Price, A. H., Cairns, J. E., Horton, P., Jones, H. G., & Griffiths, H. (2002). Linking drought-resistance mechanisms to drought avoidance in upland rice using a QTL approach: progress and new opportunities to integrate stomatal and mesophyll responses. *Journal of Experimental Botany*, *53*, 989–1004.

Prinsen, H. C. M. T., Schiebergen-Bronkhorst, B.G.M., Roeleveld, M. W., Jans, J.J.M., de Sain van Velden, M.G.M. Visser, G., van Hasselt, P. M., & Verhoeven-Duif, N. M. (2016). Rapid quantification of underivatized amino acids in plasma by hydrophilic interaction liquid chromatography (HILIC) coupled with tandem mass-spectrometry. *Journal of Inherited Metabolic Disease*, *39*, 651–660.

Pyngrope, S., Bhoomika, K., & Dubey, R. S. (2013). Reactive oxygen species, ascorbate-glutathione pool, and enzymes of their metabolism in drought-sensitive and tolerant indica rice (*Oryza sativa* L.) seedlings subjected to progressing levels of water deficit. *Protoplasma*, *250*, 585–600.

Qiao, M., Hong, C., Jiao, Y., Hou, S., & Gao, H. (2024). Impacts of drought on photosynthesis in major food crops and the related mechanisms of plant responses to drought. *Plants*, *13*, 1808.

Rabilloud, T., & Lescuyer, P. (2014). The proteomic to biology inference, a frequently overlooked concern in the interpretation of proteomic data: A plea for functional validation. *Proteomics*, *14*, 157–161.

Rahbarian, R., Khavari-Nejad, R., Ganjeali, A., Bagheri, A., & Najafi, F. (2011). Drought stress effects on photosynthesis, chlorophyll flourescence and water relations in tolerant and susceptible chickpea (*Cicer arietinum* L.) genotypes. *ACTA Biologica Cracoviensia Series Botanica, 53,* 47–56.

Rahman, S., Shaheed, M. S., Mehboob-Ur-Rahman, & Malik, T. A. (2000). Evaluation of excised leaf water loss and relative water content, as screening techiques for breeding drought resistant wheat. *Pakistan Journal of Botany, 3,* 663–665.

Rakkammal, K., Priya, A., Pandian, S., Maharajan, T., Rathinapriya, P., Satish, L., Ceasar, S. A., Sohn, S., & Ramesh, M. (2022). Conventional and omics approaches for understanding the abiotic stress response in cereal crops — An updated overview. *Plants, 11,* 2852.

Reddy, A. R., Chaitanya, K. V., & Vivekanandan, M. (2004). Drought-induced responses of photosynthesis and antioxidant metabolism in higher plants. *Journal of Plant Physiology, 161,* 1189–1202.

Reddy, B. V. ., Ramesh, S., Reddy, P. ., & Kumar, A. . (2009). Genetic enhancement for drought tolerance in sorghum. In J. Janick (Ed.), *Plant Breeding Reviews* (pp. 198–222). John Wiley and Sons Inc.

Rezayian, M., Niknam, V., & Ebrahimzadeh, H. (2018). Effects of drought stress on the seedling growth, development, and metabolic activity in different cultivars of canola. *Soil Science and Plant Nutrition, 64,* 360–369.

Rhee, S. Y., & Mutwil, M. (2014). Towards revealing the functions of all genes in plants. *Trend in Plant Science, 19,* 212–221.

Rhodes, D., & Hanson, A. D. (1993). Quaternary ammonium and tertiary sulfonium compounds in higher plants. *Annual Review of Plant Physiology and Plant Molecular Biology, 44,* 357–384.

Rizhsky, L., Liang, H., & Mittler, R. (2002). The combined effect of drought stress and heat shock on gene xpression in tobacco. *Plant Physiology, 130,* 1143–1151.

Saad-allah, K. M., Nessem, A. A., Ebrahim, M. K. H., & Gad, D. (2022). Evaluation of drought tolerance of five maize genotypes by virtue of physiological and molecular responses. *Agronomy, 12,* 59.

Saeidi, M., Moradi, F., & Abdoli, M. (2017). Impact of drought stress on yield, photosynthesis rate, and sugar alcohols contents in wheat after anthesis in semiarid region of Iran. *Arid Land Research and Management, 31,* 204–218.

Salam, U., Ullah, S., Tang, Z. H., Elateeq, A. A., Khan, Y., Khan, J., Khan, A., & Ali, S. (2023). Plant metabolomics: An overview of the role of primary and secondary metabolites against different environmental stress factors. *Life, 13,* 706.

Salehi-Lisar, S. Y., & Bakhshayeshan-Agdam, H. (2016). Drought stress in plants; Causes, consequences, and tolerance. In D. J. B. and L. S. P. T. M. A. Hossain, S. H. Wani, S. Bhattacharjee (Ed.), *Drought Stress Tolerance in Plants*. Springer, Cham.

Sallam, A., Alqudah, A. M., Dawood, M. F. A., Baenziger, P. S., & Börner, A. (2019). Drought stress tolerance in wheat and barley: Advances in physiology, breeding and genetics research. *International Journal of Molecular Sciences, 20,* 1–36.

Samarah, N. H. (2005). Effects of drought stress on growth and yield of barley. *Agronomy for Sustainable Development, 23,* 145–149.

Sanders, G. J., & Arndt, S. K. (2012). Osmotic adjustment under drought conditions. In R. Aroca (Ed.), *Plant Responses to Drought Stress* (pp. 199–229). Springer-Velag, Berlin, Heidelberg.

Sarto, M. V. M., Sarto, J. R. W., Rampim, L., Rosset, J. S., Bassegio, D., Costa, P. F. da, & Inagaki, A. M. (2017). Wheat phenology and yield under drought: A review. *Australian Journal of Crop Science, 11*, 941–946.

Schulze, W. X., Altenbuchinger, M., He, M., Kränzlein, M., & Zörb, C. (2021). Proteome profiling of repeated drought stress reveals genotype-specific responses and memory effects in maize. *Plant Physiology and Biochemistry*, *159*, 67–79.

Seki, M., Umezawa, T., Urano, K., & Shinozaki, K. (2007). Regulatory metabolic networks in drought stress responses. *Current Opinion in Plant Biology*, *10*, 296–302.

Seleiman, M. F., Al-Suhaibani, N., Ali, N., Akmal, M., Alotaibi, M., Refay, Y., Dindaroglu, T., Abdul-Wajid, H. H., & Battaglia, M. L. (2021). Drought stress impacts on plants and different approaches to alleviate its adverse effects. *Plants*, *10*, 259.

Shao, H. B., Chu, L. Y., Jaleel, C. A., & Zhao, C. X. (2008). Water-deficit stress-induced anatomical changes in higher plants. *Comptes Rendus Biologies, 331*, 215–225.

Sharma, P., Jha, A. B., Dubey, R. S., & Pessarakli, M. (2012). Reactive oxygen species, oxidative damage, and antioxidative defense mechanism in plants under stressful conditions. *Journal of Botany*, *2012*, 1–26.

Shavrukov, Y., Kurishbayev, A., Jatayev, S., Shvidchenko, V., Zotova, L., Koekemoer, F., De Groot, S., Soole, K., & Langridge, P. (2017). Early flowering as a drought escape mechanism in plants: How can it aid wheat production? *Frontiers in Plant Science*, *8*, 1950.

Shehzadi, A., Akram, N. A., Ali, A., & Ashraf, M. (2019). Exogenously applied glycinebetaine induced alteration in some key physio-biochemical attributes and plant anatomical features in water stressed oat (*Avena sativa* L.) plants. *Journal of Arid Land*, *11*, 292–305.

Shinozaki, K., & Yamaguchi-Shinozaki, K. (1997). Gene expression and signal transduction in water-stress response. *Plant Physiology*, *11*, 327–334.

Shinozaki, K., & Yamaguchi-Shinozaki, K. (2007). Gene networks involved in drought stress response and tolerance. *Journal of Experimental Botany, 58*, 221–227.

Singh, D., & Laxmi, A. (2015). Transcriptional regulation of drought response: a tortuous network of transcriptional factors. *Frontiers in Plant Science*, *6*, 895.

Singh, M., Kumar, J., Singh, S., Singh, V. P., & Prasad, S. M. (2015). Roles of osmoprotectants in improving salinity and drought tolerance in plants: a review. *Reviews in Environmental Science and Biotechnology*, *14,* 407–426.

Singh, P. K., Indoliya, Y., Agrawal, L., Awasthi, S., Deeba, F., Dwivedi, S., Chakrabarty, D., Shirke, P. A., Pandey, V., Singh, N., Parkash, O., & Kanta, S. (2022). Genomic and proteomic responses to drought stress and biotechnological interventions for enhanced drought tolerance in plants. *Current Plant Biology*, *29*, 100239.

Singh, S., Gupta, A. K., & Kaur, N. (2012). Differential responses of antioxidative defence system to long-term field drought in wheat (*Triticum aestivum* L.) genotypes differing in drought tolerance. *Journal of Agronomy and Crop Science, 198*, 185–195.

Sivanich, M. K., Gu, T., Tabang, D. N., & Li, L. (2022). Recent advances in isobaric labeling and applications in quantitative proteomics. *Proteomics*, *22*, e2100256.

Steinberg, T. H. (2009). Protein gel staining methods: An introduction and overview. *Methods in Enzymology*, *463*, 541–563.

Stout, D. G., & Simpson, G. M. (1978). Drought resistance of Sorghum bicolor .L. drought avoidance mechanisms related to leaf water status. *Canadian Journal of Plant Science*, *58*, 213–224.

Sugumar, T., Shen, G., Smith, J., & Zhang, H. (2024). Creating climate-resilient crops by increasing drought, heat, and salt tolerance. *Plants*, *13*, 1238.

Sultan, M. A. R. ., Hui, L., Yang, L. J., & Xian, Z. H. (2012). Assessment of drought tolerance of some Triticum L. species through physiological indices. *Czech Journal of Genetics and Plant Breeding*, *4*, 178–184.

Sun, J., Li, J., Wang, M., Song, Z., & Liu, J. (2021). Protein quality control in plant organelles: Current progress and future perspectives. *Molecular Plant*, *14*, 95–114.

Sur, T. (2013). iTRAQ , a new prospect of toxicogenomics. *International Journal of Human Genetics*, *13*, 33–40.

Suzuki, N., Rivero, R. M., Shulaev, V., Blumwald, E., & Mittler, R. (2014). Abiotic and biotic stress combinations. *New Phytologist*, *203*, 32–43.

Szabados, L., & Savouré, A. (2010). Proline: a multifunctional amino acid. *Trends in Plant Science*, *15*, 89–97.

Szklarczyk, D., Kirsch, R., Koutrouli, M., Nastou, K., Mehryary, F., Hachilif, R., Gable, A. L., Fang, T., Doncheva, N. T., Pyysalo, S., Bork, P., Jensen, L. J., & Von Mering, C. (2023). The STRING database in 2023: protein–protein association networks and functional enrichment analyses for any sequenced genome of interest. *Nucleic Acids Research*, *51*, D638–D646.

Tadesse, W., Bishaw, Z., & Assefa, S. (2019). Wheat production and breeding in Sub-Saharan Africa: Challenges and opportunities in the face of climate change. *International Journal of Climate Change Strategies and Management*, *11*, 696–715.

Taiz, L., & Zeiger, E. (2012). *Plant Physiology* (5th ed.). Sunderland, Massachusetts U.S.A.: Sinauer Associates Inc.

Takahashi, F., Kuromori, T., Sato, H., & Shinozaki, K. (2018). Regulatory gene networks in drought stress responses and resistance in plants. In M. Iwaya-Inoue, M., Sakurai, M., Uemura (Ed.), *Survival Strategies in Extreme Cold and Desiccation*. Singapore, Japan: Springer Nature.

Tan, C. B., Lim, S. Y., & Lau, S. (2017). Proteomics in commercial crops : An overview. *Journal of Proteomics*, *169*, 176–188.

Tardieu, F., Simonneau, T., & Muller, B. (2018). The physiological basis of drought tolerance in crop plants: A scenario-dependent probabilistic approach. *Annual Review of Plant Biology*, *69*, 733–759.

Thanmalagan, R. R., Jayaprakash, A., Roy, A., Arunachalam, A., & Lakshmi, P. T. V. (2022). A review on applications of plant network biology to understand the drought stress response in economically important cereal crops. *Plant Gene*, *29*, 100345.

The UniProt Consortium. (2023). UniProt: the Universal Protein Knowledgebase in 2023. *Nucleic Acids Research*, *51*, D523–D531.

Thomas, P. D. (2017). The Gene Otology and the meaning of biological function. *Methods Molecular Biology, 1446*, 15–24.

Todaka, D., & Takahashi, F. (2019). ABA-responsive gene expression in response to drought stress: cellular regulation and long-distance signaling. *Advances in Botanical Research*, *92*, 1–31.

Turner, N. C., & Begg, J. E. (1981). Plant-water relations and adaptations. *Plant and Soil*, *58*, 97–13.

Verslues, P. E., & Juenger, T. E. (2011). Drought, metabolites, and Arabidopsis natural variation: a promising combination for understanding adaptation to water-limited environments. *Current Opinion in Plant Biology*, *14*, 240–245.

Vessal, S., Arefian, M., & Siddique, K. H. M. (2020). Proteomic responses to progressive dehydration stress in leaves of chickpea seedlings. *BMC Genomics*, *523*, 1–15.

Vineeth, T. V., Kumar, P., & Krishna, G. K. (2016). Bioregulators protected photosynthetic machinery by inducing expression of photorespiratory genes under water stress in chickpea. *Photosynthetica*, *54*, 234–242.

Vinocur, B., & Altman, A. (2005). Recent advances in engineering plant tolerance to abiotic stress: Achievements and limitations. *Current Opinion in Biotechnology*, *16*, 123–132.

Wang, D., Pan, Y., Zhao, X., Zhu, L., Fu, B., & Li, Z. (2011). Genome-wide temporal-spatial gene expression profiling of drought responsiveness in rice. *BMC Genomics*, *12*, 149.

Wang, G. P., Zhang, X. Y., Li, F., Luo, Y., & Wang, W. (2010). Overaccumulation of glycine betaine enhances tolerance to drought and heat stress in wheat leaves in the protection of photosynthesis. *Photosynthetica*, *48*, 117–126.

Wang, J., Zhang, X., Han, Z., Feng, H., Wang, Y., Kang, J., Han, X., Wang, L., Wang, C., Li, H., & Ma, G. (2022). Analysis of physiological indicators associated with drought tolerance in wheat under drought and re-watering Conditions. *Antioxidants*, *11*, 2266.

Wang, W., Vinocur, B., & Altman, A. (2003). Plant responses to drought, salinity and extreme temperatures: towards genetic engineering for stress tolerance. *Planta*, *218*, 1–14.

Wang, Y., Peng, C., Zhan, Y., Yu, L., Li, M., & Li, J. (2017). Comparative proteomic analysis of two sugar beet cultivars with contrasting drought tolerance. *Journal of Plant Growth Regulation*, *36*, 537–549.

Wang, Y., Zhang, X., Huang, G., Feng, F., Liu, X., Guo, R., Gu, F., Zhong, X., & Mei, X. (2019). iTRAQ-based quantitative analysis of responsive proteins under PEG-induced drought stress in wheat leaves. *International Journal of Molecular Sciences*, *20*, 2621.

Wellburn, A. R. (1994). The spectral determination of chlorophylls a and b, as well as total carotenoids, using various solvents with spectrophotometers of different resolution. *Journal of Plant Physiology*, *144*, 307–313.

Wilhite, D. A., & Glantz, M. H. (1985). Understanding: The drought phenomenon: The role of definitions. *Water International*, *10*, 111–120.

Wu, G. Q., Wang, C. M., Su, Y. Y., Zhang, J. J., Feng, R. J., & Liang, N. (2014). Assessment of drought tolerance in seedlings of sugar beet (*Beta vulgaris* L.) cultivars using inorganic and organic solutes accumulation criteria. *Soil Science and Plant Nutrition, 60*, 565–576.

Wu, W. W., Wang, G., Baek, S. J., & Shen, R.-F. (2006). Comparative study of three proteomic quantitative methods, DIGE, cICAT, and iTRAQ, using 2D Gel-or LC-MALDI TOF/TOF. *Journal of Proteome Research, 5,* 651–658.

Xiong, L., & Zhu, J.-K. (2002). Molecular and genetic aspects of plant responses to osmotic stress. *Plant, Cell and Environment, 25*, 131–139.

Xu, C., Garrett, W. M., Sullivan, J., Caperna, T. J., & Natarajan, S. (2006). Separation and identification of soybean leaf proteins by two-dimensional gel electrophoresis and mass spectrometry. *Phytochemistry, 67*, 2431–2440.

Xu, Y., Song, D., Qi, X., Asad, M., Wang, S., Tong, X., Jiang, Y., & Wang, S. (2023). Physiological responses and transcriptome analysis of soybean under gradual water deficit. *Frontiers in Plant Science, 14*, 1269884.

Xu, Z., Lai, X., Ren, Y., Yang, H., Wang, H., Wang, C., Xia, J., Wang, Z., Yang, Z., Geng, H., Shi, X., & Zhang, Y. (2023). Impact of drought stress on yield-related agronomic traits of different genotypes in spring wheat. *Agronomy, 13,* 2968.

Yao, T., Zhang, J., Xie, M., Yuan, G., Tschaplinski, T. J., Muchero, W., & Chen, J. G. (2021). Transcriptional regulation of drought response in arabidopsis and woody plants. *Frontiers in Plant Science, 11*, 572137.

Ye, J., Coulouris, G., Zaretskaya, I., Cutcutache, I., Rozen, S., & Madden, T. L. (2012). Primer-BLAST: A tool to design target-specific primers for polymerase chain reaction. *BioMed Central Bioinformatics*, 134.

Yoshida, T., Mogami, J., & Yamaguchi-Shinozaki, K. (2014). ABA-dependent and ABA-independent signaling in response to osmotic stress in plants. *Current Opinion in Plant Biology, 21,* 133–139.

Yoshimura, K., Masuda, A., Kuwano, M., Yokota, A., & Akashi, K. (2007). Programmed proteome response for drought avoidance/tolerance in the root of a C3 xerophyte (Wild watermelon) under water deficits. *Plant and Cell Physiology, 49,* 226–241.

Yu, X., James, A. T., Yang, A., Jones, A., Mendoza-Porras, O., Bétrix, C.-A., Ma, H., Colgrave, M. L., Yu, X., James, A. T., Yang, A., Jones, A., Mendoza-Porras, O., Bétrix, C.-A., Ma, H., & Colgrave, M. L. (2016). A comparative proteomic study of drought-tolerant and drought-sensitive soybean seedlings under drought stress. *Crop and Pasture Science*, *67*, 528–540.

Yuan, L., Liu, X., Luo, M., Yang, S., & Wu, K. (2013). Involvement of histone modifications in plant abiotic stress responses. *Journal of Integrative Plant Biology, 55*, 892–901.

Zandalinas, S. I., Mittler, R., Balfagón, D., Arbona, V., & Gómez-cadenas, A. (2018). Plant adaptations to the combination of drought and high temperatures. *Physiologia Plantarum, 162,* 2–12.

Zargar, S. M., Gupta, N., Mir, R. A., & Rai, V. (2016). Shift from gel based to gel free proteomics to unlock unknown regulatory network in plants: A comprehensive review. *Journal of Advanced Research in Biotechnology, 1*, 1–19.

Zargar, S. M., Mir, R. A., Ebinezer, L. B., Masi, A., Hami, A., Manzoor, M., Salgotra, R. K., Sofi, N. R., Mushtaq, R., Rohila, J. S., & Rakwal, R. (2022). Physiological and multi-omics approaches for explaining drought stress tolerance and supporting sustainable production of rice. *Frontiers in Plant Science*, *12*, 3242.

Zenda, T., Liu, S., Wang, X., Jin, H., & Liu, G. (2018). Comparative proteomic and physiological analyses of two divergent maize inbred lines provide more insights into drought-stress tolerance mechanisms. *International Journal of Molecular Sciences*, *19*, 3225.

Zeng, W., Peng, Y., Zhao, X., Wu, B., Chen, F., Ren, B., Zhuang, Z., Gao, Q., & Ding, Y. (2019). Comparative proteomics analysis of the seedling root response of drought-sensitive and drought-tolerant maize varieties to drought stress. *International Journal of Molecular Sciences*, *20*, 2793.

Zhang, J., Nguyen, H. T., & Blum, A. (1999). Genetic analysis of osmotic adjustment in crop plants. *Journal of Experimental Botany*, *50*, 291–302.

Zhao, Y., Gao, C., Shi, F., Yun, L., Jia, Y., & Wen, J. (2018). Transcriptomic and proteomic analyses of drought responsive genes and proteins in *Agropyron mongolicum* Keng. *Current Plant Biology*, *14*, 19–29.

Zheng, H., Yang, Z., Wang, W., Guo, S., Li, Z., Liu, K., & Sui, N. (2020). Transcriptome analysis of maize inbred lines differing in drought tolerance provides novel insights into the molecular mechanisms of drought responses in roots. *Plant Physiology and Biochemistry*, *149*, 11–26.

Zhou, Q., Li, Y., Wang, X., Yan, C., Ma, C., Liu, J., & Dong, S. (2022). Effects of different drought degrees on physiological characteristics and endogenous hormones of soybean. *Plants*, *11*, 2282.

Zhou, R., Yu, X., Ottosen, C., Rosenqvist, E., Zhao, L., Wang, Y., & Yu, W. (2017). Drought stress had a predominant effect over heat stress on three tomato cultivars subjected to combined stress. *BMC Plant Biology*, *17*, 1–13.

Zhu, J. K. (2016). Abiotic stress signaling and responses in plants. *Cell*, *167*, 313–324.

Zhu, Y., Luo, X., Nawaz, G., Yin, J., & Yang, J. (2020). Physiological and biochemical responses of four cassava cultivars to drought stress. *Scientific Reports*, *10*, 6968.

APPENDICES

Table A1.1: Preparation of hydrogen peroxide standards.

Concentration (µM)	**20 mM K_2HPO_4 (µl)**	**H_2O (µl)**	**500 mM KI (µl)**	**5 mM H_2O_2 (µl)**
***0**	187.5	187.5	375	0
250	187.5	150	375	37.5
500	187.5	112.5	375	75
750	187.5	75	375	112.5
1000	187.5	37.5	375	150
1250	187.5	0	375	187.5

*blank solution

Table A1.2: Preparation of resolving and stacking gels for gel electrophoresis.

Reagents	**12%(v/v) Resolving gel**	**5%(v/v) Stacking gel**
Distilled water	4.3	3.6
40% Acryl-bisacrylamide mix	3	0.625
0.5M Tris-HCL (pH 6.8)	-	0.63
1.5M Tris-HCL (pH 8.8)	2.5	-
10% SDS	0.1	0.05
10% APS	0.1	0.05
TEMED	0.006	0.005
Total volume	**10 ml**	**5 ml**